ATTACHMENT 2

(GPU Letter to NRC dated March 4, 1991)

Nuclear

GPU Nuclear Corporation
One Upper Pond Road
Parsippany, New Jersey 07054
201-316-7000
TELEX 136-482
Writer's Direct Dial Number

March 4, 1991
5000-91-2026
C320-91-2035

U. S. Nuclear Regulatory Commission
Att: Document Control Desk
Washington, DC 20555

Gentlemen:

Subject: Oyster Creek Nuclear Generating Station (OCNGS)
Docket No. 50-219
License No. DPR-16
Oyster Creek Drywell Containment

References: (1) GPUN letter dated December 5, 1990 - Drywell Structural Reports and Water Intrusion Summary

In the Reference 1 letter, GPUN committed to provide to you the structural design reports supporting drywell sand removal at Oyster Creek. As you know, our investigations indicate strongly that the presence of sand is a major contributor to the high corrosion rates observed in the sandbed region (elevation 8'-11" to 12'-3") of the drywell; for that reason we consider sand removal to be an important element in our program to eliminate the corrosion threat to drywell integrity.

Attachment I to this letter provides this information in the form of GE Reports Index No. 9-3 and 9-4, "An ASME Section VIII Evaluation of the Oyster Creek Drywell for Without Sand Case Stress and Stability Analysis." This two (2) part report covers the structural analysis of the Oyster Creek drywell with the sand cushion removed and conservatively assumes a uniform drywell sandbed region corroded thickness of 0.736" at the end of Cycle 13 operation. The report demonstrates that if the sand cushion were removed the drywell would remain in full compliance with ASME Code requirements.

Further measurements of the drywell shell thickness are being made during the current 13R outage and will serve as a basis for refined corrosion rate projections. Assuming that these updated corrosion rate projections are consistent with the Attachment I analysis, GPUN plans to proceed with the removal of the drywell sand cushion during Cycle 13 operation as a prudent and positive step in arresting corrosion at Oyster Creek.

RZ:C3202035

If you have any questions or comments on this submittal or the overall drywell corrosion program, please contact Mr. Michael Laggart, Manager, Corporate Nuclear Licensing at (201) 316-7968.

Sincerely,

J. C. DeVine, Jr.
Vice President,
Technical Functions

Attachment
JCD/RZ/plp

cc: Administrator, Region 1
Senior NRC Resident Inspector
Oyster Creek NRC Project Manager

DRF # 00664
INDEX No. 9-3
REV. 0

AN ASME SECTION VIII EVALUATION OF OYSTER CREEK DRYWELL FOR WITHOUT SAND CASE

PART I

STRESS ANALYSIS

February 1991

prepared for

GPU Nuclear Corporation
Parsippany, New Jersey

prepared by

GE Nuclear Energy
San Jose, California

DRF # 00664
INDEX NO. 9-3, REV. 0

AN ASME SECTION VIII EVALUATION OF OYSTER CREEK DRYWELL FOR WITHOUT SAND CASE

PART I

STRESS ANALYSIS

Prepared by: C.D. Frederickson

C.D. Frederickson, Senior Engineer
Materials Monitoring &
Structural Analysis Services

C.D. Frederickson for GWC

G. W. Contreras, Engineer
Materials Monitoring &
Structural Analysis Services

Reviewed by: H. S. Mehta

H. S. Mehta, Principal Engineer
Materials Monitoring &
Structural Analysis Services

Approved by: S. Ranganath

S. Ranganath, Manager
Materials Monitoring &
Structural Analysis Services

TABLE OF CONTENTS

	Page No.
1. INTRODUCTION	1-1
1.1 Background	1-1
1.2 Supplementary Code Stress Analyses	1-2
1.3 Scope of Present Analysis	1-3
1.4 Report Outline	1-3
1.5 References	1-3
2. ANALYSIS BASES	2-1
2.1 Drywell Geometry and Materials	2-1
2.2 ASME Code Allowable Values	2-3
2.2.1 Thickness Reductions From Local Corrosion Effects	2-4
2.2.2 Allowable Stresses for Post-Accident Condition	2-5
2.3 Load Magnitudes and Combinations	2-5
2.4 Temperature Gradients	2-6
2.5 References	2-7
3. DRYWELL FINITE ELEMENT ANALYSIS	3-1
3.1 Description of Finite Element Models	3-1
3.1.1 Axisymmetric Model	3-1
3.1.2 Pie Slice Finite Element Model	3-1
3.2 Load Application on Pie Slice Model	3-2
3.2.1 Gravity Loads	3-3
3.2.2 Pressure Load	3-3
3.2.3 Seismic Loads	3-4
3.3 Stress Results for Various Load Cases and Combinations	3-4

TABLE OF CONTENTS (CONT'D)

	Page No.
3.4 Temperature Stress Analysis	3-5
3.5 References	3-6
4. SEISMIC LOAD DEFINITION	4-1
4.1 Finite Element Model	4-1
4.2 Dynamic Analysis Methodology and Response Spectra	4-1
4.3 Post-Accident Seismic Analysis	4-2
4.4 Analysis for Relative Support Displacement Effects	4-2
4.5 References	4-3
5. CODE STRESS EVALUATION	5-1
5.1 Code Stress Evaluation of Regions Above the Lower Sphere	5-1
5.2 Elastic Stress Analysis of Sandbed and Lower Sphere	5-2
5.2.1 Small Displacement Solution Results	5-2
5.2.2 Large Displacement Solution Results	5-4
5.3 Code Evaluation of the Sandbed and Lower Sphere	5-4
5.3.1 Primary Stress Evaluation	5-4
5.3.2 Extent of Local Primary Membrane Stress	5-5
5.3.3 Primary Plus Secondary Stress Evaluation	5-6
6. SUMMARY AND CONCLUSIONS	6-1
APPENDIX A DETAILED RESULTS FOR AXISYMMETRIC MODEL TEMPERATURE STRESS ANALYSIS	

LIST OF TABLES

Table No.	Title	Page No.
2-1	As-designed and Projected 95% Confidence thicknesses used in the Code Stress Evaluation	2-8
2-2	Allowable Stresses for Drywell Shell in Section VIII Analysis	2-9
2-3	Allowable Stresses for Post-Accident Condition	2-10
2-4	Load Combinations specified in the Parsons Report (Reference 2-3)	2-11
2-5a	Dead Weight Loads	2-12
2-5b	Penetration Loads	2-13
2-5c	Live Loads	2-15
3-1	Load Cases Considered in the Finite Element Analysis	3-7
3-2	Adjusted Weight Densities of Shell to Account for Compressible Material Weight	3-8
3-3	Oyster Creek Drywell Additional Weights - Refueling Condition	3-9
3-4	Oyster Creek Drywell Additional Weights - Accident and Post-Accident Condition	3-10
3-5	Hydrostatic Pressures for Post-Accident Condition	3-11

LIST OF TABLES (CONT'D)

Table No.	Title	Page No.
3-6	Meridional Seismic Stresses at Four Sections	3-12
3-7	Application of Loads to Match Seismic Stresses - Accident Condition	3-13
3-8	Application of Loads to Match Seismic Stresses - Post-Accident Condition	3-14
3-9	Description of Load Combinations in Terms of Unit Load Case Sum	3-15
5-1a	Comparison of Calculated Stresses to Code Allowable Values (Nominal Drywell Wall Thicknesses Above Lower Sphere)	5-7
5-1b	Comparison of Calculated Stresses to Code Allowable Values (95% Projected Drywell Wall Thicknesses Above Lower Sphere)	5-8
5-2a	Comparison of Calculated Primary Stresses to Code Allowable Values (Small Displacement; Lower Sphere and Sandbed)	5-9
5-2b	Comparison of Calculated Primary Stresses to Code Allowable Values (Large Displacement; Lower Sphere and Sandbed)	5-10
5-3a	Comparison of Calculated Primary Plus Secondary Stresses to Code Allowable Values (Small Displacement; Lower Sphere and Sandbed)	5-11

LIST OF TABLES (CONT'D)

Table No.	Title	Page No.
5-3b	Comparison of Calculated Primary Plus Secondary Stresses to Code Allowable Values (Large Displacement; Lower Sphere and Sandbed)	5-12

LIST OF FIGURES

Figure No.	FIGURE	Page No.
1-1	Drywell Configuration	1-5
3-1	Complete Axisymmetric Finite Element Model of Drywell	3-16
3-2	Sand Bed Region of Drywell Finite Element Model	3-17
3-3	Knuckle Region of Drywell Finite Element Model	3-18
3-4	Cylindrical Region of Drywell Finite Element Model	3-19
3-5	Upper Cylindrical Region of Drywell Finite Element Model	3-20
3-6	Oyster Creek Drywell Pie Slice Finite Element Model	3-21
3-7	Inside Closeup View of Lower Drywell Section	3-22
3-8	Application of Loading to Simulate Seismic Stresses	3-23
3-9	Below Curb Drywell Model Nodalization for Temperature Analysis During Accident Condition	3-24

LIST OF FIGURES (CONT'D)

Figure No.	FIGURE	Page No.
3-10	Example of Calculated Temperature Distribution at Various Elapsed Times	3-25
3-11	Meridional Stress Distribution in the Sand Bed Region from Temperature Distribution at t=210 Seconds	3-26
3-12	Circumferential Stress Distribution in the Sand Bed Region from Temperature Distribution at t=210 Seconds	3-27
5-1	Circumferential Stresses for Accident Condition V-1 in 'With Sand' and 'Without Sand' Cases - Small Displacement	5-13
5-2	Plot of Accident Condition V-1 Meridional Stresses for 'Without Sand' Case - Small Displacement	5-14
5-3	Circumferential Membrane Stress Distribution Using Small Displacement Option	5-15
5-4	Circumferential Membrane Stress Magnitudes at Four Meridional Planes in Sandbed Region - Small Displacement	5-16
5-5	Beam With Transverse Plus Axial Loading	5-17
5-6	Circumferential Membrane Stress Distribution Using Large Displacement Option	5-18

LIST OF FIGURES (CONT'D)

Figure No.	FIGURE	Page No.
5-7	Comparison of Circumferential Membrane Stress Magnitudes With Large and Small Displacement Options	5-19
5-8	Circumferential Membrane Stress Magnitudes at Four Meridional Planes in Sandbed Region - Large Displacement	5-20

1. INTRODUCTION

1.1 Background

The Oyster Creek Nuclear Generating Station utilizes a GE BWR Nuclear Steam Supply System and a steel Mark I pressure suppression type containment vessel system. The pressure suppression system consists of a drywell, a pressure suppression chamber (torus) which stores a large volume of water and a connecting vent system between the drywell and the water pool. The drywell, sometimes referred to as the containment vessel or containment structure, houses the reactor vessel, reactor coolant recirculation loops, and other components associated with the reactor system.

Figure 1-1 shows the drywell along with the pertinent dimensions. The drywell is a combination of a sphere, cylinder and 2:1 ellipsoidal dome and it resembles an inverted light bulb. The spherical portion of drywell near the base includes a sandbed region that provides an elastic transition zone which is intended to ameliorate abrupt thermal and mechanical discontinuities. The pressure suppression system was designed, analyzed and constructed by Chicago Bridge & Iron Company (CBI).

A recent inspection of the steel shell (November 1986) prior to restart from the 11R outage in the sandbed region revealed that some degradation of the shell had taken place during the years since completion of construction. Subsequent inspections also indicated minor thickness degradations in the upper spherical and cylindrical sections of the drywell.

A detailed description of the previous analyses pertaining to Oyster Creek drywell is given in Reference 1-1. An ASME Code stress analysis addressing the drywell thickness degradation is documented in Reference 1-2. The analyses in Reference 1-2 are based on the present configuration in the sandbed region, i.e., it is assumed that the sand is present. One of the option GPUN is exploring to mitigate further

corrosion in the sandbed region, is to remove the sand. The purpose of the stress analyses presented in this report is to evaluate the drywell per ASME Section VIII for this modification.

1.2 Supplementary Code Stress Analyses

The Code of record for the stress analysis of Oyster Creek drywell is Section VIII, 1962 Edition and Nuclear case interpretations 1270 N-5, 1274 N-5 and 1272 N-5. The CBI stress report (Reference 1-3) augmented by the recent GE report (Reference 1-2) constitutes the Section VIII Code stress report of record for the drywell. The GE report is a supplementary stress report to the CBI stress report and addresses aspects of Code compliance as they relate to the local wall thinning observed in the Oyster Creek drywell. The stress analyses in this report as in the previous GE report [1-2] are guided by GPUN Technical Specification for primary containment analysis [1-4].

Based on the ultrasonic (UT) inspection results, the projected 95% confidence thickness value for the drywell shell in the sandbed region is 0.736 inch. However, in several previous Oyster Creek drywell analyses, as discussed in Reference 1-1, a conservative thickness value of 0.700 inch was used. A shell thickness of 0.700 inch in the sandbed region was used in the stress analyses documented in Reference 1-2.

In the first part of the stress analysis report of Reference 1-2, the nominal or as-designed thicknesses were assumed everywhere except in the sand bed region. The thickness in the sand bed region was assumed as 0.700 inch compared to the as-designed thickness of 1.154 inch. Later, the local thinning in areas other than the sand bed region of drywell was addressed. The second part of Reference 1-2 report addressed the buckling evaluation of drywell shell.

1.3 Scope of Present Analysis

The stress analyses described in this report address the case when the sand has been removed from the sandbed region (called the 'without sand case'). A companion report [1-5] addresses the buckling evaluation for this case.

The finite element models used in the Reference 1-2 analyses were modified for this case by removing the spring elements representing sand stiffness. It will be shown that this change affects only the stresses in the sandbed and adjacent region. The stresses in the other regions of the drywell are essentially unaffected.

1.4 Report Outline

Section 2 of the report describes the drywell geometry, materials, ASME Code allowables and load combinations used in the evaluation of applied stresses. Also discussed is the temperature gradient definition in the sand bed region under DBA conditions. Section 3 includes the details of drywell finite element analysis. Seismic load analyses are covered in Section 4.

Section 5 presents the Code stress evaluation results to meet the Code criteria. Finally, the summary and conclusions are discussed in Section 6. The Appendix includes calculated stresses from some of the unit load cases.

1.5 References

1-1 Yekta, M., "OC Drywell Structural Evaluations," GPUN Technical Data Report No. 926, Rev. 1, February 6,1989.

1-2 a. "An ASME Section VIII Evaluation of the Oyster Creek Drywell - Part 1 - Stress Analysis," GE Index # 9-1, DRF # 00664 (November 1990).

b. "An ASME Section VIII Evaluation of the Oyster Creek Drywell - Part 2 - Stability Evaluation," GE Index # 9-2, DRF # 00664 (November 1990).

1-3 "Structural Design of the Pressure Suppression Containment Vessels," by Chicago Bridge & Iron Co..Contract # 9-0971, 1965.

1-4 GPUN Specification SP-1302-53-044, Technical Specification for Primary Containment Analysis - Oyster Creek Nuclear Generating Station; Rev. 2, October 1990.

1-5 "An ASME Section VIII Evaluation of the Oyster Creek Drywell for Without Sand Case - Part 2 - Stability Evaluation," GE Index # 9-4, DRF # 00664 (February 1991).

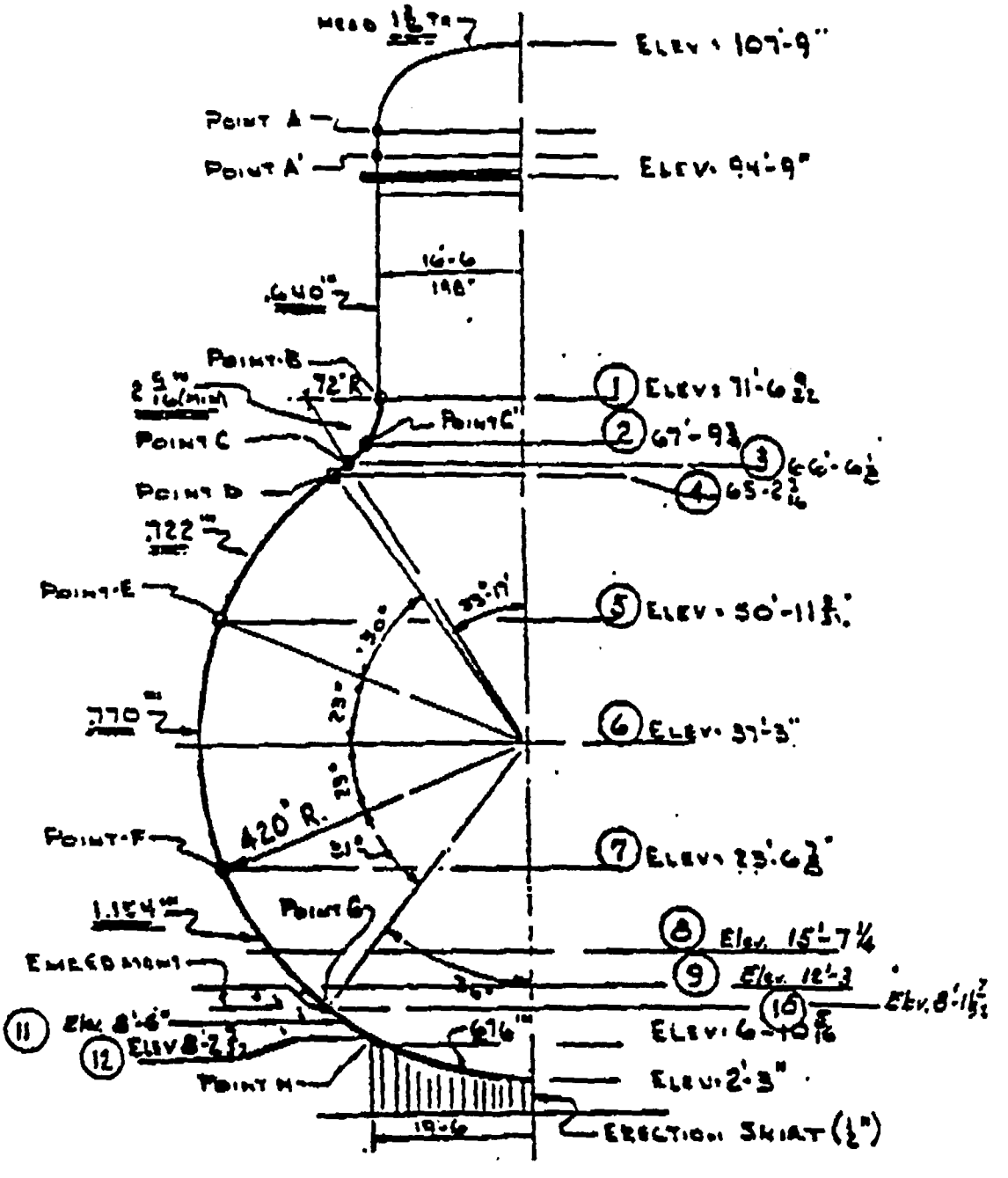

Figure 1-1 Drywell Configuration

2. ANALYSIS BASES

2.1 Drywell Geometry and Materials

The spherical section has an inside diameter of 70 ft. which intersects the 33 ft. diameter cylindrical portion. A transition knuckle is provided at the connection of the sphere to the cylinder (Figure 1-1). The drywell is 105'-6" high. The plate thicknesses vary from a maximum of 2.625 in. at the transition between the sphere and the cylinder down to a minimum of 0.640 in. in the cylinder. The head wall thickness is 1.188 in.

The head, which is 33 ft. in diameter, is made with a double tongue and groove seal which permits periodic checks for tightness. Ten vent pipes, 6'-6" in diameter, are equally spaced around the circumference to connect the drywell to the vent header inside the pressure suppression chamber.

The drywell interior is filled with concrete to elevation 10'-3" to provide a level floor. Concrete curbs follow the contour of the vessel up to elevation 12'-3" with cutouts around the vent lines.

On the exterior, the drywell is encapsulated in concrete of varying thickness from the base elevation up to the elevation of the top head. From there, the concrete continues vertically to the level of the top of the spent fuel pool.

The base of the drywell is supported on a concrete pedestal conforming to the curvature of the vessel. A structural steel skirt was first installed to provide interim support for the vessel during erection. A portion of the steel skirt was left in place which serves as one of the shear rings that provides horizontal restraint for the drywell during an earthquake.

The proximity of the biological shield concrete surface to the steel shell varies with the elevation. The concrete is in full contact with the shell over the bottom of the sphere at its invert elevation 2'-3"

up to elevation 8'-11 1/4". At that point, the concrete is stepped back 15 inches radially to form a pocket which continues up to elevation 12'-3". That pocket is currently filled with sand which forms a cushion which is intended to smooth the transition of the shell plate from a condition of fully clamped between two concrete masses to a free standing condition. This sand filled pocket is referred to here as the sandbed. In the analyses described in this report it is assumed that the sand has been removed. Up from elevation 12'-3" there is a 3-inch gap between the drywell and the concrete biological shield wall which is filled with foam material that provides insulation but no structural support.

An upper lateral seismic restraint, attached to the cylindrical portion of the drywell at elevation 82'-6", allows for thermal, deadweight, and pressure radial deflection, but not for lateral movement due to seismic excitation. All penetrations for piping, instrumentation lines, vent ducts, electrical lines, equipment accesses, and personnel entrance have expansion joints and double seals where applicable.

The materials of construction for the drywell are given in Specification S-2299-4 [2-1]. The drywell shell, i.e., the sphere, cylinder, dome, and transitions, was constructed from SA-212, Grade B High Tensile Strength Carbon-Silicon Steel Plates for Boilers and other Pressure Vessels ordered to SA-300 specification.

The following steels were used in the construction of penetrations, reinforcements, and appurtenances:

SA-300 Steel Plates for Pressure Vessels for Service at Low Temperatures.

SA-333 Seamless and Welded Steel Pipe for Low Temperature Service.

SA-350 Forged or Rolled Carbon and Alloy Steel Flanges, Forged Fittings, and Valves and Parts for Low Temperature Service.

ASTM A-36 Structural Steel.

Table 2-1 shows the as-designed thicknesses used in the Code stress evaluation of the drywell shell [1-2]. Also shown in the same Table are the projected 95% confidence thickness values in the locally corroded areas [2-2]. These latter thicknesses are used in the primary stress evaluation presented in Subsection 5.2.

2.2 ASME Code Allowable Values

The Oyster Creek drywell vessel was designed, fabricated and erected in accordance with the 1962 Edition of ASME Code, Section VIII and Code Cases 1270N-5, 1271N and 1272N-5.

The Code Case 1272 N-5 limits the general membrane stresses to 1.1 times the allowable stress values given in Table UCS-23 of Section VIII. The combined general membrane, general bending, and local membrane stresses are limited to 1.5 times the general membrane stress allowables. Finally, the Code Case limits the sum of the primary plus secondary stresses to three times the allowable stresses given in Table UCS-23. The allowable stress value given in Table UCS-23 for SA 212, Grade B is 17500 psi. Accordingly, the allowable stress values for various categories of stresses are shown in Table 2-2.

The original Code of record and the Code Cases do not provide specific guidance in two areas. The first relates to the size of a region of increased membrane stress due to thickness reductions from local or general corrosion effects, and the second pertains to the allowable stresses for service level C or post-accident conditions. In the first case, guidance was sought from Subsection NE of Section III. The justification for the use of this guidance is provided in a report prepared by Dr. W.E. Cooper of Teledyne [2-5]. In the latter case, the Standard Review Plan document was used as guidance with details discussed in Reference 2-6. The allowable limits obtained are discussed next.

2.2.1 Thickness Reductions from Local Corrosion Effects

Consideration of local corrosion effects can be achieved by application of the requirements for Local Primary Membrane Stresses. A thorough discussion of this is presented in Reference 2-5. The discussion presented here is extracted from that reference.

The NE-3213.10 definition of Local Primary Membrane Stress is:

> Cases arise in which a membrane stress produced by pressure or other mechanical loading and associated with a primary or discontinuity effect produces excessive distortion in the transfer of load to other portions of the structure. Conservatism requires that such a stress be classified as local primary membrane stress even though it has some characteristics of a secondary stress. A stress region may be considered local if the distance over which the membrane stress intensity exceeds 1.1 S_{mc} does not extend in the meridional direction more than 1.0/(Rt), where R is the minimum midsurface radius of curvature and t is the minimum thickness in the region considered. Regions of local primary membrane stress intensity involving axisymmetric membrane stress distributions which exceed 1.1 S_{mc} shall not be closer in the meridional direction than 2.5/(Rt), where R is defined as $(R_1+R_2)/2$ and t is defined as $(t_1+t_2)/2$, where t_1 and t_2 are the minimum thicknesses at each of the regions considered, and R_1 and R_2 are the minimum midsurface radii of curvature at these regions where the membrane stress intensity exceeds 1.1 S_{mc}. Discrete regions of local membrane stress intensity, such as those resulting from concentrated loads acting on brackets, where the membrane stress intensity exceeds 1.1 S_{mc} shall be spaced so that there is no overlapping of the areas in which the membrane stress intensity exceeds 1.1 S_{mc}.

The value of S_{mc} from NE of Section III is equivalent to 1.1 S from Section VIII.

There is no Code limit for the extent of the region in which the membrane stress exceeds 1.0 S_{mc} but is less than $1.1S_{mc}$. This 10% variation in the allowable stress was provided because of the "beam on elastic foundation" effects of such local regions, the stress decays as one moves away from the thin region, but overshoots general membrane stress value by a small amount as the effects dampen out with distance. Thus, this provision is not equivalent to a 10% increase in the allowable stress which can be taken advantage of in the original design. However, given a design which satisfies the general Code intent, as the Oyster Creek drywell does as originally constructed, it is not a violation of Subsection NE requirements for the membrane stress to be between $1.0S_{mc}$ and $1.1S_{mc}$ over significant distances.

Based on the preceding discussion, a limit of $1.1S_{mc}$ will be used in evaluating the general membrane stresses in areas of the drywell where reduced thicknesses are specified.

2.2.2 Allowable Stresses for Post-Accident Condition

In the post-accident condition, the drywell is flooded to elevation 74'-6". The allowable stress values for this condition are given in Table 3.8.2-1 of Reference 2-4. Table 2-3 shows the allowable stress values used for the post-accident condition.

2.3 Load Magnitudes and Combinations

The loads to be considered in the Oyster Creek drywell stress analysis, and the load combinations are specified in Reference 1-4. References 2-1 and 2-3 also contain similar descriptions of the loads and load combinations. Table 2-4 shows these load combinations. The Cases I and II pertain to test loads imposed on the drywell prior to plant startup. These loads are enveloped by the loads specified in Case V - Accident Condition. Therefore, separate calculations were not conducted for Cases I and II.

A comparison of the load combinations shown in Table 2-4 and those given in Reference 2-4 is covered in Reference 2-6. From that comparison it was concluded that the load combinations in Table 2-4 essentially envelope those described in Reference 2-4.

The dead load, live load and other equipment loads used in the stress calculations were obtained from an earlier study by CBI [Reference No. 2.4.3 of Reference 1-4], and are shown in Tables 2-5a though 2-5c. In the dead weight loading, the weight of the compressible material attached to the drywell was separately added. This weight was taken as 10 lbs. per sq. ft. of drywell surface [Reference No. 2.4.2 of Reference 1-4]. The additional weight on the cylindrical portion of the drywell during the refueling was obtained from Reference No. 2.4.3 in Reference 1-4 as 561 lbs/inch of drywell cylindrical region circumference.

The stresses from seismic loads were separately calculated as described in Section 4.

2.4 Temperature Gradients

The drywell shell is essentially at a uniform temperature during all of the operating conditions except the accident condition. During the accident condition it is assumed that the drywell shell except the region below the curb (i.e., the sand bed region) is at the same temperature as that of the environment inside the drywell. An analysis of the meridional temperature distribution in the sand bed region during the accident condition was reported in Reference 1-4.

The meridional temperature results in Reference 1-4 are given as a function of elapsed time from the start of the accident condition to 4500 seconds. These temperature distributions are used in Section 3 to calculate the stresses.

2.5 References

2-1 Technical Specification S-2299-4; Design, Furnishing, Erection and Testing of the Reactor Drywell. and Suppression Chamber Containment Vessels (1964).

2-2 "Forcasted Drywell Thicknesses to 14R," letter dated October 5, 1990 from S.C. Tumminelli of GPUN to H.S. Mehta of GE, dated.

2-3 "Primary Containment Design Report," prepared by The Ralph M. Parsons Company, FSAR Amendment 15.

2-4 Nuclear Regulatory Commission Standard Review Plan, Section 3.8.2, Steel Containment, Rev. 1, July 1981.

2-5 "Justification for use of Section III, Subsection NE, Guidance in Evaluating the Oyster Creek Drywell," Appendix A to letter dated December 21, 1990 from H.S. Mehta of GE to S.C. Tumminelli of GPUN.

2-6 "Comparison of FDSAR and SRP Load Combinations," Appendix D to letter dated December 21, 1990 from H.S. Mehta of GE to S.C. Tumminelli of GPUN.

TABLE 2-1

As-designed and Projected 95% Confidence thicknesses used in the Code Stress Evaluation

Drywell Region	As-designed Thicknesses (in)	Projected 95% 14R Thicknesses (in)
Cylindrical Region	0.640	0.619*
Knuckle	2.625	2.625
Upper Spherical Region	0.722	0.677
Middle Spherical Region	0.770	0.723
Lower Spherical Region Except Sand Bed Area	1.154	1.154
Sand Bed Region	1.154	0.736

* no on-going corrosion

TABLE 2-2

Allowable Stresses for Drywell Shell in Section VIII Analysis

(Except Post-Accident Condition)

<u>Primary Stresses</u>	
General membrane	19300 psi
General membrane plus bending	29000 psi
<u>Primary plus Secondary Stresses</u>	
Surface stresses including thermal effects	3x17500 or 52500 psi

NOTE: The general membrane stress allowable value of 19300 psi is equal to 1.1x17500, where 17500 psi is the allowable stress value for the drywell material in Table UCS-23 of Section VIII.

TABLE 2-3

Allowable Stresses for Post-Accident Condition

Primary Stresses

General Membrane	38000 psi
General Membrane plus Bending	1.5x General membrane or 57000 psi

Secondary Stresses

Primary plus Secondary	70000 psi

NOTE: The above allowable stresses are based Standard Review Plan, Section 3.8.2., Steel Containment

Table 2-4

Load Combinations specified in the Parsons Report (Reference 2-3)

CASE I - INITIAL TEST CONDITION
Deadweight + Design Pressure (62 psi) + Seismic (2 x DBE)

CASE II - FINAL TEST CONDITION
Deadweight + Design Pressure (35 psi) + Seismic (2 x DBE)

CASE III - NORMAL OPERATING CONDITION
Deadweight + Pressure (2 psi external) + Seismic (2 x DBE)

CASE IV - REFUELING CONDITION
Deadweight + Pressure (2 psi external) + Water load at water seal @ 118'-3" + Seismic (2 x DBE)

CASE V - ACCIDENT CONDITION
Deadweight + Pressure (62 psi & 175 F or 35 psi & 281 F) + Seismic (2 x DBE)

CASE VI - POST ACCIDENT CONDITION
Deadweight + Water Load @ 74' 6" + Seismic (2 x DBE)

Notes: (1) The loads shown above predominate. Reference 2-3 contains all of the loads.

(2) DBE is the design basis earthquake.

TABLE 2.5a
Dead Weight Loads

Item	Elevation (ft.)	Weight in lbs
Upper Header	60.00	36000
Lower Header	40.00	41000
Upper Weld Pads	65.00	40000
Middle Weld Pads	60.00	40000
Lower Weld Pads	56.00	48000
Top Flange	95.75	20100
Bottom Flange	93.75	20700
Stabilizers	82.17	21650
Upper Beam Seats	50.00	1102000
Lower Beam Seats	22.00	556000
12 Ft Diam. EQ DOOR	30.25	48000
Personnel Lock	30.00	64100
Vents	15.56	50000
13 Ft Diam EQ DOOR	30.25	57000
Upper Weld Pads	65.00	12000
Middle Weld Pads	60.00	19200
Lower Weld Pads	56.00	8400

TABLE 2-5b
Penetration Loads

Penetration ID	Elevation (ft.)	Weight in lbs
x - 54A	87.00	1000
x - 5 A Thru H	16.00	150000
x - 6	16.00	6000
x - 7A Thru D	30.00	45600
x - 8	26.00	2450
x - 9A, 9B	34.00	22600
x - 10, 11	26.00	8650
x - 12, 45	31.00	16500
x - 13A, 13B	33.00	15450
x - 14,15,39B	70.00	5750
x - 43, 44	54.00	7850
x - 16A,B	73.00	8850
x - 17	90.00	2750
x - 18, 19	20.00	900
x - 20,21,22	40.00	850
x - 23,24,34A,B	20.00	6000
x - 25	90.00	3750
x - 27	90.00	1000
x - 28A-G	34.00	5450
x - 30AB, 32A	16.00	3700
x - 31AB, 53	16.00	3750
x - 26	20.00	3900
x - 35A Thru G	16.00	900

TABLE 2-5b (Cont'd)
Penetration Loads

Penetration ID	Elevation (ft.)	Weight in lbs
x - 36	60.00	700
x - 37 A Thru D	40.00	8100
x - 38A Thru D	40.00	8100
x - 42	20.00	400
x - 39A	30.00	850
x - 40 AB, 46A	30.00	2400
x - 46B, 52	30.00	1650
x - 49, 50	35.00	1500
x - 51	32.00	750
x - 100AB, 104B	40.00	2500
x - 105A,D+107A	40.00	2500
x - 100C,D,G+104	40.00	4150
x - 105B,C+106B	40.00	2550
x - 100E, 103A,10	40.00	2500
x - 102B	40.00	850
x - 101A-F	40.00	5100
x - 104BD	40.00	1650
x - 54B	90.00	1000
x - 55 A+B	90.00	2000
x - 102A,104A,10	40.00	2650
x - 100F,103B	40.00	1850
x - 29A,B,47,48	90.00	4000
x - 32B,33A,33B	16.00	3750
x - 40CD	36.00	1550
x - 41	90.00	500

TABLE 2-5c

Live Loads

Item	Elevation (ft.)	Weight in lbs
Upper Header	60.00	4200
Lower Header	40.00	7150
Upper Weld Pads	65.00	20000
Middle Weld Pads	60.00	20000
Lower Weld Pads	56.00	24000
Equip Door	30.25	100000
Personnel Lock	30.00	15000

3. DRYWELL FINITE ELEMENT ANALYSIS

3.1 Description of Finite Element Models

The drywell was modelled for finite element analysis using the ANSYS computer program [3-1]. Two finite element models, an axisymmetric model and a 36° pie slice model, were used in the stress analysis. Both of these models are essentially the same as those used in the stress analyses [1-2] except that the elements representing sand stiffness were eliminated. The axisymmetric model was used in determining the stresses for the seismic and the thermal gradient load cases. The pie slice model was used for dead weight and pressure load cases and to evaluate the stresses for load combinations. The pie slice model includes the effect of vent pipes and the reinforcing ring on the stress state in the sandbed and adjacent region.

3.1.1 Axisymmetric Model

The axisymmetric model is shown in Figures 3-1 through 3-5, where Figure 3-1 is an overview, and Figures 3-2, 3-3, 3-4, and 3-5 show the sand bed, knuckle, cylindrical, and upper most cylindrical regions, respectively. The geometry as described in Subsection 2.1, along with References 3-2 and 3-3, was used in generating this model.

The model was developed using axisymmetric solid elements (STIF 25), with the lower most portion being fixed in all directions. This element has asymmetric load capability which was required for the seismic evaluation. Seismic evaluations are discussed in Section 4.

3.1.2 Pie Slice Finite Element Model

Taking advantage of symmetry of the drywell with 10 ventlines, a 36° section was modeled. Figure 3-6 shows the 36° pie slice finite element model of the drywell. This model includes the drywell shell

from the base of the sandbed region to the top of the elliptical head and the vent and vent header. The torus is not included in this model because the bellows provide a very flexible connection which does not allow significant structural interaction between the drywell and torus. The various colors in Figure 3-6 represent the different shell thicknesses of the drywell and ventline. Figure 3-7 shows the view from the inside of the drywell with the gussets and the vent jet deflector.

The drywell and vent shell are modeled using the 3-dimensional plastic quadrilateral shell (STIF43) element. At a distance of 76 inches from the drywell shell, the ventline modeling was simplified by using beam elements. The transition from shell to beam elements is made by extending rigid beam elements from a node along the centerline of the vent radially outward to each of the shell nodes of the ventline. ANSYS STIF4 beam elements are then connected to this centerline node to model the axial and bending stiffness of the ventline and header. Spring (STIF14) elements are used to model the vertical header supports inside the torus. ANSYS STIF4 beam elements are also used to model the stiffeners in the cylindrical region of the drywell.

Symmetric boundary conditions are defined for both edges of the 36° drywell segment. This allows the nodes at this boundary to move radially outward from the drywell centerline and vertically, but not in the circumferential direction. Rotations are also fixed in two directions to prevent the boundary from rotating out of the plane of symmetry. Nodes at the bottom edge of the drywell are fixed in all directions to simulate the fixity of the shell within the concrete foundation.

3.2 Load Application on Pie Slice Model

The loads are applied to the drywell finite element model in the manner which most accurately represents the actual loads anticipated on the drywell. Details on the application of loads are discussed in the following paragraphs.

3.2.1 Gravity Loads

The gravity loads include dead weight loads of the drywell shell, weight of the compressible material and penetrations and live loads. The drywell shell loads are imposed on the model by defining the weight density of the shell material and applying a vertical acceleration of 1.0 g to simulate gravity. The ANSYS program automatically distributes the loads consistent with the mass and acceleration. The compressible material weight of 10 lb/ft^2 is added by adjusting the weight density of the shell to also include the compressible material. The adjusted weight densities for the various shell thicknesses are summarized in Table 3-2.

The additional dead weights, penetration weights and live loads are applied as additional nodal masses to the model. As shown on Table 3-3 for the refueling condition case, the total additional mass is summed for each 5 foot elevation of the drywell. The total is then divided by 10 for the 36° section assuming that the mass is evenly distributed around the perimeter of the drywell. The resulting mass is then applied uniformly to a set of nodes at the desired elevation as shown in Table 3-3. These applied masses automatically impose gravity loads on the drywell model with the defined acceleration of 1g. The same method is used to apply the additional masses to the model for the accident and the post-accident conditions as summarized in Table 3-4.

3.2.2 Pressure Load

The appropriate pressure load is applied to the internal/external faces of all of the drywell and vent shell elements. The axial stress at the transition from vent shell to beam elements is simulated by applying equivalent axial forces to the nodes of the shell elements. In the post-accident condition, the drywell is assumed to be flooded to elevation 74'-6" (894 inches). Using a water density of 62.3 lb/ft^3 (0.0361 lb/in^3), the pressure gradient versus elevation is calculated as shown in Table 3-5. The hydrostatic pressure at the

bottom of the sandbed region is calculated to be 28.3 psi. According to the elevation of the element centerline, the appropriate pressures are applied to the inside surface of the shell elements.

3.2.3 Seismic Loads

Seismic inertia and displacement stresses were first calculated using the axisymmetric model. The seismic meridional stresses determined from the axisymmetric model were then imposed on the pie slice model by applying downward forces at four elevations of the model (A: 23'-7",B: 37'-3",C: 50'-11" and D: 88'-9") as shown on Figure 3-8. Using this method, the meridional stresses calculated from the axisymmetric model are duplicated at four sections of the pie slice model including 1) the mid-elevation of the sandbed region, 2) 17.25° below the equator, 3) 5.75° above the equator and 4) just above the knuckle region. These four sections were chosen to most accurately represent the loading in the lower drywell while also providing a reasonably accurate stress distribution in the upper drywell. Table 3-6 shows the meridional stress magnitudes at the four sections.

Unit loads are then applied to the pie slice model in separate load steps at each elevation shown in Figure 3-8. The resulting stresses at the four sections of interest are then averaged for each of the applied unit loads. By solving four equations with four unknowns, the correct loads are determined to match the stresses shown in Table 3-6 at the four sections. The calculation for the correct loads are shown in Tables 3-7 and 3-8 for the accident and post-accident conditions, respectively.

3.3 Stress Results for Various Load Cases and Combinations

Only the two orthogonal stress components - meridional and circumferential - are significant at the maximum stress locations in the drywell shell. A review of the component stresses indicated that the calculated shear stress magnitudes are insignificant compared to the values for the total meridional and circumferential stresses. Therefore, the orthogonal stress magnitudes and the principal stress

magnitudes were essentially the same. Also, the maximum stress was equivalent to the stress intensity at the locations evaluated.

The stresses for the seismic inertia, seismic displacement and temperature load cases (see Table 3-1) were calculated using the axisymmetric model. The details of the temperature stress analysis is described in the next Subsection and the procedures used in the calculation of the seismic stresses are covered in Section 4. The calculated values of the membrane and membrane plus bending stresses for temperature case are tabulated in Appendix A.

The seismic stresses were incorporated in the pie slice model to determine the overall stress resultants for the accident and post-accident load combinations. The temperature stresses determined from the axisymmetric model were separately added to the accident condition stresses obtained from the pie slice model. The multipliers applied to the various unit load cases (Table 3-1) to obtain total stresses for a particular load combination are shown in Table 3-9. The resulting stresses for these load combinations are discussed and compared with the Code allowables in Section 5.

3.4 Temperature Stress Analysis

The thermal response in the sand bed region to a DBA LOCA has been analyzed by GPU in Reference 1-4. Figure 3-9 shows the meridional nodes below the drywell floor, for which the calculated temperatures as a function of elapsed time are reported in Reference 1-4. An example of the calculated temperatures is shown in Figure 3-10.

From a review of the temperature distributions, two intermediate time steps were identified as possibly yielding the most severe thermal stresses. At 60 seconds, the largest temperature gradient occurs over a two inch meridional length. At 210 seconds, the maximum temperature is achieved. In addition, a third time step, 690 seconds, was evaluated to verify that a more deeply penetrating temperature condition would not result in higher stresses than the first two cases.

The predominant stresses for each of these cases occurred near the top of the sand bed region (near the 0.736" to 1.154" transition) and were in the circumferential and meridional directions. It was found that the thermal stresses at 210 seconds yielded the more severe stress condition. Figures 3-11 and 3-12 show the meridional and circumferential stress distributions in the sand bed region.

3.5 References

3-1 Gabriel J. DeSalvo, Ph.D. and John A. Swanson, Ph.D, "ANSYS Engineering Analysis System User's Manual," Revision 4.1, Swanson Analysis System, Inc. Houston, PA, March 1, 1983.

3-2 CB&I Drwg. 9-0971 sheet number 4, Rev. 1, "Drywell - Field Weld Joint"

3-3 CB&I Drwg. 9-0971 sheet number 7, Rev. 5, "Drywell - Cylindrical Shell & Top Head"

TABLE 3-1

Load Cases Considered in the Finite Element Analysis

Case No.	Loading
1	Pressure
2	Gravity-1 (Accident Condition)
3	Gravity-2 (Refueling)
4*	Unflooded Seismic
5*	Flooded Seismic
6	Flooded Hydrostatic Pressure
7*	Seismic Relative Support Displacement
8*	Temperature Gradient During DBA

* Load Cases Analyzed by Axisymmetric Finite Element Model

TABLE 3-2

Adjusted Weight Densities of Shell to Account for Compressible Material Weight

Shell Thickness(in.)	Adjusted Weight Density (lb/in^3)
1.154	0.343
0.770	0.373
0.722	0.379
2.563	0.310
0.640	0.392
1.250	0.339

TABLE 3-3

Oyster Creek Drywell Additional Weights - Refueling Condition

ELEVATION (feet)	DEAD WEIGHT (lbf)	PENETR. WEIGHT (lbf)	& MISC. LOADS (lbf)	TOTAL LOAD (lbf)	5 FOOT RANGE LOAD	LOAD PER 36 DEG. (lbf)	# OF ELEMENTS	NODES OF APPLICATION	LOAD PER FULL NODE (lbf)	LOAD PER HALF NODE (lbf)
15.56	50000			50000						
16		168100		168100						
20		11200		11200						
** 15-20					229300	22930	6	116-119	3822	1911
22#	556000			556000						
** 21-25#					556000	55600	8	161-169	6950	3475
26		11100		11100						
30	64100	51500		115600						
30.25	105000		100000	205000						
** 26-30					331700	33170	8	179-187	4146	2073
31		16500		16500						
32		750		750						
33		15450		15450						
34		28050		28050						
35		1500		1500						
** 31-35					62250	6225	8	188-196	778	389
36		1550		1550						
40	41000	43350		84350						
** 36-40					85900	8590	8	197-205	1074	537
50#	1102000			1102000						
** 45-50#					1102000	110200	8	418-426	13775	6888
54		7850		7850						
** 51-55					7850	785	8	436-444	98	49
56	56400		24000	80400						
60	95200	700	20000	115900						
** 56-60					196300	19630	8	454-462	2454	1227
65	52000		20000	72000						
** 61-65					72000	7200	8	472-480	900	450
70		5750		5750						
** 66-70					5750	575	8	508-516	72	36
73		8850		8850						
** 71-75					8850	885	8	526-534	111	55
82.17	21650			21650						
** 81-85					21650	2165	8	553-561	271	135
87		1000		1000						
90		15000		15000						
** 86-90					16000	1600	8	571-579	200	100
93.75	20700			20700						
94.75#			698000	698000						
95.75	20100			20100						
** 91-96					738800	73880	8	589-597	9235	4618
TOTALS:	2184150	388200	862000	3434350	3434350	343435				

- LOAD TO BE APPLIED IN VERTICAL DIRECTION ONLY.

& - MISCELLANEOUS LOADS INCLUDE 698000 LB WATER WEIGHT AT 94.75 FT. ELEVATION 100000 LB EQUIPMENT DOOR WEIGHT AT 30.25 FT. ELEVATION AND WELD PAD LIVE LOADS OF 24000, 20000 AND 20000 AT 56, 60 AND 65 FT. ELEVATIONS

REFWGT.WK1

TABLE 3-4

Oyster Creek Drywell Additional Weights
Accident and Post-Accident Condition

ELEVATION (feet)	DEAD WEIGHT (lbf)	PENETR. WEIGHT (lbf)	& MISC. LOADS (lbf)	TOTAL LOAD (lbf)	5 FOOT RANGE LOAD	LOAD PER 36 DEG. (lbf)	# OF ELEMENTS	NODES OF APPLICATION	LOAD PER FULL NODE (lbf)	LOAD PER HALF NODE (lbf)
15.58	50000			50000						
16		168100		168100						
20		11200		11200						
** 15-20					229300	22930	6	116-119	3822	1911
22#	556000			556000						
** 21-25#					556000	55600	8	161-169	6950	3475
26		11100		11100						
30	64100	51500		115600						
30.25	105000			105000						
** 26-30					231700	23170	8	179-187	2896	1448
31		16500		16500						
32		750		750						
33		15450		15450						
34		28050		28050						
35		1500		1500						
** 31-35					62250	6225	8	188-196	778	389
36		1550		1550						
40	41000	43350		84350						
** 36-40					85900	8590	8	197-205	1074	537
50#	1102000			1102000						
** 45-50#					1102000	110200	8	418-426	13775	6888
54		7850		7850						
** 51-55					7850	785	8	436-444	98	49
56	56400			56400						
60	95200	700		95900						
** 56-60					152300	15230	8	454-462	1904	952
65	52000			52000						
** 61-65					52000	5200	8	472-480	650	325
70		5750		5750						
** 66-70					5750	575	8	508-516	72	36
73		8850		8850						
** 71-75					8850	885	8	526-534	111	55
82.17	21650			21650						
** 81-85					21650	2165	8	553-561	271	135
87		1000		1000						
90		15000		15000						
** 86-90					16000	1600	8	571-579	200	100
93.75	20700			20700						
95.75	20100			20100						
** 91-98					40800	4080	8	589-597	510	255
TOTALS:	2184150	388200	0	2572350	2572350	257235				

- LOAD TO BE APPLIED IN VERTICAL DIRECTION ONLY.
& - NO MISCELLANEOUS LOADS FOR THIS CONDITION.

FLOODWGT.WK1

TABLE 3-5

Hydrostatic Pressures for Post-Accident Condition

WATER DENSITY: 62.32 lb/ft3
0.03606 lb/in3

FLOODED ELEV: 74.5 ft
894 inches

ELEMENTS ABOVE NODES	ANGLE ABOVE EQUATOR (degrees)	ELEVATION (inch)	DEPTH (inch)	PRESSURE (psi)	ELEMENTS
27	-53.32	110.2	783.8	28.3	1-12
40	-51.97	116.2	777.8	28.1	13-24
53	-50.62	122.4	771.6	27.8	25-36
66	-49.27	128.8	765.2	27.6	37-48
79	-47.50	137.3	756.7	27.3	49-51, 61-66 ,55-57
92	-46.20	143.9	750.1	27.1	52-54, 138-141 ,58-60
102	-44.35	153.4	740.6	26.7	142-147, 240-242, 257-259
108	-41.89	166.6	727.4	26.2	148-151, 243, 256
112	-39.43	180.2	713.8	25.7	152-155, 244, 255
116	-36.93	194.6	699.4	25.2	156-159, 245, 254
120	-34.40	209.7	684.3	24.7	160-165, 246, 253
124	-31.87	225.2	668.8	24.1	166-173, 247, 252
130	-29.33	241.3	652.7	23.5	174-183, 248-251
138	-26.80	257.6	636.4	23.0	184-195
148	-24.27	274.4	619.6	22.3	196-207
161	-20.13	302.5	591.5	21.3	208-215
170	-14.38	342.7	551.3	19.9	216-223
179	-8.63	384.0	510.0	18.4	224-231
188	-2.88	425.9	468.1	16.9	232-239
197	2.88	468.1	425.9	15.4	430-437
400	8.63	510.0	384.0	13.8	438-445
409	14.38	551.3	342.7	12.4	446-453
418	20.13	591.5	302.5	10.9	454-461
427	25.50	627.8	266.2	9.6	462-469
436	30.50	660.2	233.8	8.4	470-477
445	35.50	690.9	203.1	7.3	478-485
454	40.50	719.8	174.2	6.3	486-493
463	45.50	746.6	147.4	5.3	494-501
472	50.50	771.1	122.9	4.4	502-509
481	54.86	790.5	103.5	3.7	510-517
490	-	805.6	88.4	3.2	518-525
499	-	820.7	73.3	2.6	526-533
508	-	835.7	58.3	2.1	534-541
517	-	850.8	43.2	1.6	542-549
526	-	885.3	8.7	0.3	550-557
-	-	187.3	706.7	25.5	340-399 (Ventline)

FLOODP.WK1

TABLE 3-6

Meridional Seismic Stresses at Four Sections

Section	Elevation (inches)	2-D Shell Model Node	Meridional Stresses Accident (psi)	Meridional Stresses Post-Accident (psi)
A) Middle of Sandbed	119	32	1258	1288
B) 17.25° Below Equator	323	302	295	585
C) 5.75° Above Equator	489	461	214	616
D) Above Knuckle	1037	1037	216	808

TABLE 3-7

Application of Loads to Match Seismic Stresses - Accident Condition

COMPRESSIVE STRESSES FROM 2-D ANALYSIS	SECTION:	1	2	3	4
	2-D NODE:	32	302	461	1037
	ELEV:	119.3"	322.5"	489.1"	912.3"
		2-D SEISMIC STRESSES AT SECTION (psi)			
0.058" SEISMIC DEFLECTION:		788.67	155.54	103.46	85.31
HORIZ. PLUS VERTICAL SEISMIC INERTIA:		469.55	139.44	110.13	130.21
TOTAL SEISMIC COMPRESSIVE STRESSES:		1258.22	294.98	213.59	215.52

3-D INPUT LOAD SECTION	INPUT 3-D UNIT LOAD DESCRIPTION	SECTION:	1	2	3	4
		3-D NODES:	53-65	170-178	400-408	526-534
		ELEV:	119.3"	322.5"	489.1"	912.3"
			3-D STRESSES AT SECTION (psi)			
A	1000 lbs at nodes 563 through 569		85.43	37.94	34.94	55.23
B	500 lbs at 427&435, 1000 lbs at 428-434		89.88	39.92	36.76	0.00
C	500 lbs at 197&205, 1000 lbs at 198-204		97.64	43.37	0.00	0.00
D	500 lbs at 161&169, 1000 lbs at 162-168		89.85	0.00	0.00	0.00
	DESIRED COMPRESSIVE STRESSES (psi):		1258.22	294.98	213.59	215.52

3-D INPUT LOAD SECTION	LOAD TO BE APPLIED TO MATCH 2-D STRESSES		RESULTING STRESSES AT SECTION (psi)			
A	3902.2		333.37	148.05	136.34	215.52
B	2101.4		188.87	83.89	77.25	0.00
C	1453.8		141.93	63.04	0.00	0.00
D	6811.6		594.05	0.00	0.00	0.00
		SUM:	1258.22	294.98	213.59	215.52

SEISUNFL.WK1

TABLE 3-8

Application of Loads to Match Seismic Stresses
Post-Accident Condition

COMPRESSIVE STRESSES FROM 2-D ANALYSIS	SECTION:	1	2	3	4
	2-D NODE:	32	302	461	1037
	ELEV:	119.3"	322.5"	489.1"	912.3"
		2-D SEISMIC STRESSES AT SECTION (psi)			
0.058" SEISMIC DEFLECTION:		788.67	155.54	103.46	85.31
HORIZ. PLUS VERTICAL SEISMIC INERTIA:		499.79	429.39	512.76	723.14
TOTAL SEISMIC COMPRESSIVE STRESSES:		1288.46	584.93	616.22	808.45

3-D INPUT LOAD SECTION	INPUT 3-D UNIT LOAD DESCRIPTION	SECTION:	1	2	3	4
		3-D NODES:	53-85	170-178	400-408	526-534
		ELEV:	119.3"	322.5"	489.1"	912.3"
			3-D STRESSES AT SECTION (psi)			
A	1000 lbs at nodes 563 through 569		85.43	37.94	34.94	55.23
B	500 lbs at 427&435, 1000 lbs at 428-434		89.88	39.92	36.76	0.00
C	500 lbs at 197&205, 1000 lbs at 198-204		97.64	43.37	0.00	0.00
D	500 lbs at 161&169, 1000 lbs at 162-168		89.85	0.00	0.00	0.00
	DESIRED COMPRESSIVE STRESSES (psi):		1288.46	584.93	616.22	808.45

3-D INPUT LOAD SECTION	LOAD TO BE APPLIED TO MATCH 2-D STRESSES		RESULTING STRESSES AT SECTION (psi)			
A	14637.9		1250.51	555.36	511.45	808.45
B	2850.2		256.17	113.78	104.77	0.00
C	-1841.7		-189.58	-84.21	0.00	0.00
D	-318.8		-28.64	0.00	0.00	0.00
		SUM:	1288.46	584.93	616.22	808.45

SEISFL.WK1

TABLE 3-9

Description of Load Combinations in Terms of Unit Load Case Sum

Load Combination	Load Comb. Case(4)	Constituent Load Cases
Normal Operating Condition(3)	III	- (Case 1)x0.03226 + Case 2 ± Case 4 ± Case 7
Refueling Condition	IV	- (Case 1)x0.03226 + Case 3 ± Case 4 ± Case 7
Accident Condition - 1	V-1	+ Case 1 + Case 2 ± Case 4 ± Case 7 + Case 8
Accident Condition - 2	V-2	+ (Case 1)x0.565 + Case 2 ± Case 4 ± Case 7 + Case 8
Post-Accident Condition	VI	+ Case 2 ± Case 5 + Case 6 ± Case 7

Notes: (1) For load combination definition see Reference 2-3.

(2) For unit load case description see Table 3-1.

(3) Normal Operation also includes live load due to personnel lock.

(4) Load Combination Case Numbers are based on Table 2-44

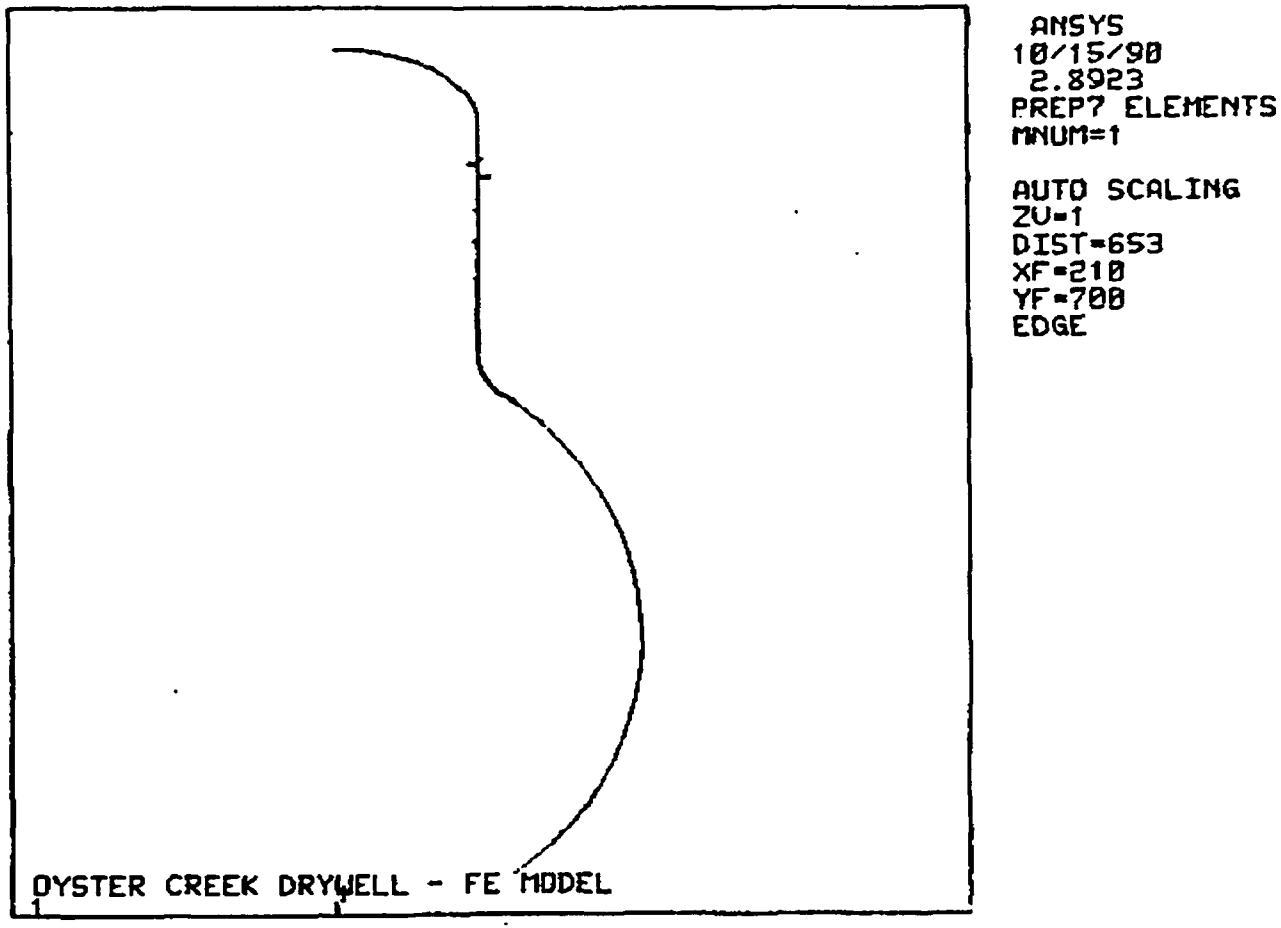

Figure 3-1 Complete Finite Element Model of Drywell

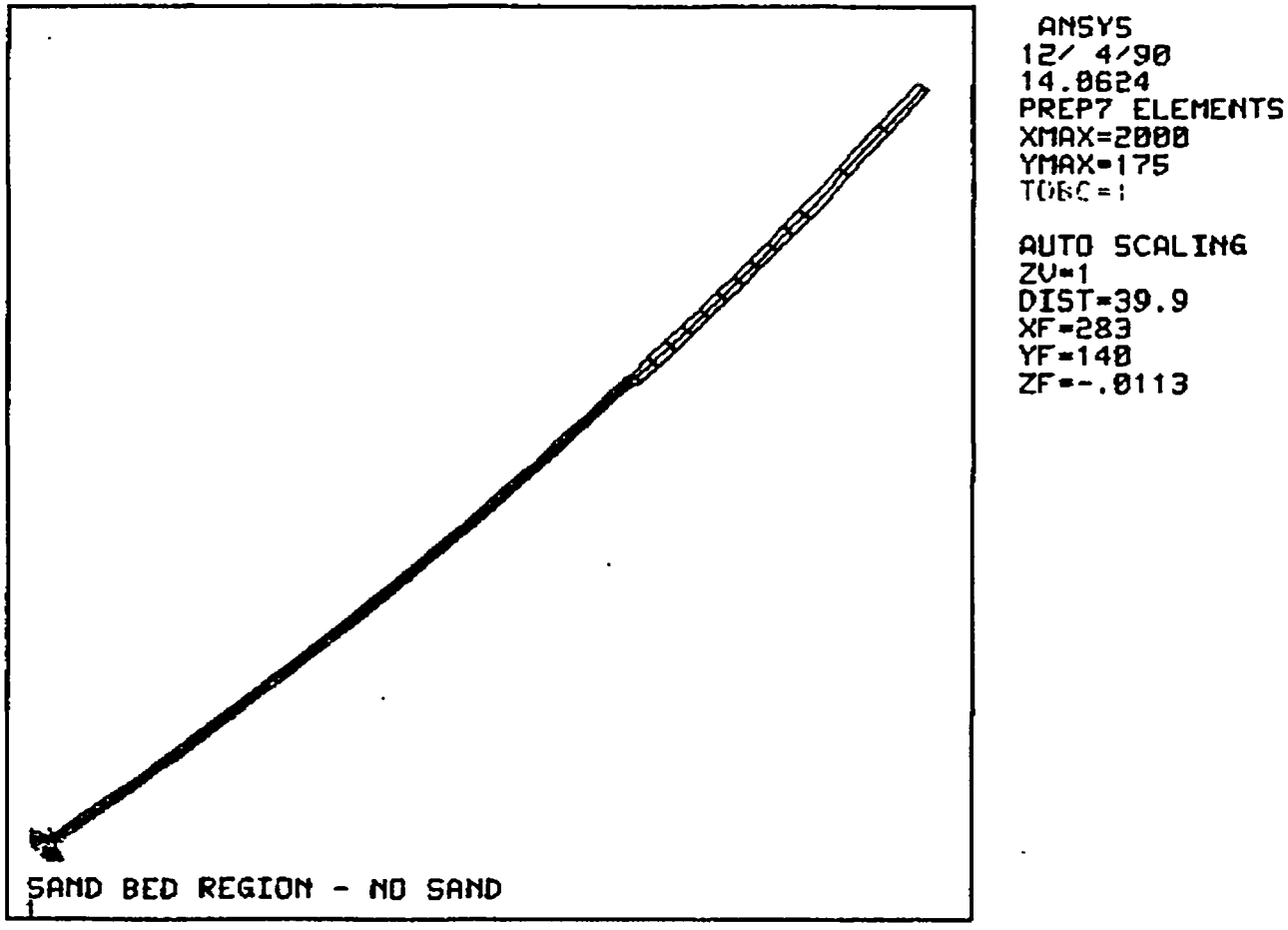

Figure 3-2 Sand Bed Region of Drywell Finite Element Model

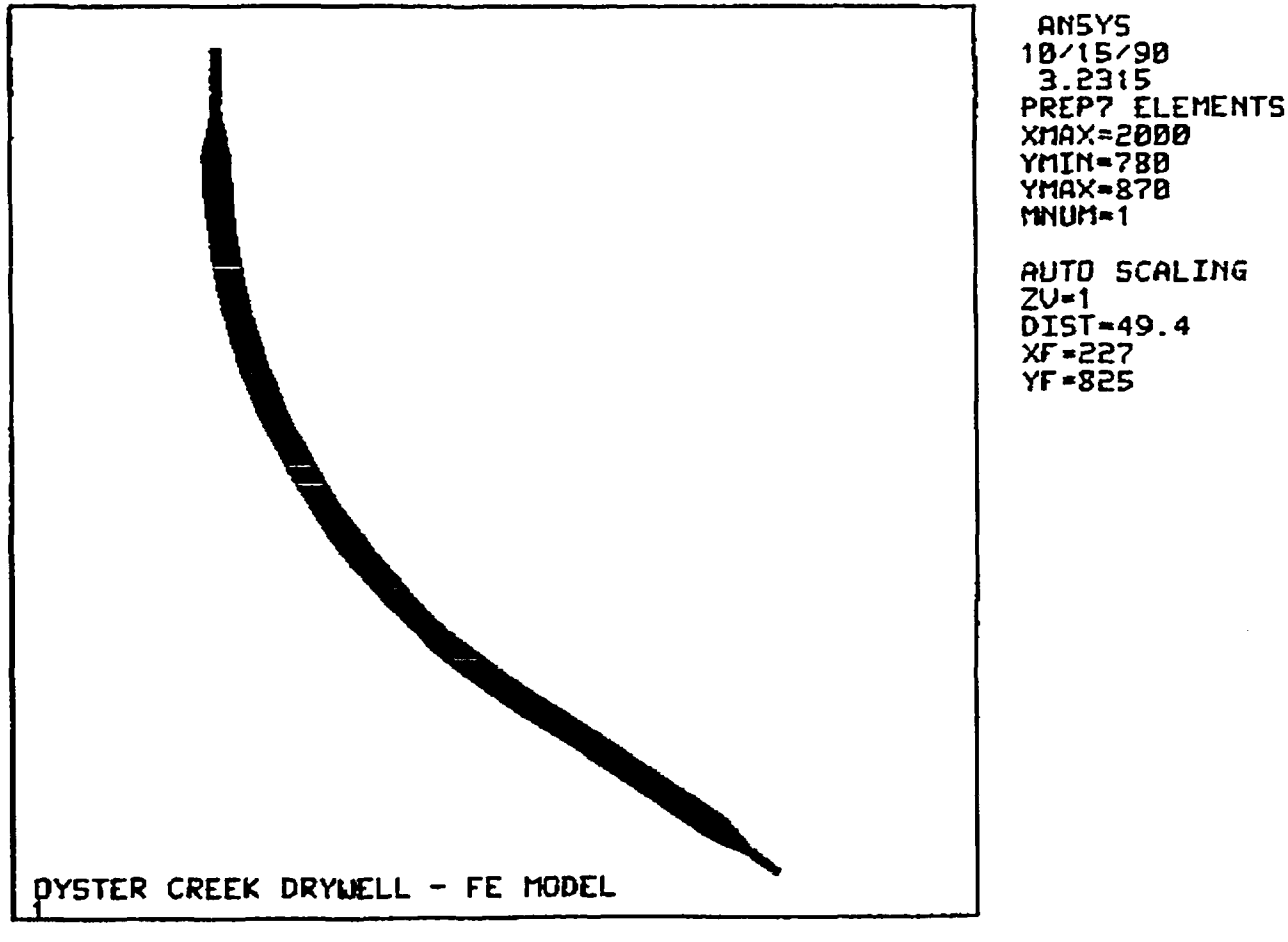

Figure 3-3 Knuckle Region of Drywell Finite Element Model

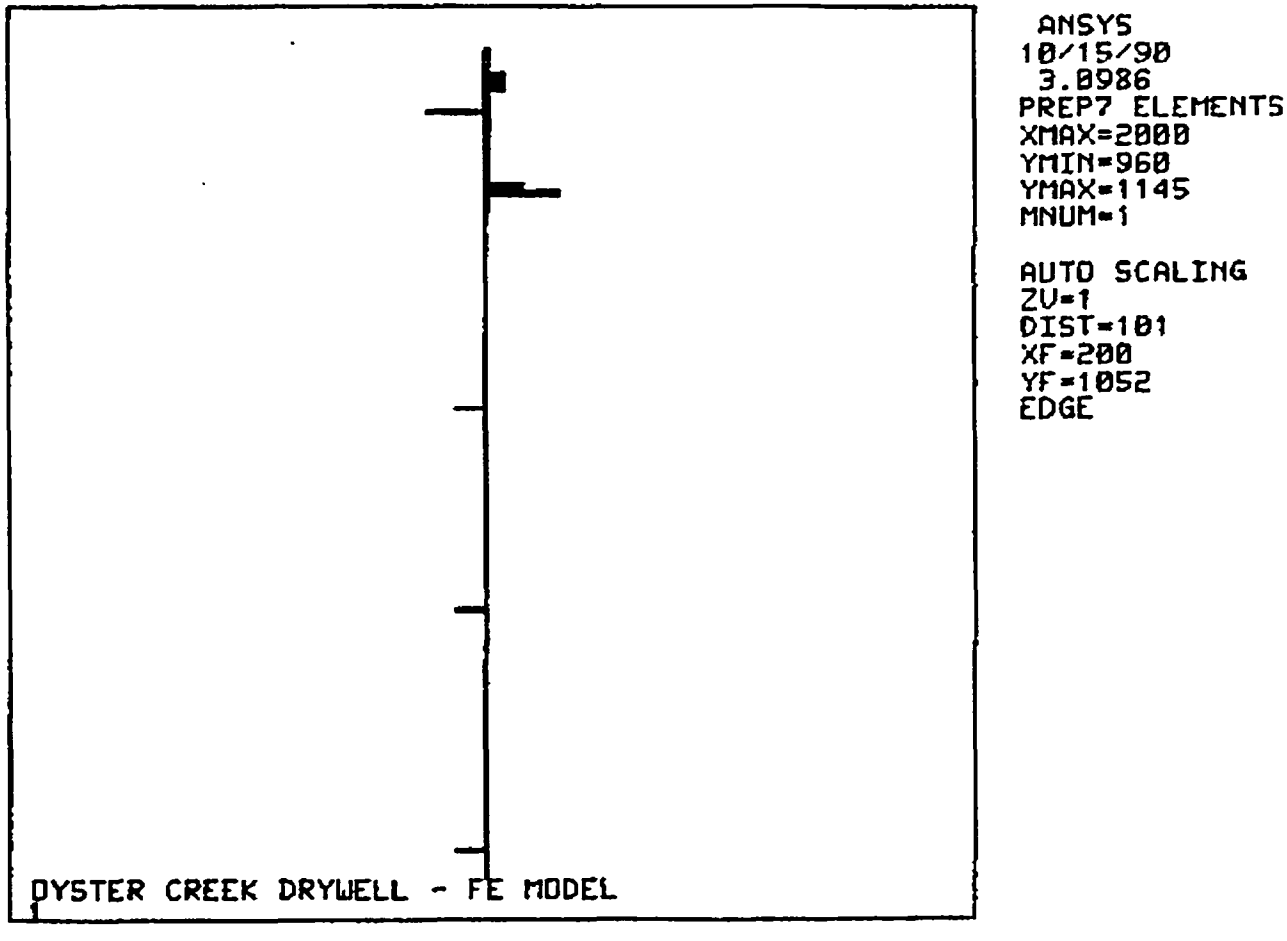

Figure 3-4 Cylindrical Region of Drywell Finite Element Model

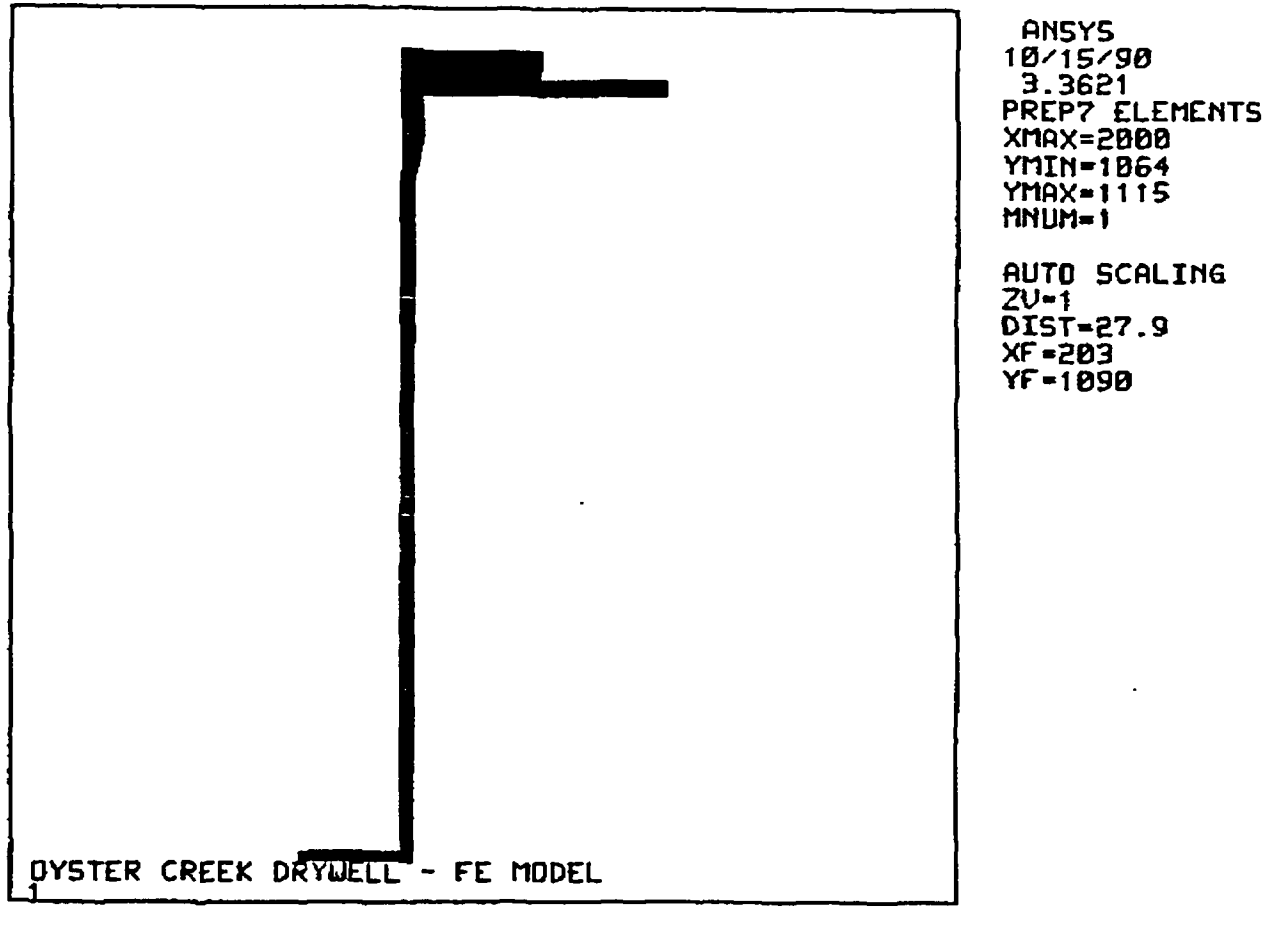

Figure 3-5 Upper Cylindrical Region of Drywell Finite Element Model

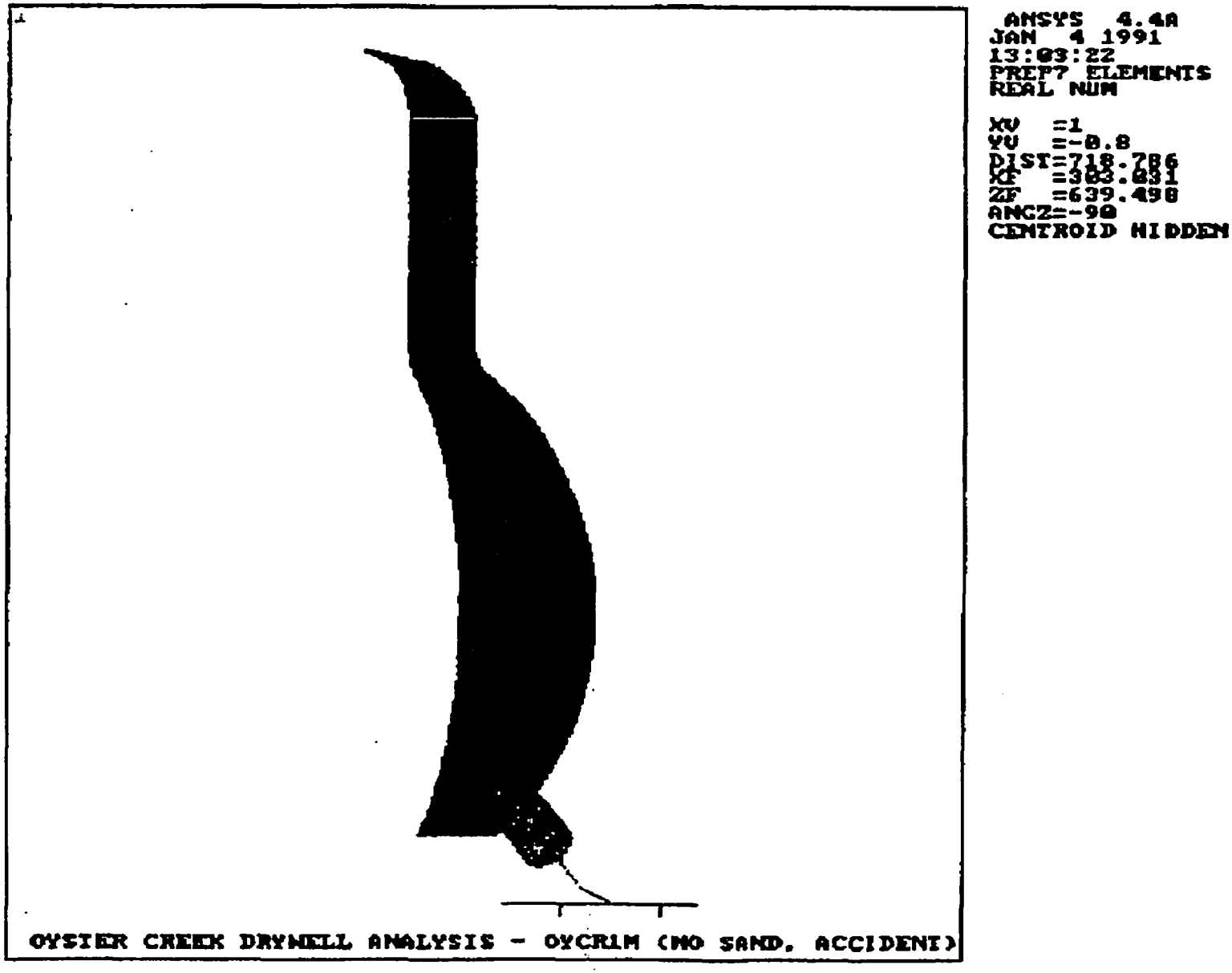

Figure 3-6 Oyster Creek Drywell Pie Slice Finite Element Model

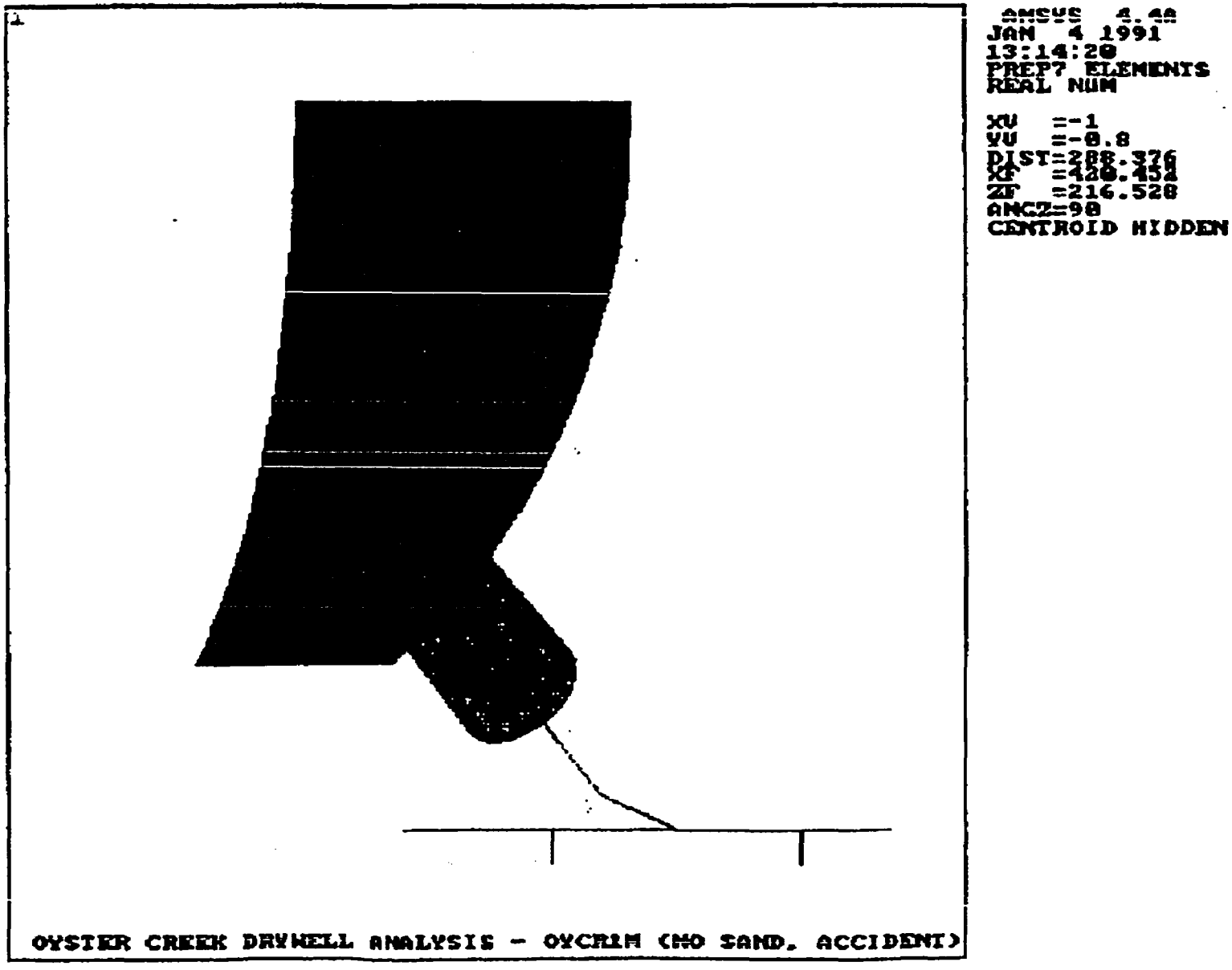

Figure 3-7 Inside Closeup View of Lower Drywell Section

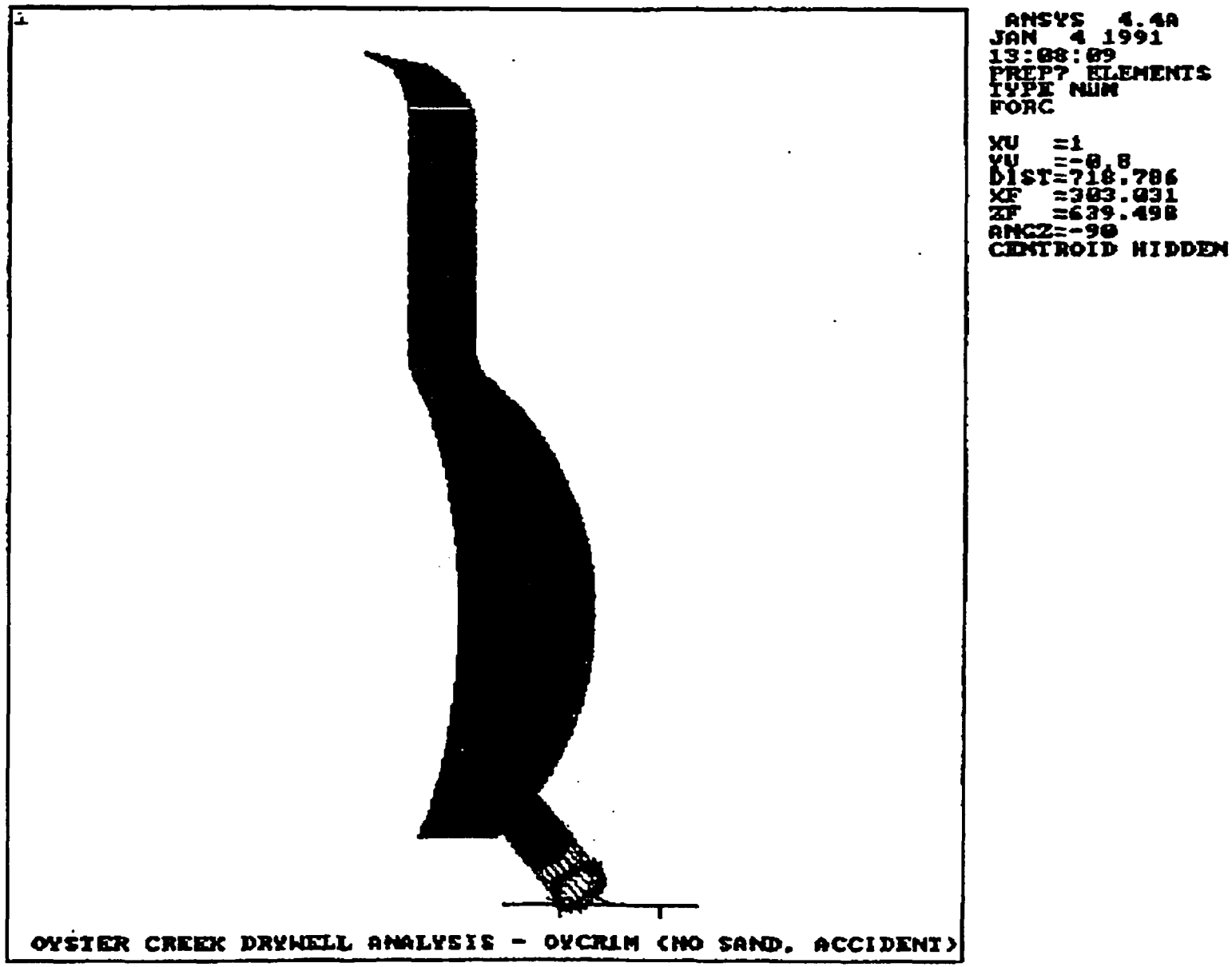

Figure 3-8 Application of Loading to Simulate Seismic Stresses

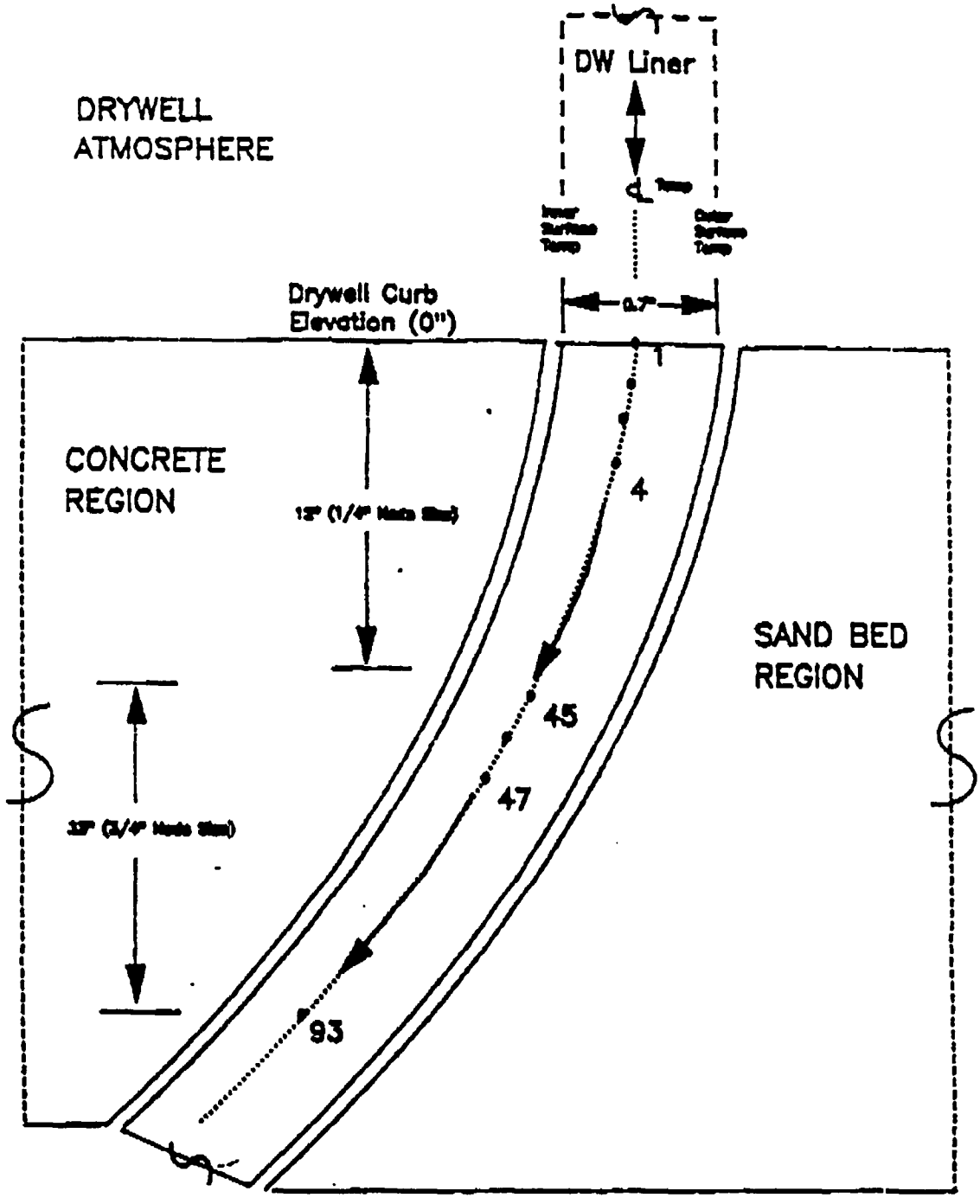

Figure 3-9 Below Curb Drywell Model Nodalization for Temperature Analysis During Accident Condition

TIME (SECONDS)

DIST IN INCH	110	120	150	180	210	240	270	300
	TEMPERATURE IN DEGREES F							
0	247.3	248.6	250.5	251.3	251.8	251.7	251.7	251.7
0.25	228.6	230.7	234.9	237.3	239.1	240.1	240.9	241.5
0.5	210.6	213.4	219.6	223.6	226.6	228.5	230.1	231.3
0.75	193.7	197.1	205	210.3	214.3	217.2	219.6	221.3
1	178	181.9	191	197.5	202.6	206.1	209	211.6
1.25	163.7	167.9	178	185.6	191	195.6	198.9	201.8
1.5	150.9	155.3	165.9	175.9	180.2	185.1	189.2	192.5
1.75	139.7	144	154.9	163.3	170	175.6	179.8	183.6
2	130.1	134.2	144.9	153.5	160.6	166.2	171	175
2.25	121.8	125.7	136	144.5	151.6	157.6	162.6	166.9
2.5	115	118.5	128.2	136.5	143.5	149.6	154.7	159.2
2.75	109.3	112.5	121.6	129.3	136.2	142.2	147.6	152
3	104.7	107.5	115.5	122.9	129.6	135.5	140.7	145.3
3.25	101.1	103.6	110.6	117.6	123.7	129.6	134.5	139
3.5	98.25	100.2	106.6	112.6	118.5	123.9	128.8	133.3
3.75	96.03	97.66	103	108.5	113.9	119	123.7	128
4	94.35	95.66	100.1	105	109.9	114.6	119.1	123.3
4.25	93.1	94.13	97.83	102.1	106.6	110.8	115	118.9
4.5	92.18	92.98	96	99.6	103.5	107.6	111.3	115
4.75	91.51	92.12	94.54	97.59	101	104.5	108.1	111.6
5	91.03	91.69	93.61	95.95	98.89	102	105.3	108.5
5.25	90.69	91.04	92.53	94.63	97.16	99.92	102.8	105.8
5.5	90.46	90.71	91.86	93.56	95.69	98.11	100.7	103.6
5.75	90.3	90.48	91.35	92.72	94.51	96.59	98.88	101.3
6	90.2	90.32	90.98	92.06	93.56	95.32	97.33	99.48
6.25	90.12	90.21	90.7	91.55	92.76	94.27	96.01	97.92
6.5	90.08	90.14	90.49	91.15	92.16	93.41	94.91	96.58
6.75	90.05	90.09	90.34	90.85	91.66	92.7	93.98	95.44
7	90.03	90.06	90.24	90.62	91.25	92.12	93.21	94.48
7.25	90.02	90.04	90.16	90.45	90.95	91.66	92.57	93.66
7.5	90.01	90.02	90.11	90.33	90.71	91.29	92.05	92.98
7.75	90.01	90.01	90.07	90.23	90.53	91	91.63	92.41
8	90	90.01	90.05	90.16	90.39	90.76	91.28	91.95
8.25	90	90	90.03	90.11	90.29	90.58	91	91.56
8.5	90	90	90.02	90.08	90.21	90.44	90.78	91.24
8.75	90	90	90.01	90.06	90.15	90.33	90.61	90.99
9	90	90	90.01	90.04	90.11	90.25	90.47	90.78
9.25	90	90	90.01	90.03	90.08	90.18	90.36	90.61
9.5	90	90	90	90.02	90.06	90.14	90.27	90.48
9.75	90	90	90	90.01	90.04	90.1	90.21	90.37
10	90	90	90	90.01	90.03	90.07	90.15	90.29
10.25	90	90	90	90	90.02	90.05	90.12	90.22
10.5	90	90	90	90	90.01	90.04	90.09	90.17
10.75	90	90	90	90	90.01	90.03	90.06	90.13
11	90	90	90	90	90.01	90.02	90.05	90.1
11.25	90	90	90	90	90	90.01	90.03	90.07
11.5	90	90	90	90	90	90.01	90.02	90.05
11.75	90	90	90	90	90	90.01	90.02	90.04
12	90	90	90	90	90	90	90.01	90.03
12.75	90	90	90	90	90	90	90	90.01
13.5	90	90	90	90	90	90	90	90
14.25	90	90	90	90	90	90	90	90
15	90	90	90	90	90	90	90	90
15.75	90	90	90	90	90	90	90	90
16.5	90	90	90	90	90	90	90	90
17.25	90	90	90	90	90	90	90	90
18	90	90	90	90	90	90	90	90
18.75	90	90	90	90	90	90	90	90
19.5	90	90	90	90	90	90	90	90
20.25	90	90	90	90	90	90	90	90
21	90	90	90	90	90	90	90	90
21.75	90	90	90	90	90	90	90	90
22.5	90	90	90	90	90	90	90	90
23.25	90	90	90	90	90	90	90	90
24	90	90	90	90	90	90	90	90
24.75	90	90	90	90	90	90	90	90
25.5	90	90	90	90	90	90	90	90
26.25	90	90	90	90	90	90	90	90
27	90	90	90	90	90	90	90	90
27.75	90	90	90	90	90	90	90	90
28.5	90	90	90	90	90	90	90	90
29.25	90	90	90	90	90	90	90	90
30	90	90	90	90	90	90	90	90
30.75	90	90	90	90	90	90	90	90

Figure 3-10 Example of Calculated Temperature Distribution at Various Elapsed Times

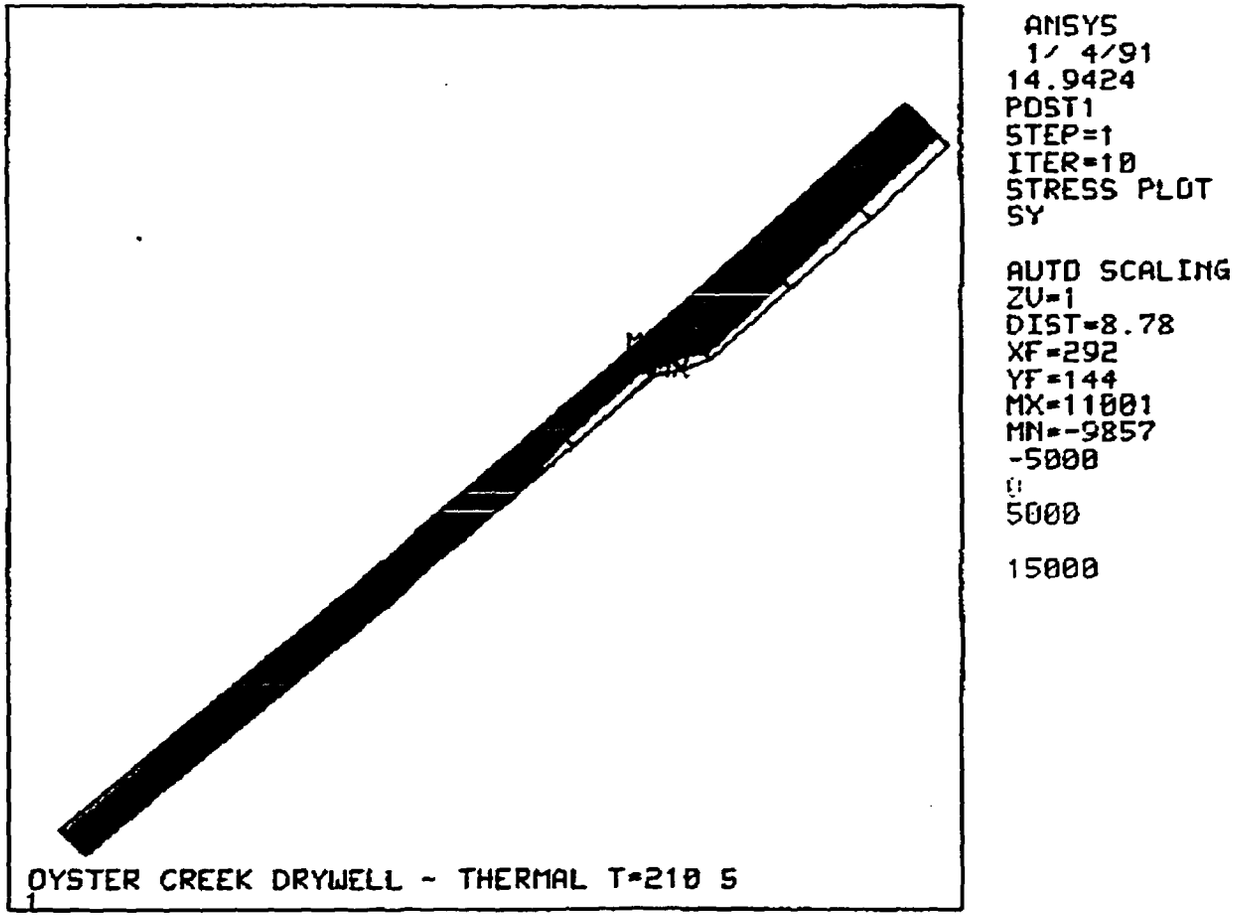

Figure 3-11 Meridional Stress Distribution in the Sand Bed Region From Temperature Distribution at t=210 Seconds

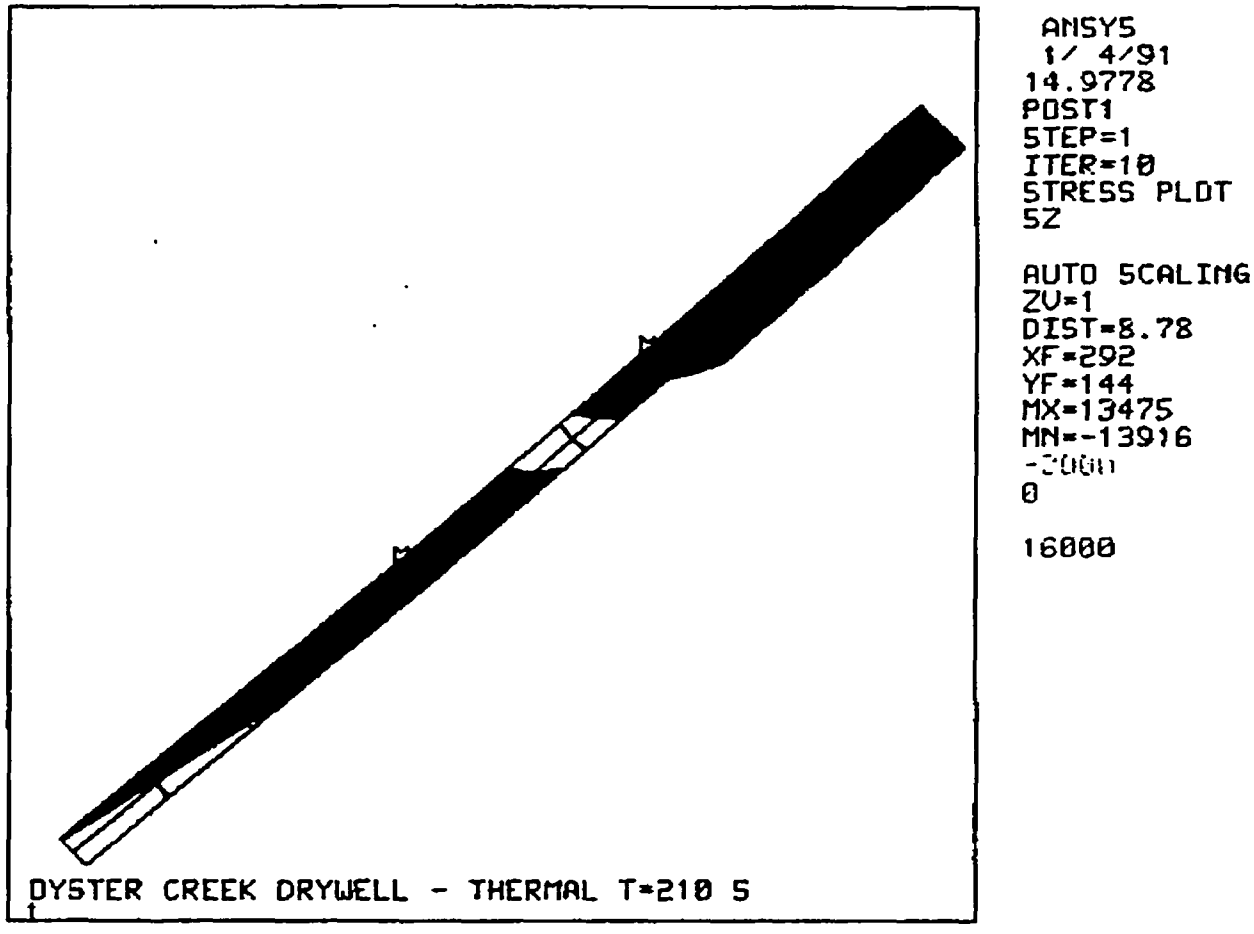

Figure 3-12 Circumferential Stress Distribution in the Sand Bed Region From Temperature Distribution at t=210 Seconds

4. SEISMIC LOAD DEFINITION

This section briefly describes the general methodology followed in the seismic evaluation of the drywell. A detailed report on the seismic analysis methodology and the results is included in Reference 4-1.

4.1 Finite Element Model

The axisymmetric finite element model was used in the seismic analysis. All of the concentrated loads listed in Tables 2-5a and 2-5b were included in both the flooded and unflooded seismic analyses. Since the lower and upper beams connect to the drywell through pads, the beam weights do not act during the horizontal earthquake excitation. Therefore, the beam weights are active only in the vertical direction. In addition, the live loads listed in Table 2-5c were included in the unflooded seismic analysis.

The drywell is constrained at the "reactor building/drywell/star truss" interface at elevation 82'-6" and at its base. The upper constraint was implemented in the finite element analysis by restraining the middle node in the horizontal direction at this elevation. The base constraint is as before, i.e., all nodes fixed.

4.2 Dynamic Analysis Methodology and Response Spectra

The seismic input motion spectra were provided by GPUN in Reference 1-4. The seismic motion spectra were for two locations: at the mat foundation and at the upper constraint. Since the ANSYS program can only accept one input spectrum, the input spectra at the two elevations were enveloped.

The response spectrum dynamic analyses were first conducted for frequencies up to the ZPA frequencies of the input motion spectra. The response contributions due to the truncated higher frequency modes

were calculated by static analyses in which the total model mass is subjected to support accelerations. These were taken as ZPA accelerations for each of the orthogonal spatial directions. All colinear modal response contributions were combined by the Double Sum Method and the spatial contributions by the SRSS method. The response contributions due to the truncated higher frequency modes were combined with the response totals due to the lower frequency modes included in the analysis by the SRSS method. The resulting total colinear inertia responses were combined with the corresponding responses due to relative support motion by the absolute sum method. These stresses were then combined with the stresses from other loads (e.g., pressure, thermal, etc.) for the Code evaluation.

4.3 Post-Accident Seismic Analysis

In the post-accident condition, the drywell is flooded to elevation 74'-6". The weight of the water was lumped at several elevations along the meridian of the drywell. Based on previous experience, the fluid-structure interaction effects were assumed as negligible and the hydrodynamic mass of water was assumed as 80% of the total mass of water which would fill an empty drywell. This exclusion of 20% mass reasonably accounts for the volume of RPV, shield wall and pedestal.

4.4 Analysis for Relative Support Displacement Effects

The drywell is fixed at its base and is laterally constrained by the reactor building at elevation 82'-6". During seismic excitation, the reactor building would experience relative displacement between the drywell constraint elevation and the basemat. Since the reactor building is much stiffer and much more massive than the drywell, it will take the drywell for a 'ride' during relative support displacement. Therefore, the stresses in the drywell due to relative support displacement were determined and added to those from the seismic inertia loads.

The horizontal relative displacement of the drywell upper support with respect to the drywell at the basemat was specified as 0.058 inch for 2xDBE condition [1-4]. The stresses from this relative displacement were obtained by applying a horizontal displacement of 0.058 inch at the upper support elevation.

4.5 References

4-1 "Seismic Analysis Details," Appendix B of letter dated December 21, 1990 from H.S. Mehta of GE to S.C. Tumminelli of GPUN.

5. CODE STRESS EVALUATION

Sections 3 and 4 describe the analyses for shell stresses for the various unit load cases and the limiting load combinations V and VI. The stress analysis for the 'with sand case' in Reference 1-2a has shown that the accident condition, load combination V-1, and the post-accident condition, load combination VI, represent the limiting load combinations for the Code stress evaluation. This was also determined to be the case for the 'without sand' configuration considered in this report. The removal of sand from the sandbed region affects the stresses only in the sandbed and the adjacent lower spherical region. Therefore, the Code stress evaluation of these regions is described separately from the other regions of the drywell.

5.1 Code Stress Evaluation of Regions Above the Lower Sphere

Figure 5-1 shows a plot of the accident condition membrane circumferential stresses for the 'with' and 'without' sand cases as a function of meridional distance. Stresses in both the sandbed and the other drywell regions are included in Figure 5-1. It is seen that in the other regions the stress magnitudes for the two cases are essentially identical.

From the preceding it is clear that the stresses in the other regions (i.e., other than the sandbed and the adjacent lower spherical region) are unaffected by removing the sand. Nevertheless, for completeness, the calculated stress magnitudes for these regions from Reference 1-2a are repeated in Tables 5-1a and 5-1b.

The stress magnitudes shown in Tables 5-1a and 5-1b are computed using elastic small displacement analysis. As discussed in Subsection 5.2, the stresses in the sandbed and lower sphere regions were also evaluated using elastic large displacement analysis. A comparison of the component stresses from the small and large displacement solutions for the drywell regions above the lower sphere showed insignificant differences.

In order to evaluate the impact on the penetration analyses, a comparison of the radial and meridional displacements at the equator plane of the sphere (elevation 37'-3") for the with and without sand cases was performed. The comparison showed that the radial displacements in the two cases were essentially identical but the meridional or vertical displacements differed by ≈ 0.042 inch for load combination V-1. This difference was judged to be small compared to the calculated vertical thermal displacement of ≈ 0.5 inch for the accident condition load combination V-2.

5.2 Elastic Stress Analysis of Sandbed and Lower Sphere

5.2.1 Small Displacement Solution Results

The maximum stresses are along the meridional boundary of the model (i.e., the plane of symmetry between the vents), so the stresses along this boundary will be considered first. Figure 5-2 shows the plot of meridional membrane stress magnitudes for the accident condition V-1 as a function of meridional distance from the bottom of the sandbed. A comparison of the membrane stress magnitudes in Figures 5-1 'without sand' case and Figure 5-2 shows that the circumferential stress is higher than the meridional stress in both the sandbed region and the lower spherical region. This is expected since the absence of sand springs allows more radial displacement of the drywell shell under dead weight and internal pressure. Figure 5-3 shows a plot of the membrane circumferential stress distribution. The maximum value of the circumferential membrane stress is ≈ 23.0 ksi. Further, this stress exceeds 1.1 S_{mc} (21.2 ksi) for a meridional distance of ≈ 26 inches (see Figure 5-1).

The Code (NE-3213.10) states that cases arise in which a membrane stress produced by pressure or other mechanical loading and associated with a primary or discontinuity effect produces excessive distortion in the transfer of load to other portions of the structure. Such a membrane stress is conservatively classified by the Code as local primary membrane stress. The Code limits the magnitude of this stress to 1.5 S_{mc} (29.0 ksi). A stressed region may be considered local if

the distance over which the membrane stress intensity exceeds 1.1 S_{mc} does not extend in the meridional direction more than 1.0/(Rt). With R=420 in. and t=0.736 inch in the sandbed region, 1.0/(Rt) is equal to 17.6 inches. Thus, the maximum value of the circumferential membrane stress (23.0 ksi) meets the Code stress limit (29.0 ksi) but its meridional extent over 1.1 S_{mc} is greater than 1.0/(Rt).

The meridional extent of 26 in. occurs only at the plane of symmetry between the vent lines. The extent is less at other meridional planes. Figure 5-4 shows the meridional extent of circumferential membrane stress above 1.1 S_{mc} at four meridional planes. Using a weighted average over the circumference of the model, the meridional extent was calculated as 14 inches. This average value is less than 1.0/(Rt) and, thus, meets the meridional extent criterion given in NE-3213.10.

The objective of the Code in limiting the meridional extent and magnitude of the local primary membrane stress is to preclude excessive distortion in the transfer of load to other portions of the structure, since such distortion could invalidate the elastic analysis. The small displacement results showed that the maximum radial displacement in the sandbed region was 0.28 inch for the accident condition V-1. This is less than half the modeled thickness of the drywell in that region and, therefore, is judged not to be excessive.

The small displacement analysis conducted previously is conservative because the stiffening effect of the tensile in-plane stresses is not considered. This effect would tend to reduce the local radial deflection (thus, also the local circumferential stress) of the drywell shell in the sandbed region. For example, consider the case of a beam subjected to both transverse and tensile axial loads as shown in Figure 5-5. A small displacement analysis of this configuration considers the bending moments based on the transverse load only. The bending stresses and deflections of the beam are overpredicted based on these bending moments. In a real structure, tensile axial loads in combination with the deflections of the beam

produced by transverse loads creates an opposing bending moment. As a result the overall bending moment is reduced, leading to smaller bending deflections and stresses. This stiffening effect can be included only by conducting a large displacement analysis.

5.2.2 Large Displacement Solution Results

Based on the preceding discussion, a large displacement analysis was conducted using the same pie slice model and the accident condition V-1 loads. A large displacement analysis can be conducted using the ANSYS code by activating the KAY(6) key. When this option is chosen, the ANSYS program first calculates displacements of the structure based on a small displacement analysis. The geometry of the structure is then updated based on the calculated displacements. The loads are again applied to the structure and the displacements are recalculated. The geometry of the structure is continually updated and the displacements are recalculated until the maximum displacement change between successive iterations is reduced below the selected convergence criteria. A convergence criteria of 0.01 inch was chosen for this analysis. In this manner, the ANSYS code accurately accounts for the stiffening of the structure due to in-plane tensile stresses.

Figure 5-6 shows the distribution of membrane circumferential stress. Figure 5-7 shows a plot of membrane circumferential stress as a function of meridional distance when the large displacement option in ANSYS was used. For comparison, the stress results from the small displacement solution (Figure 5-1) are also shown in Figure 5-7. It is seen that the maximum value from the large displacement solution is ≈ 21.5 ksi (compared to ≈ 23 ksi in the small displacement analysis), and it exceeds 1.1 S_{mc} (21.2 ksi) over a maximum distance of only 11 inches at the meridional plane between the vent lines. This is clearly less than the 1.0 $\sqrt{(Rt)}$ distance of 17.6 in.

Figure 5-8 shows the circumferential membrane stress magnitudes at four different meridional planes based on large displacement solution. Using a weighted average over the circumference of the model, the meridional extent was calculated as ≈ 2 in.

5.3 Code Evaluation of the Sandbed and Lower Sphere

5.3.1 Primary Stress Evaluation

Tables 5-2a and 5-2b show the maximum values of primary stresses for the accident condition load combination V-1, and the Code allowable values for the small and large displacement solutions, respectively. In the primary membrane stress category, the calculated stress intensities for the sandbed region are based on the average values. The peak value of the circumferential membrane stress in the sandbed region was compared with the local primary membrane stress limits.

As expected, a comparison of Tables 5-2a and 5-2b shows that the calculated stress magnitudes using the large displacement option are in general slightly lower than those obtained using the small displacement option. The differences in the stresses are larger in the sandbed region where the radial displacements are larger. The calculated primary stress magnitudes in the sandbed region and lower sphere meet the Code stress limits.

5.3.2 Extent of Local Primary Membrane Stress

Paragraph NE-3213.10 of the Code states that a stresses region may be considered local if the distance over which the membrane stress intensity exceeds 1.1 S_{mc} does not extend in the meridional direction more than 1.0/(Rt), which is ≈ 17.6 inches. When the small displacement solution is used (5.2.1), the membrane circumferential stress magnitude in the sandbed region exceeds 1.1 S_{mc} over a meridional distance of ≈ 26 inches at the plane of symmetry between the vent lines. However, this distance was found to be 14 inches using a weighted average considering other meridionals.

Furthermore, this distance of 26 inches at the plane of symmetry between the vent lines was reduced to ≈ 11 inches when the large displacement solution was used in which the stiffness matrix is updated based on the deformed shape. Therefore, it is concluded that

the circumferential stress in the sandbed region meets the meridional extent criterion of the Code Paragraph NE-3213.10.

5.3.3 Primary Plus Secondary Stress Evaluation

Only two load cases result in significant secondary stresses in the shell. The first is the temperature gradient (accident condition V-1) which produces secondary stresses in the sandbed and lower sphere. The second is the post-accident condition which produces discontinuity bending moments in the shell at the bottom of the sandbed. The post-accident load combination case VI controls. Tables 5-3a and 5-3b show the calculated values of primary plus secondary stresses and a comparison with the allowable values for small and large displacement solutions, respectively. All of the calculated primary plus secondary stress values are within the Code allowable values.

TABLE 5-1a

Comparison of Calculated Stresses to Code Allowable Values
(Nominal Drywell Wall Thicknesses Above Lower Sphere)
Limiting Load Combination - V-1

Drywell Region	Stress Categ.	Calc. Stress Magnitude, Max. (psi)	Allowable Stress (psi)
Cylinder (t=0.640 in.)	Prim. Memb.	19200	19300
	Prim. Memb. + Bending	20280	29000
Knuckle (t=2.625 in.)	Prim. Memb.	18430	19300
	Prim. Memb. + Bending	20620	29000
Upper Sphere (t=0.722 in.)	Prim. Memb.	19090	19300
	Prim. Memb. + Bending	26350	29000
Middle Sphere (t=0.770 in.)	Prim. Memb.	18460	19300
	Prim. Memb. + Bending	23110	29000

TABLE 5-1b

Comparison of Calculated Stresses to Code Allowable Values
(95% Projected Drywell Wall Thicknesses Above Lower Sphere)
Limiting Load Combination - V-1

Drywell Region	Stress Categ.	Calc. Stress Magnitude, Max. (psi)	Allowable Stress (psi)
Cylinder (t=0.619 in.)	Prim. Memb.	19850	21200
	Prim. Memb. + Bending	20970	29000
Upper Sphere (t=0.677 in.)	Prim. Memb.	20360	21200
	Prim. Memb. + Bending	28100	29000
Middle Sphere (t=0.723 in.)	Prim. Memb.	19660	21200
	Prim. Memb. + Bending	24610	29000

TABLE 5-2a

Comparison of Calculated Primary Stresses to Code Allowable Values
(Small Displacement; Lower Sphere and Sandbed)
Limiting Load Combination - V-1

Drywell Region	Stress Categ.	Calc. Stress Magnitude, Max. (psi)	Allowable Stress (psi)
Lower Sphere (t=1.154 in.)	Prim. Memb.	13800	21200
	Local Prim. Memb.	17690	29000
	Prim. Memb. + Bending	17800	29000
Sandbed (t=0.736 in.)	Prim. Memb.	17430	21200
	Local Prim. Memb.	22970	29000
	Prim. Memb. + Bending	24950	29000

TABLE 5-2b

Comparison of Calculated Primary Stresses to Code Allowable Values
(Large Displacement; Lower Sphere and Sandbed)
Limiting Load Combination - V-1

Drywell Region	Stress Categ.	Calc. Stress Magnitude, Max. (psi)	Allowable Stress (psi)
Lower Sphere (t=1.154 in.)	Prim. Memb.	13940	21200
	Local Prim. Memb.	17530	29000
	Prim. Memb. + Bending	17640	29000
Sandbed (t=0.736 in.)	Prim. Memb.	16540	21200
	Local Prim. Memb.	21540	29000
	Prim. Memb. + Bending	23130	29000

TABLE 5-3a

Comparison of Calculated Primary Plus Secondary Stresses
to Code Allowable Values
(Small Displacement -Lower Sphere and Sandbed)

Drywell Region	Stress Categ.	Calc. Stress Magnitude, Max. (psi)	Allowable Stress (psi)
Lower Sphere (t=1.154 in.)	Prim. + Sec. (Acc. Load Cond. V-1)	29020	52500
	Prim. + Sec. (Post-Acc. Load Cond. VI)	30280	70000
Sandbed Region (t=0.736 in.)	Prim. + Sec. (Acc. Load Cond. V-1)	38420	52500
	Prim. + Sec. (Post-Acc. Load Cond. VI)	67020	70000

TABLE 5-3b

Comparison of Calculated Primary Plus Secondary Stresses
to Code Allowable Values
(Large Displacement -Lower Sphere and Sandbed)

Drywell Region	Stress Categ.	Calc. Stress Magnitude, Max. (psi)	Allowable Stress (psi)
Lower Sphere (t=1.154 in.)	Prim. + Sec. (Acc. Load Cond. V-1)	28860	52500
	Prim. + Sec. (Post-Acc. Load Cond. VI)	30280	70000
Sandbed Region (t=0.736 in.)	Prim. + Sec. (Acc. Load Cond. V-1)	36600	52500
	Prim. + Sec. (Post-Acc. Load Cond. VI)	67020	70000

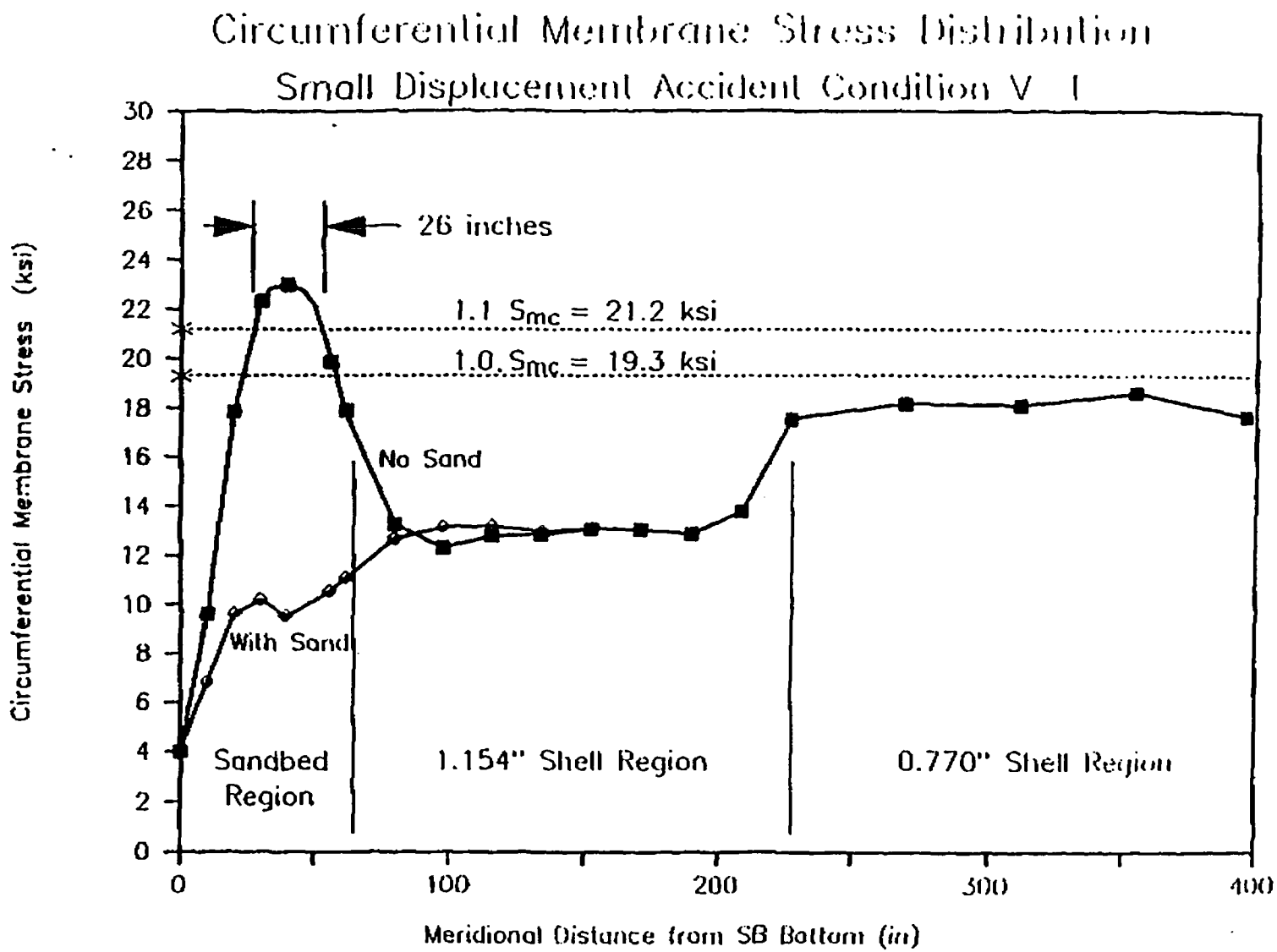

ACCDNT4A.DRW

Figure 5-1 Circumferential Stresses for Accident Condition V-1 in 'With Sand' and 'Without Sand' Cases - Small Displacement

QRF # 00664
INDEX NO. 9-3, REV. 0

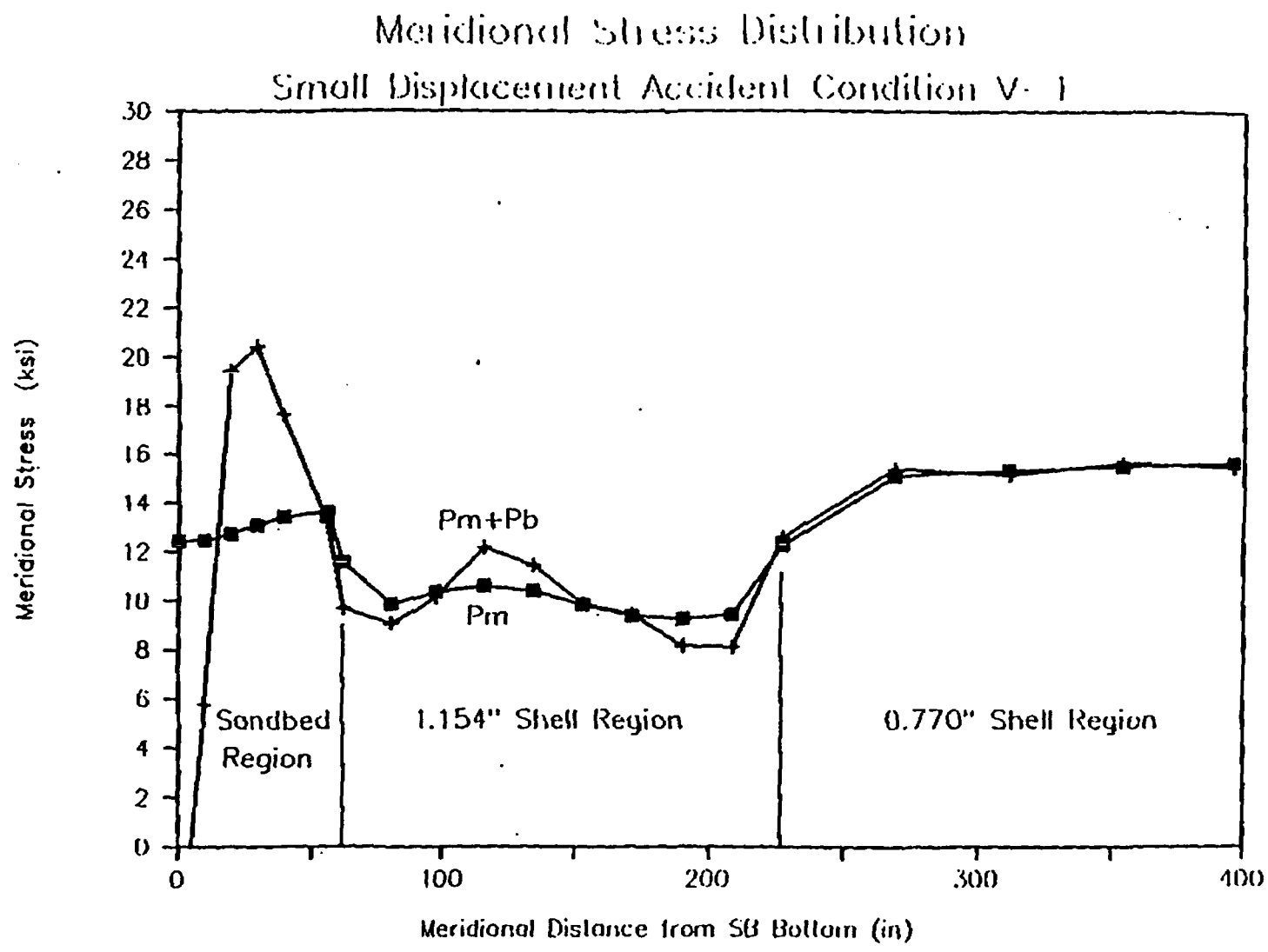

OYCR1M2.DRW

Figure 5-2 Plot of Accident Condition V-1 Meridional Stresses for 'Without Sand' Case - Small Displacement

DRF # 00564
INDEX NO. 9-3, REV. 0

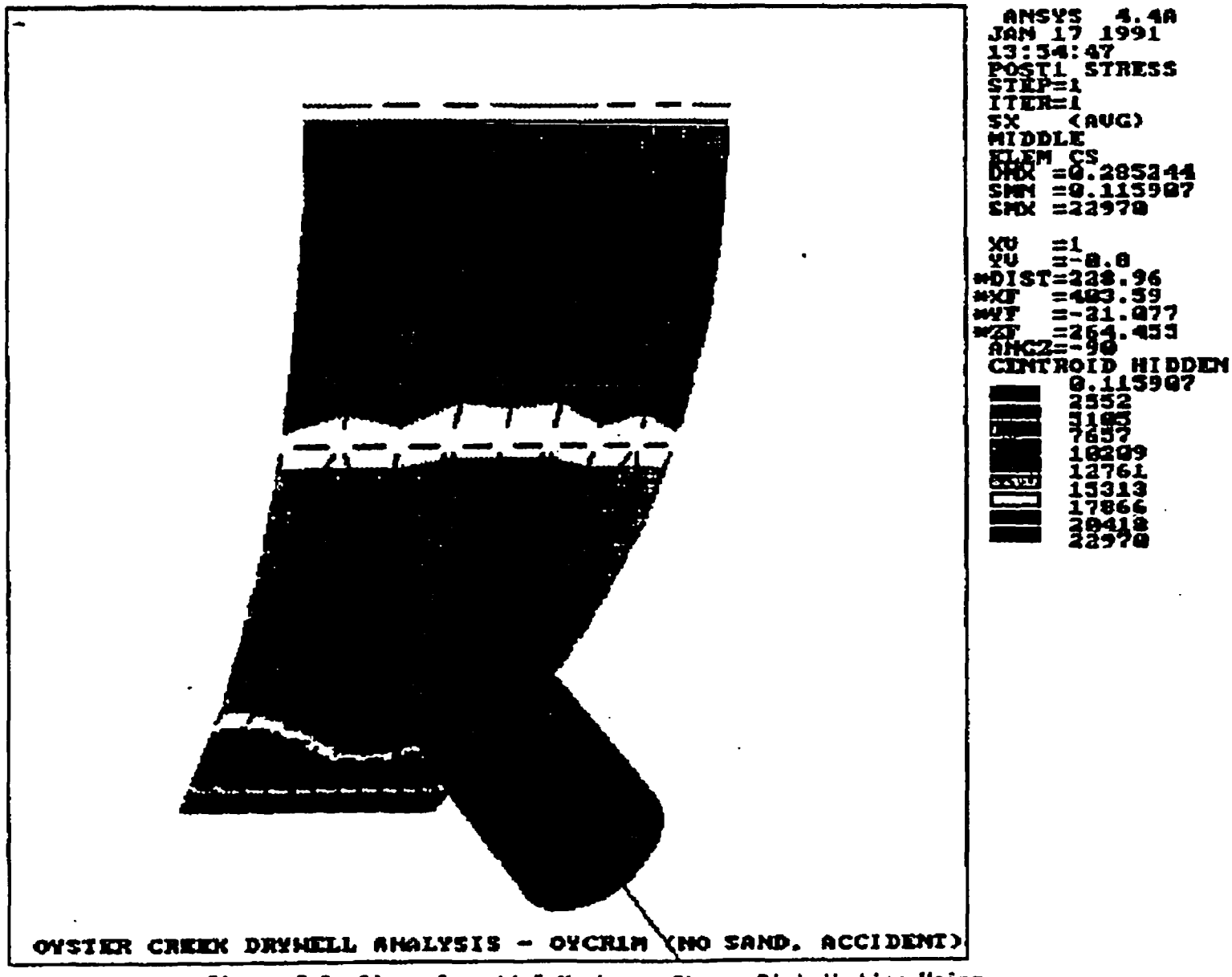

Figure 5-3 Circumferential Membrane Stress Distribution Using Small Displacement Option.

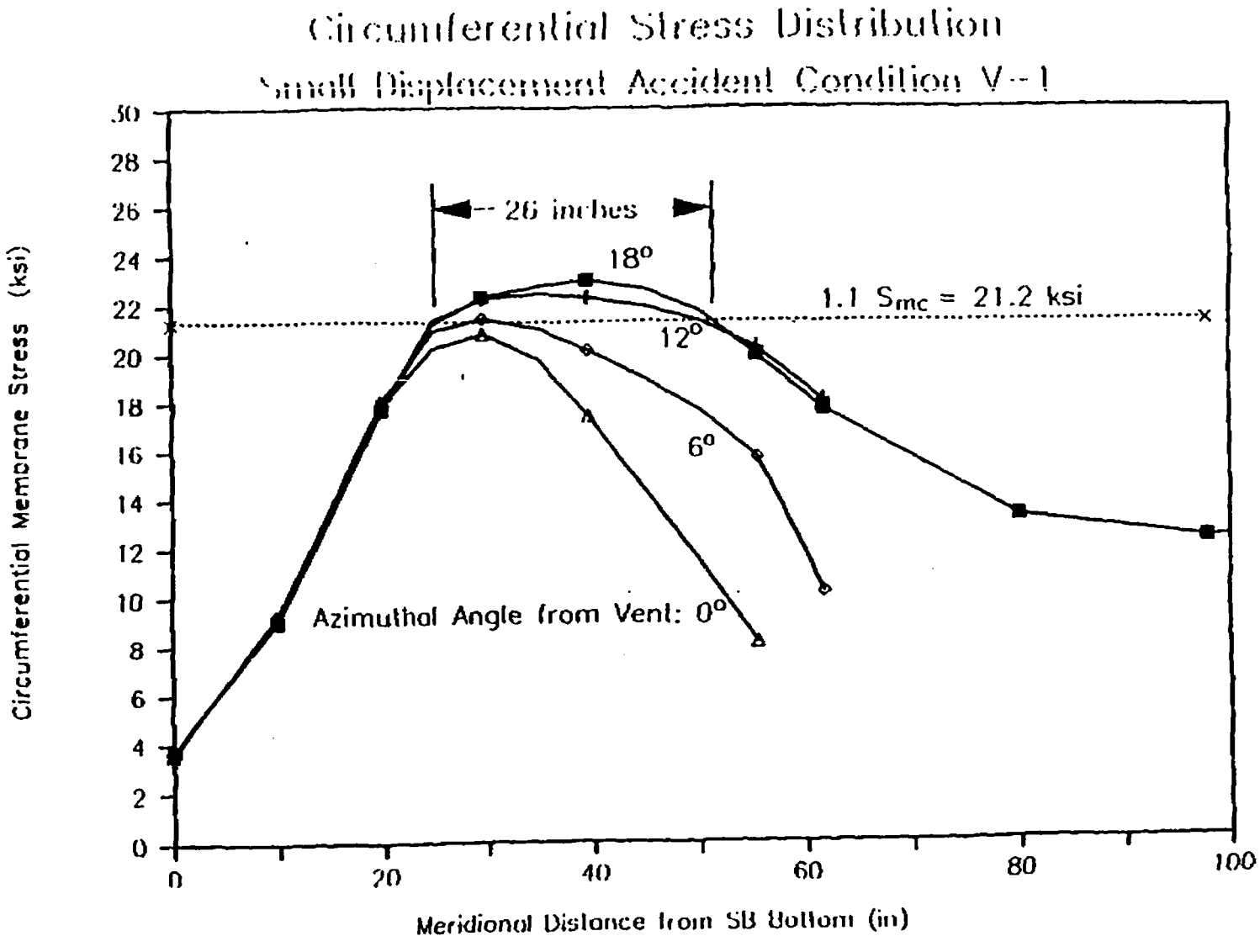

ACCDN15A.DRW

Figure 5-4 Circumferential Membrane Stress Magnitudes at Four Meridional Planes in Sandbed Region - Small Displacement

DRF # 00664
INDEX NO. 9-3, REV. 0

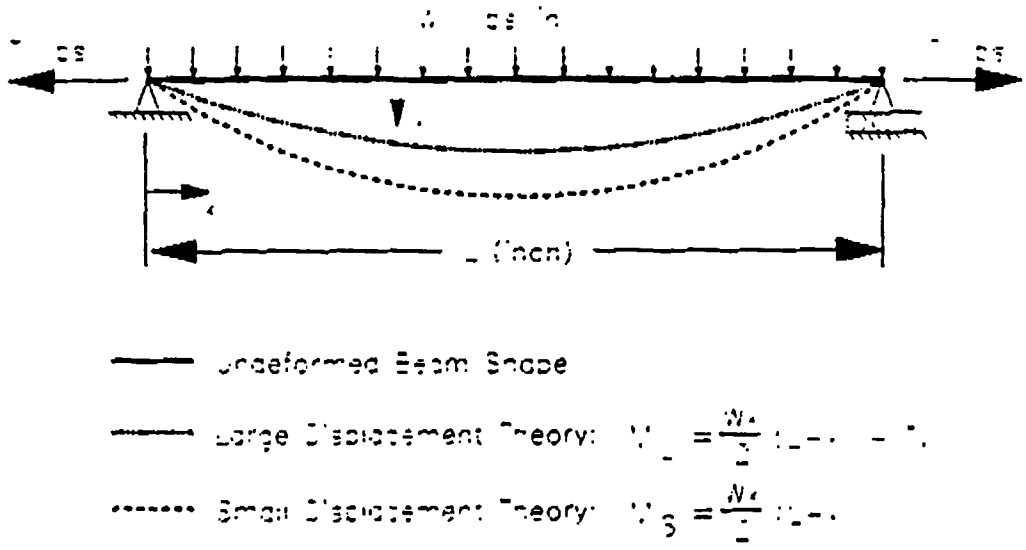

Figure 5-5 Beam With Transverse Plus Axial Loading

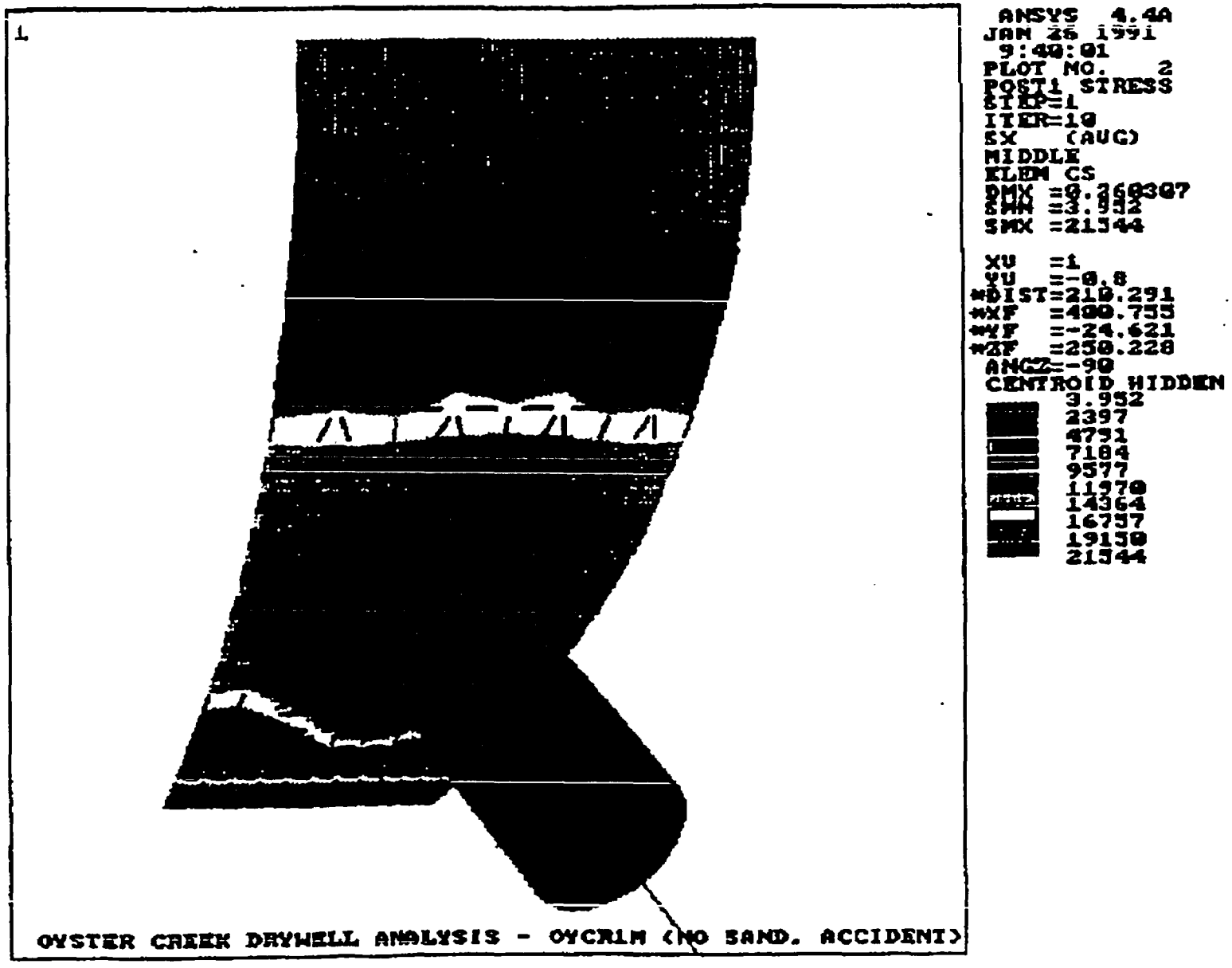

Figure 5-6 Circumferential Membrane Stress Distribution Using Large Displacement Option.

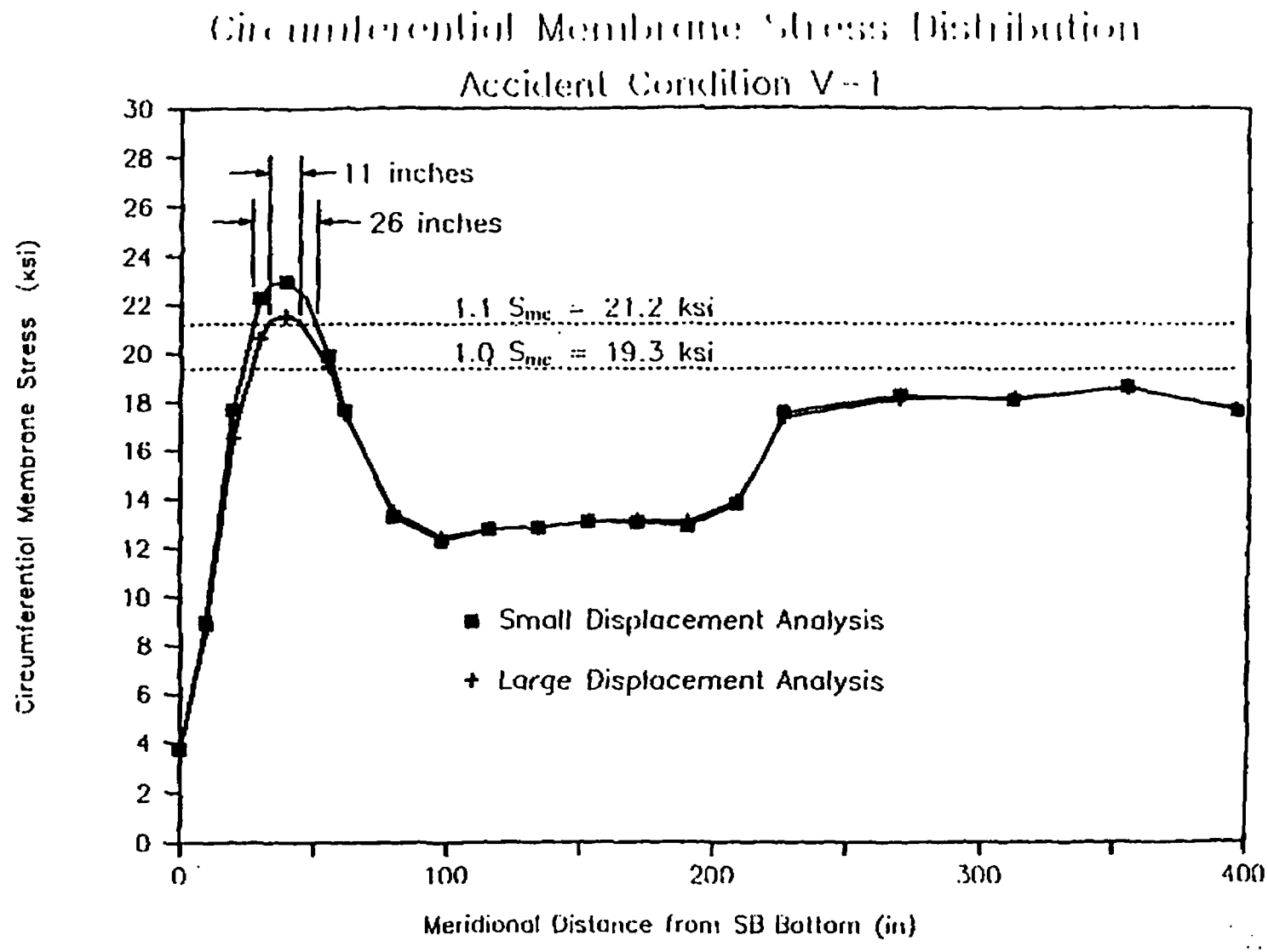

ACCDNT7A.DRW

Figure 5-7 Comparison of Circumferential Membrane Stress Magnitudes With Large and Small Displacement Options

ORF # 00664
INDEX NO. 9-3, REV. 0

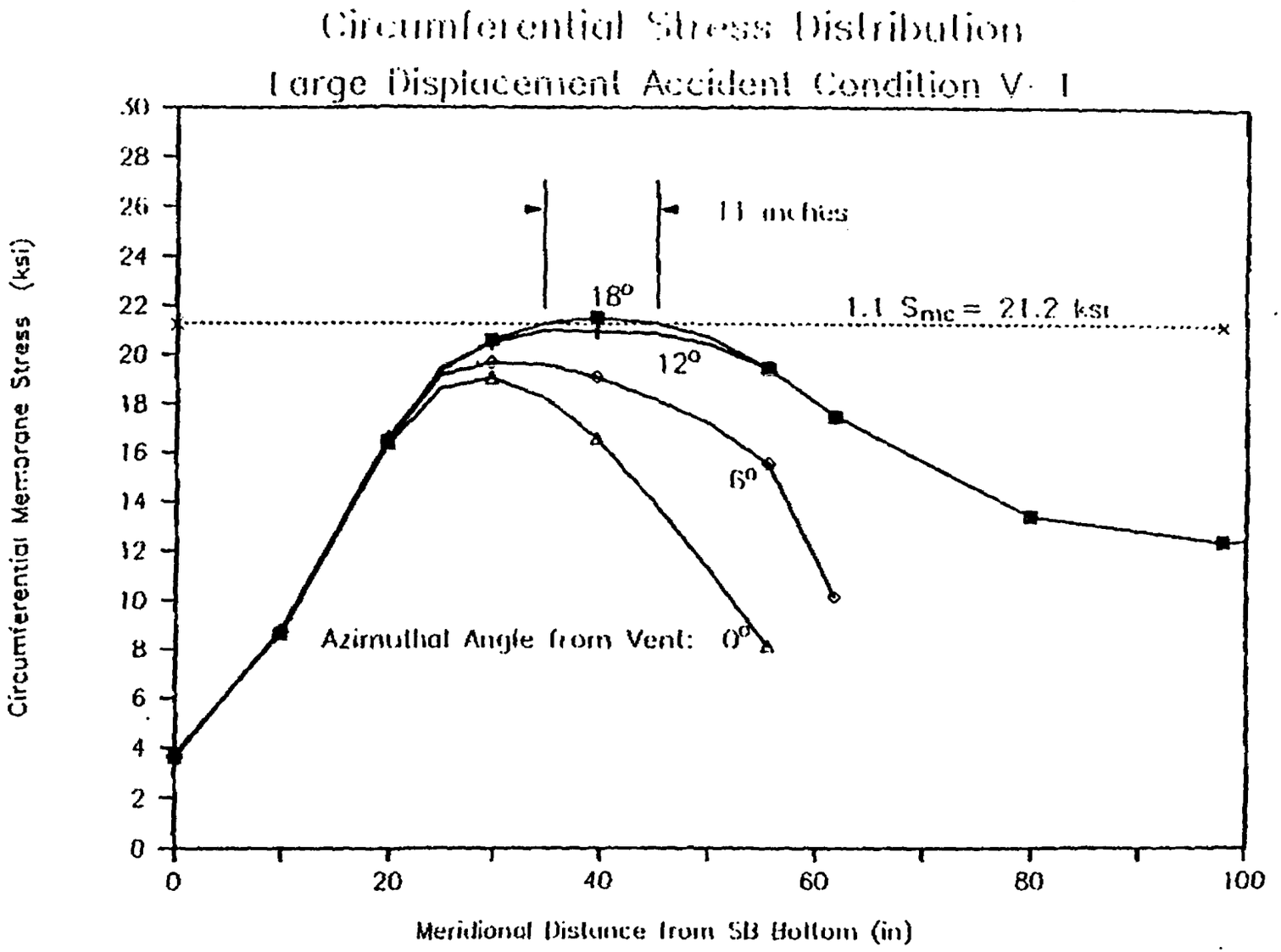

ACCUNT6A.DRW

Figure 5-6 Circumferential Membrane Stress Magnitudes at Four Meridional Planes in Sandbed Region - Large Displacement

DRF # 00664
INDEX NO. 9-3, REV. 0

6. SUMMARY AND CONCLUSIONS

This report is a supplementary report to the Code stress report (Reference 1-2) of record and addresses aspects of Code compliance as they relate to the local wall thinning observed and the removal of sand from the sandbed region in the Oyster Creek drywell. The loads and load combinations used in the analysis were based on the previous drywell stress analyses and the GPUN technical specification (Reference 1-4). In developing the allowable stress limits guidance was taken from Subsection NE of Section III, ASME Code where the Code of record, Section VIII and Code Case 1272N-5, is not explicit.

The stress analysis first considered a model in which everywhere as-designed thicknesses were used except in the sandbed region where the thickness was assumed as 0.736 inch. This served as a basis for evaluating the stresses for the 95% confidence projected thicknesses to 14R.

The highest stresses were determined to be from the Case V-1 and VI load combinations in all the different regions of the drywell. It was shown that the primary and secondary stresses are within the allowable limits for both conditions (as-designed thicknesses and 95% projected 14R thicknesses). At the plane of symmetry between the vent lines, the meridional extent of the circumferential membrane stress above $1.1S_{mc}$, was in excess of $1.0\sqrt{(Rt)}$. However, using a weighted average considering other meridional planes, this distance was less than $1.0\sqrt{(Rt)}$. Furthermore, a large displacement solution indicated the extent at the symmetry plane to be also less than $1.0\sqrt{(Rt)}$. This clearly satisfied the Code criterion for the extent of local primary membrane stress.

It is concluded that the Oyster Creek drywell shell will continue to meet the Code of record requirements at least up to 14R with the sand removed from the sandbed region. The analysis for buckling capability of the drywell shell without sand is contained in a companion GE report (Reference 1-5).

APPENDIX A

DETAILED RESULTS FOR AXISYMMETRIC MODEL TEMPERATURE STRESS ANALYSIS

This appendix presents a summary of the finite element analysis results for the temperature stress case (Load Case No. 8 in Table 3-1). The stresses reported in these tables are the nodal stresses. Since there are three nodes across the thickness of the drywell shell (e.g., see Figure 3-3), the stress at the center node is essentially a membrane stress. The difference between the stress at an inner or the outer node and the middle node is indicative of the bending stress at that section.

In each of the stress tables, the second and third columns from the left show the radial and vertical coordinates of the center nodes. Four stress components (three normal stresses and one shear stress) are listed for each of the inner, middle and the outer nodes.

Table 2-1 shows the wall thicknesses in the various regions of the drywell. To help assess the maximum stress levels, the range of node numbers associated with each wall thickness are given below:

Drywell Region	Node Number Range
Sandbed Region	1 through 96
Lower Spherical Region except Sandbed Area	100 through 237
Middle Spherical Region	241 through 603
Upper Spherical Region	604 through 876
Knuckle	880 through 942
Cylindrical Region	946 through 1449

ter Creek Raw Data for Thermal Stress at 210 seconds - No Sand

				Outside Nodes					Middle Nodes					Inside Nodes			
ode	X (inch)	Y (inch)	Theta (degrees)	Node	Radial SX (psi)	Meridional SY (psi)	Hoop SZ (psi)	SXY (psi)	Node	Radial SX (psi)	Meridional SY (psi)	Hoop SZ (psi)	SXY (psi)	Node	Radial SX (psi)	Meridional SY (psi)	Hoop SZ (psi)	SXY (psi)
2	247.06	106.93	36.00	1	226.09	1034.01	380.65	-9.14	2	-6.29	-8.65	-3.20	-6.90	3	-238.43	-1053.61	-387.87	-4.21
5	248.68	108.10	36.27	4	-62.03	985.03	271.56	-8.96	5	3.34	-8.66	-12.63	-6.88	6	68.72	-1004.52	-297.76	-4.42
8	250.28	109.28	36.54	7	18.78	872.26	231.35	-8.94	8	0.65	-8.80	-49.55	-7.00	9	-17.18	-891.83	-331.27	-4.76
11	251.87	110.46	36.81	10	-4.22	743.82	133.30	-9.02	11	1.10	-9.26	-106.80	-7.36	12	6.59	-764.10	-347.65	-5.42
14	253.45	111.66	37.08	13	1.69	609.76	23.76	-9.43	14	0.81	-10.17	-182.09	-8.02	15	0.10	-631.47	-388.54	-6.38
17	255.03	112.86	37.35	16	-0.58	459.81	-106.18	-10.20	17	0.64	-11.55	-271.83	-9.07	18	2.00	-484.13	-435.98	-7.76
20	256.61	114.06	37.62	19	-0.61	288.40	-257.49	-11.37	20	0.46	-13.55	-372.39	-10.57	21	1.63	-316.12	-487.59	-9.65
23	258.18	115.28	37.89	22	-1.40	86.88	-423.52	-12.97	23	0.18	-16.11	-479.58	-12.56	24	1.81	-119.42	-535.80	-12.09
26	259.74	116.50	38.16	25	-1.98	-152.78	-603.70	-14.98	26	-0.04	-19.39	-588.56	-15.06	27	1.87	114.41	-573.30	-15.16
29	261.30	117.73	38.43	28	-2.78	-439.10	-795.23	-17.41	29	-0.46	-23.16	-693.60	-18.06	30	1.78	393.65	-591.68	-18.81
32	262.85	118.97	38.70	31	-3.42	-780.08	-993.77	-20.13	32	-0.75	-27.66	-787.92	-21.52	33	1.73	726.71	-581.34	-23.13
35	264.39	120.21	38.98	34	-4.36	-1182.93	-1193.91	-23.18	35	-1.39	-32.38	-863.45	-25.39	36	1.30	1120.45	-532.04	-27.94
38	265.93	121.46	39.25	37	-4.91	-1652.58	-1387.74	-26.24	38	-1.74	-37.77	-910.68	-29.54	39	1.03	1581.18	-431.99	-33.34
41	267.47	122.72	39.52	40	-5.97	-2192.89	-1565.98	-29.41	41	-2.69	-42.79	-918.57	-33.82	42	0.03	2111.54	-269.35	-38.90
44	269.00	123.99	39.79	43	-6.20	-2802.51	-1715.52	-32.09	44	-3.01	-48.36	-874.40	-38.02	45	-0.52	2713.00	-30.40	-44.81
47	270.52	125.26	40.06	46	-7.38	-3478.59	-1822.08	-34.55	47	-4.46	-52.48	-763.87	-41.85	48	-2.42	3380.10	297.18	-50.23
50	272.03	126.54	40.33	49	-6.85	-4208.92	-1865.70	-35.67	50	-4.49	-57.08	-571.08	-44.97	51	-3.22	4106.08	728.07	-55.56
53	273.54	127.83	40.60	52	-8.24	-4980.26	-1828.71	-36.18	53	-6.69	-58.39	-278.98	-46.96	54	-6.44	4872.00	1272.68	-59.25
56	275.05	129.13	40.87	55	-6.16	-5763.37	-1678.89	-34.03	56	-5.97	-60.51	130.60	-47.29	57	-7.28	5659.14	1944.74	-62.32
59	276.54	130.43	41.14	58	-8.10	-6531.01	-1392.12	-30.95	59	-9.34	-56.11	675.68	-45.39	60	-12.29	6428.10	2748.54	-61.83
62	278.04	131.74	41.41	61	-3.20	-7230.80	-935.66	-23.06	62	-7.04	-53.90	1374.72	-40.55	63	-12.78	7146.60	3694.30	-60.29
65	279.54	133.07	41.68	64	-6.63	-7818.72	-271.20	-14.20	65	-13.01	-39.78	2254.64	-31.96	66	-21.46	7746.21	4784.93	-52.12
68	281.03	134.41	41.96	67	3.67	-8200.93	843.46	2.54	68	-6.63	-31.34	3322.91	-18.67	69	-19.12	8171.78	6014.92	-42.49
71	282.52	135.75	42.23	70	-2.54	-8313.58	1828.22	19.01	71	-16.73	-1.40	4587.72	0.07	72	-33.16	8308.43	7349.11	-21.43
74	284.01	137.11	42.50	73	18.71	-8015.78	3341.44	48.55	74	-2.78	13.73	6052.16	25.40	75	-24.45	8091.46	8779.96	-0.36
77	285.48	138.47	42.78	76	3.35	-7240.83	5179.99	73.93	77	-21.43	67.73	7707.77	57.98	78	-48.22	7350.12	10230.17	39.81
80	286.96	139.83	43.05	79	38.07	-5780.86	7407.65	120.94	80	7.18	87.33	9530.91	99.05	81	-25.38	6026.09	11677.57	75.06
83	288.42	141.21	43.33	82	12.42	-3599.93	9913.37	153.88	83	-27.11	182.58	11429.45	148.67	84	-67.78	3865.39	12917.21	142.37
86	289.88	142.59	43.60	85	56.15	-427.51	12302.47	221.60	86	23.22	215.99	12886.75	206.92	87	-10.11	869.81	13474.75	191.84
89	291.33	143.98	43.87	88	52.43	3582.20	12454.55	246.39	89	-16.56	394.74	11868.16	266.24	90	-84.78	-3247.12	11144.07	287.76
92	292.77	145.37	44.15	91	-131.59	8527.28	6323.45	306.60	92	-20.60	355.34	4258.37	305.94	93	91.71	-7947.40	2150.06	307.38
95	294.21	146.77	44.42	94	703.92	11000.93	-8125.28	1694.61	95	66.02	-12.80	-11318.26	-267.26	96	289.00	-9858.70	-13916.42	-182.15
98	294.65	147.04	44.49	97	1072.89	8060.70	-8625.81	2643.90	96	-131.17	561.36	-10877.87	-727.93	99	200.89	-6526.92	-13138.37	-564.42
101	295.06	147.31	44.56	100	31.35	5771.47	-9376.01	1086.78	101	-391.95	974.74	-10499.76	-116.71	102	-253.59	-7181.17	-12462.12	-291.51
104	296.51	148.72	44.83	103	28.09	6870.25	-7417.07	103.83	104	27.27	165.66	-9013.26	105.53	105	28.74	-6780.11	-10683.19	109.97
107	297.92	150.14	45.10	106	-5.45	7802.93	-5629.43	32.02	107	17.57	37.99	-7569.98	66.37	108	43.12	-7020.35	-9460.61	103.21

ster Creek Raw Data for Thermal Stress at 210 seconds - No Sand

				Outside Nodes							Middle Nodes						Inside Nodes		
Node	X (inch)	Y (inch)	Theta (degrees)	Node	Radial SX (psi)	Meridional SY (psi)	Hoop SZ (psi)	SXY (psi)	Node	Radial SX (psi)	Meridional SY (psi)	Hoop SZ (psi)	SXY (psi)	Node	Radial SX (psi)	Meridional SY (psi)	Hoop SZ (psi)	SXY (psi)
110	299.33	151.56	45.37	109	-26.01	8227.45	-4115.90	17.47	110	-13.52	58.61	-8216.64	33.43	111	1.82	-8219.11	-8352.30	52.51
113	300.74	152.89	45.65	112	2.54	8430.21	-2787.41	-18.71	113	13.59	1.86	-5003.42	6.92	114	27.62	-8414.57	-7218.38	35.53
116	302.13	154.42	45.92	115	-11.79	8342.41	-1695.31	-33.27	116	-3.55	-2.18	-3923.80	-14.30	117	7.71	-8401.38	-6171.25	7.78
119	303.52	155.87	46.19	118	0.89	8089.45	-779.80	-51.47	119	6.37	-26.78	-2976.28	-30.59	120	14.83	-8161.44	-5180.91	-6.74
122	304.91	157.31	46.47	121	-4.82	7679.44	-47.92	-60.21	122	0.31	-34.03	-2157.55	-42.72	123	8.31	-7781.78	-4280.01	-22.39
125	306.28	158.77	46.74	124	8.32	7172.89	536.22	-68.36	125	6.23	-43.87	-1458.13	-51.20	126	6.89	-7285.78	-3462.47	-31.40
128	307.65	160.23	47.01	127	-26.28	6591.59	967.44	-71.28	128	-9.85	-47.72	-877.11	-56.72	129	8.96	-6714.93	-2732.34	-39.72
131	309.01	161.70	47.28	130	49.14	5741.73	1255.64	-82.07	131	32.25	-49.25	-371.53	-59.80	132	26.44	-5858.08	-2005.51	-35.38
134	312.35	165.36	47.96	133	23.07	4430.63	1737.09	-83.20	134	32.77	-44.56	462.83	-58.87	135	44.14	-4538.62	-818.54	-32.85
137	315.65	169.08	48.64	136	30.11	3020.76	1748.72	-66.92	137	15.85	-39.01	855.05	-50.73	138	3.07	-3109.98	-43.12	-33.40
140	318.91	172.81	49.31	139	21.10	1851.50	1528.91	-49.24	140	11.03	-30.65	966.51	-39.76	141	1.79	-1920.23	401.13	-29.58
143	322.12	176.58	49.99	142	16.22	966.89	1213.11	-33.25	143	5.40	-22.34	905.30	-28.61	144	-4.95	-1015.15	596.02	-23.60
146	325.28	180.40	50.66	145	10.49	351.91	882.73	-20.07	146	1.83	-14.76	756.51	-18.78	147	-6.62	-383.06	629.81	-17.34
149	328.40	184.25	51.34	148	6.35	-34.83	586.87	-10.24	149	-0.35	-8.94	577.73	-10.92	150	-7.01	17.20	568.64	-11.60
152	331.48	188.14	52.01	151	3.11	-245.84	347.57	-3.43	152	-1.57	-4.54	405.00	-5.17	153	-6.31	237.50	462.71	-6.98
155	334.51	192.07	52.68	154	0.74	-332.09	170.21	0.76	155	-2.17	-1.71	257.42	-1.31	156	-5.18	330.00	345.14	-3.49
158	337.49	196.03	53.36	157	-0.28	-339.77	49.71	2.88	158	-1.82	0.14	142.97	1.00	159	-3.47	341.28	238.72	-0.99
161	340.00	199.45	53.94	160	-0.54	-307.07	-14.99	3.56	161	-1.06	0.99	71.33	2.04	162	-1.69	310.29	158.12	0.43
164	342.48	202.89	54.52	163	-0.97	-257.44	-52.87	3.74	164	-1.13	1.39	20.71	2.49	165	-1.40	261.13	94.65	1.15
167	344.93	206.36	55.10	166	-0.94	-202.45	-70.61	3.47	167	-0.81	1.44	-11.90	2.51	168	-0.76	206.33	47.13	1.49
170	347.34	209.85	55.68	169	-0.91	-149.60	-74.54	2.99	170	-0.63	1.35	-38.52	2.29	171	-0.41	152.83	13.72	1.54
173	349.71	213.38	56.25	172	-0.76	-103.09	-68.67	2.40	173	-0.42	1.13	-38.85	1.93	174	-0.11	105.77	-7.86	1.43
176	352.05	218.90	56.83	175	-0.63	-64.95	-59.99	1.81	176	-0.27	0.91	-40.15	1.53	177	0.06	67.00	-20.21	1.22
179	354.35	220.48	57.41	178	-0.46	-35.54	-48.29	1.28	179	-0.14	0.67	-37.05	1.13	180	0.17	37.04	-25.75	0.98
182	356.62	224.05	57.99	181	-0.33	-14.29	-36.54	0.83	182	-0.08	0.48	-31.60	0.79	183	0.21	15.29	-26.64	0.73
185	358.85	227.66	58.57	184	-0.21	-0.01	-25.87	0.46	185	0.00	0.31	-25.24	0.50	186	0.22	0.63	-24.61	0.52
188	361.04	231.29	59.14	187	-0.13	8.65	-16.90	0.22	188	0.04	0.18	-18.95	0.28	189	0.20	-8.32	-21.01	0.33
191	363.20	234.94	59.72	190	-0.06	13.07	-9.82	0.04	191	0.06	0.09	-13.30	0.12	192	0.17	-12.94	-16.79	0.19
194	365.32	238.61	60.30	193	-0.01	14.49	-4.58	-0.07	194	0.06	0.03	-8.59	0.01	195	0.14	-14.49	-12.62	0.09
197	367.41	242.31	60.88	196	0.02	13.95	-0.96	-0.13	197	0.06	-0.01	-4.90	-0.06	198	0.10	-14.02	-8.86	0.01
200	369.45	246.03	61.45	199	0.03	12.28	1.34	-0.16	200	0.05	-0.03	-2.18	-0.09	201	0.07	-12.39	-5.72	-0.03
203	371.46	249.76	62.03	202	0.04	10.08	2.60	-0.15	203	0.04	-0.04	-0.32	-0.11	204	0.05	-10.20	-3.26	-0.06
206	373.43	253.52	62.61	205	0.04	7.78	3.13	-0.14	206	0.03	-0.04	0.85	-0.10	207	0.03	-7.85	-1.45	-0.06
209	375.38	257.30	63.19	208	0.04	5.64	3.15	-0.12	209	0.02	-0.04	1.48	-0.09	210	0.01	-5.74	-0.20	-0.06
212	377.28	261.09	63.77	211	0.03	3.81	2.87	-0.09	212	0.02	-0.03	1.73	-0.07	213	0.00	-3.89	0.58	-0.06
215	379.11	264.91	64.34	214	0.02	2.35	2.44	-0.07	215	0.01	-0.02	1.72	-0.06	216	0.00	-2.41	0.99	-0.05

ter Creek Raw Data for Thermal Stress at 210 seconds - No Sand

				Outside Nodes					Middle Nodes					Inside Nodes				
ode	X (inch)	Y (inch)	Theta (degrees)	Node	Radial SX (psi)	Meridional SY (psi)	Hoop SZ (psi)	SXY (psi)	Node	Radial SX (psi)	Meridional SY (psi)	Hoop SZ (psi)	SXY (psi)	Node	Radial SX (psi)	Meridional SY (psi)	Hoop SZ (psi)	SXY (psi)
218	380.93	268.74	64.92	217	0.02	1.27	1.95	-0.05	218	0.00	-0.02	1.55	-0.04	219	-0.01	-1.31	1.15	-0.04
221	382.71	272.59	65.50	220	0.01	0.59	1.49	-0.03	221	0.00	-0.01	1.30	-0.03	222	0.00	-0.61	1.10	-0.02
224	383.49	274.32	65.76	223	0.01	0.25	1.27	-0.02	224	0.00	-0.01	1.17	-0.02	225	-0.01	-0.27	1.07	-0.02
227	384.26	276.04	66.02	226	0.00	0.07	1.08	-0.02	227	0.00	-0.01	1.04	-0.02	228	0.00	-0.08	1.00	-0.02
230	385.03	277.78	66.27	229	0.00	-0.07	0.91	-0.01	230	0.00	0.00	0.91	-0.01	231	0.00	0.05	0.91	-0.01
233	385.79	279.51	66.53	232	0.00	-0.18	0.75	-0.01	233	0.00	0.00	0.78	-0.01	234	0.00	0.15	0.82	-0.01
236	386.54	281.25	66.79	235	0.00	-0.22	0.61	0.02	236	0.01	-0.02	0.66	-0.01	237	0.01	0.25	0.72	-0.02
239	386.75	282.00	66.90	238	-0.01	-0.35	0.51	0.06	239	0.01	-0.01	0.61	-0.03	240	0.00	0.37	0.71	-0.03
242	386.97	282.74	67.00	241	-0.02	-0.52	0.41	0.03	242	-0.01	0.00	0.56	-0.02	243	-0.01	0.50	0.70	-0.02
245	387.40	283.76	67.15	244	0.00	-0.60	0.32	0.00	245	0.00	0.00	0.49	0.00	246	0.00	0.59	0.66	0.00
248	387.82	284.77	67.30	247	0.00	-0.61	0.25	0.00	248	0.00	0.00	0.43	0.00	249	0.00	0.61	0.60	0.00
251	388.24	285.79	67.45	250	0.00	-0.62	0.19	0.00	251	0.00	0.00	0.37	0.00	252	0.00	0.62	0.55	0.00
254	388.67	286.80	67.60	253	0.00	-0.62	0.14	0.00	254	0.00	0.00	0.31	0.00	255	0.00	0.62	0.49	0.00
257	389.08	287.82	67.75	256	0.00	-0.61	0.09	0.00	257	0.00	0.00	0.27	0.00	258	0.00	0.61	0.44	0.00
260	389.50	288.84	67.90	259	0.00	-0.60	0.05	0.00	260	0.00	0.00	0.22	0.00	261	0.00	0.60	0.39	0.00
263	389.91	289.86	68.05	262	0.00	-0.58	0.01	0.00	263	0.00	0.00	0.18	0.00	264	0.00	0.58	0.35	0.00
266	390.32	290.88	68.20	265	0.00	-0.56	-0.02	0.00	266	0.00	0.00	0.14	0.00	267	0.00	0.56	0.30	0.00
269	390.73	291.90	68.35	268	0.00	-0.53	-0.05	0.00	269	0.00	0.00	0.11	0.00	270	0.00	0.53	0.26	0.00
272	391.13	292.93	68.50	271	0.00	-0.49	-0.07	0.00	272	0.00	0.00	0.08	0.00	273	0.00	0.49	0.22	0.00
275	392.28	295.87	68.93	274	0.00	-0.42	-0.11	0.01	275	0.00	0.00	0.01	0.00	276	0.00	0.42	0.13	0.00
278	393.40	298.82	69.36	277	0.00	-0.33	-0.13	0.00	278	0.00	0.00	-0.03	0.00	279	0.00	0.33	0.06	0.00
281	394.50	301.77	69.79	280	0.00	-0.24	-0.13	0.00	281	0.00	0.00	-0.06	0.00	282	0.00	0.25	0.01	0.00
284	395.58	304.74	70.22	283	0.00	-0.17	-0.12	0.00	284	0.00	0.00	-0.07	0.00	285	0.00	0.17	-0.02	0.00
287	396.64	307.71	70.65	286	0.00	-0.11	-0.10	0.00	287	0.00	0.00	-0.07	0.00	288	0.00	0.11	-0.04	0.00
290	397.67	310.69	71.08	289	0.00	-0.06	-0.09	0.00	290	0.00	0.00	-0.07	0.00	291	0.00	0.07	-0.05	0.00
293	398.68	313.68	71.51	292	0.00	-0.03	-0.07	0.00	293	0.00	0.00	-0.06	0.00	294	0.00	0.03	-0.05	0.00
296	399.67	316.68	71.94	295	0.00	0.00	-0.05	0.00	296	0.00	0.00	-0.05	0.00	297	0.00	0.00	-0.05	0.00
299	400.64	319.68	72.37	298	0.00	0.01	-0.03	0.00	299	0.00	0.00	-0.04	0.00	300	0.00	-0.01	-0.04	0.00
302	401.58	322.69	72.80	301	0.00	0.02	-0.02	0.00	302	0.00	0.00	-0.03	0.00	303	0.00	-0.02	-0.03	0.00
305	402.51	325.71	73.23	304	0.00	0.03	-0.01	0.00	305	0.00	0.00	-0.02	0.00	306	0.00	-0.03	-0.03	0.00
308	403.41	328.73	73.66	307	0.00	0.03	0.00	0.00	308	0.00	0.00	-0.01	0.00	309	0.00	-0.03	-0.02	0.00
311	404.28	331.76	74.09	310	0.00	0.02	0.00	0.00	311	0.00	0.00	-0.01	0.00	312	0.00	-0.02	-0.01	0.00
314	405.13	334.80	74.52	313	0.00	0.02	0.00	0.00	314	0.00	0.00	0.00	0.00	315	0.00	-0.02	-0.01	0.00
317	405.97	337.84	74.95	316	0.00	0.02	0.01	0.00	317	0.00	0.00	0.00	0.00	318	0.00	-0.02	-0.01	0.00
320	406.77	340.89	75.38	319	0.00	0.01	0.01	0.00	320	0.00	0.00	0.00	0.00	321	0.00	-0.01	0.00	0.00
323	407.56	343.95	75.81	322	0.00	0.01	0.01	0.00	323	0.00	0.00	0.00	0.00	324	0.00	-0.01	0.00	0.00

ter Creek Raw Data for Thermal Stress at 210 seconds - No Sand

				Outside Nodes					Middle Nodes					Inside Nodes				
Node	X (inch)	Y (inch)	Theta (degrees)	Node	Radial SX (psi)	Meridional SY (psi)	Hoop SZ (psi)	SXY (psi)	Node	Radial SX (psi)	Meridional SY (psi)	Hoop SZ (psi)	SXY (psi)	Node	Radial SX (psi)	Meridional SY (psi)	Hoop SZ (psi)	SXY (psi)
326	408.32	347.01	76.24	325	0.00	0.01	0.01	0.00	326	0.00	0.00	0.00	0.00	327	0.00	-0.01	0.00	0.00
329	409.06	350.08	76.67	328	0.00	0.00	0.00	0.00	329	0.00	0.00	0.00	0.00	330	0.00	0.00	0.00	0.00
332	409.77	353.15	77.10	331	0.00	0.00	0.00	0.00	332	0.00	0.00	0.00	0.00	333	0.00	0.00	0.00	0.00
335	410.47	356.23	77.53	334	0.00	0.00	0.00	0.00	335	0.00	0.00	0.00	0.00	336	0.00	0.00	0.00	0.00
338	411.14	359.31	77.96	337	0.00	0.00	0.00	0.00	338	0.00	0.00	0.00	0.00	339	0.00	0.00	0.00	0.00
341	411.78	362.40	78.39	340	0.00	0.00	0.00	0.00	341	0.00	0.00	0.00	0.00	342	0.00	0.00	0.00	0.00
344	412.41	365.49	78.82	343	0.00	0.00	0.00	0.00	344	0.00	0.00	0.00	0.00	345	0.00	0.00	0.00	0.00
347	413.01	368.59	79.25	346	0.00	0.00	0.00	0.00	347	0.00	0.00	0.00	0.00	348	0.00	0.00	0.00	0.00
350	413.58	371.69	79.68	349	0.00	0.00	0.00	0.00	350	0.00	0.00	0.00	0.00	351	0.00	0.00	0.00	0.00
353	414.14	374.80	80.11	352	0.00	0.00	0.00	0.00	353	0.00	0.00	0.00	0.00	354	0.00	0.00	0.00	0.00
356	414.67	377.91	80.54	355	0.00	0.00	0.00	0.00	356	0.00	0.00	0.00	0.00	357	0.00	0.00	0.00	0.00
359	415.17	381.02	80.97	358	0.00	0.00	0.00	0.00	359	0.00	0.00	0.00	0.00	360	0.00	0.00	0.00	0.00
362	415.66	384.14	81.40	361	0.00	0.00	0.00	0.00	362	0.00	0.00	0.00	0.00	363	0.00	0.00	0.00	0.00
365	416.12	387.26	81.83	364	0.00	0.00	0.00	0.00	365	0.00	0.00	0.00	0.00	366	0.00	0.00	0.00	0.00
368	416.56	390.38	82.26	367	0.00	0.00	0.00	0.00	368	0.00	0.00	0.00	0.00	369	0.00	0.00	0.00	0.00
371	416.97	393.51	82.69	370	0.00	0.00	0.00	0.00	371	0.00	0.00	0.00	0.00	372	0.00	0.00	0.00	0.00
374	417.36	396.64	83.12	373	0.00	0.00	0.00	0.00	374	0.00	0.00	0.00	0.00	375	0.00	0.00	0.00	0.00
377	417.72	399.78	83.55	376	0.00	0.00	0.00	0.00	377	0.00	0.00	0.00	0.00	378	0.00	0.00	0.00	0.00
380	418.07	402.91	83.98	379	0.00	0.00	0.00	0.00	380	0.00	0.00	0.00	0.00	381	0.00	0.00	0.00	0.00
383	418.39	406.05	84.41	382	0.00	0.00	0.00	0.00	383	0.00	0.00	0.00	0.00	384	0.00	0.00	0.00	0.00
386	418.68	409.19	84.84	385	0.00	0.00	0.00	0.00	386	0.00	0.00	0.00	0.00	387	0.00	0.00	0.00	0.00
389	418.95	412.33	85.27	388	0.00	0.00	0.00	0.00	389	0.00	0.00	0.00	0.00	390	0.00	0.00	0.00	0.00
392	419.20	415.48	85.70	391	0.00	0.00	0.00	0.00	392	0.00	0.00	0.00	0.00	393	0.00	0.00	0.00	0.00
395	419.43	418.63	86.13	394	0.00	0.00	0.00	0.00	395	0.00	0.00	0.00	0.00	396	0.00	0.00	0.00	0.00
398	419.63	421.78	86.56	397	0.00	0.00	0.00	0.00	398	0.00	0.00	0.00	0.00	399	0.00	0.00	0.00	0.00
401	419.81	424.93	86.99	400	0.00	0.00	0.00	0.00	401	0.00	0.00	0.00	0.00	402	0.00	0.00	0.00	0.00
404	419.96	428.08	87.42	403	0.00	0.00	0.00	0.00	404	0.00	0.00	0.00	0.00	405	0.00	0.00	0.00	0.00
407	420.09	431.23	87.85	406	0.00	0.00	0.00	0.00	407	0.00	0.00	0.00	0.00	408	0.00	0.00	0.00	0.00
410	420.20	434.38	88.28	409	0.00	0.00	0.00	0.00	410	0.00	0.00	0.00	0.00	411	0.00	0.00	0.00	0.00
413	420.28	437.54	88.71	412	0.00	0.00	0.00	0.00	413	0.00	0.00	0.00	0.00	414	0.00	0.00	0.00	0.00
416	420.34	440.69	89.14	415	0.00	0.00	0.00	0.00	416	0.00	0.00	0.00	0.00	417	0.00	0.00	0.00	0.00
419	420.37	443.85	89.57	418	0.00	0.00	0.00	0.00	419	0.00	0.00	0.00	0.00	420	0.00	0.00	0.00	0.00
422	420.39	447.00	90.00	421	0.00	0.00	0.00	0.00	422	0.00	0.00	0.00	0.00	423	0.00	0.00	0.00	0.00
425	420.37	450.15	90.43	424	0.00	0.00	0.00	0.00	425	0.00	0.00	0.00	0.00	426	0.00	0.00	0.00	0.00
428	420.34	453.31	90.86	427	0.00	0.00	0.00	0.00	428	0.00	0.00	0.00	0.00	429	0.00	0.00	0.00	0.00
431	420.28	456.46	91.29	430	0.00	0.00	0.00	0.00	431	0.00	0.00	0.00	0.00	432	0.00	0.00	0.00	0.00

Oyster Creek Raw Data for Thermal Stress at 210 seconds - No Sand

				Outside Nodes					Middle Nodes					Inside Nodes				
Node	X (inch)	Y (inch)	Theta (degrees)	Node	Radial SX (psi)	Meridional SY (psi)	Hoop SZ (psi)	SXY (psi)	Node	Radial SX (psi)	Meridional SY (psi)	Hoop SZ (psi)	SXY (psi)	Node	Radial SX (psi)	Meridional SY (psi)	Hoop SZ (psi)	SXY (psi)
434	420.20	459.62	91.72	433	0.00	0.00	0.00	0.00	434	0.00	0.00	0.00	0.00	435	0.00	0.00	0.00	0.00
437	420.09	462.77	92.15	436	0.00	0.00	0.00	0.00	437	0.00	0.00	0.00	0.00	438	0.00	0.00	0.00	0.00
440	419.96	465.92	92.58	439	0.00	0.00	0.00	0.00	440	0.00	0.00	0.00	0.00	441	0.00	0.00	0.00	0.00
443	419.81	469.07	93.01	442	0.00	0.00	0.00	0.00	443	0.00	0.00	0.00	0.00	444	0.00	0.00	0.00	0.00
446	419.63	472.22	93.44	445	0.00	0.00	0.00	0.00	446	0.00	0.00	0.00	0.00	447	0.00	0.00	0.00	0.00
449	419.43	475.37	93.87	448	0.00	0.00	0.00	0.00	449	0.00	0.00	0.00	0.00	450	0.00	0.00	0.00	0.00
452	419.20	478.52	94.30	451	0.00	0.00	0.00	0.00	452	0.00	0.00	0.00	0.00	453	0.00	0.00	0.00	0.00
455	418.95	481.67	94.73	454	0.00	0.00	0.00	0.00	455	0.00	0.00	0.00	0.00	456	0.00	0.00	0.00	0.00
458	418.68	484.81	95.16	457	0.00	0.00	0.00	0.00	458	0.00	0.00	0.00	0.00	459	0.00	0.00	0.00	0.00
461	418.39	487.95	95.59	460	0.00	0.00	0.00	0.00	461	0.00	0.00	0.00	0.00	462	0.00	0.00	0.00	0.00
464	418.07	491.09	96.02	463	0.00	0.00	0.00	0.00	464	0.00	0.00	0.00	0.00	465	0.00	0.00	0.00	0.00
467	417.72	494.22	96.45	466	0.00	0.00	0.00	0.00	467	0.00	0.00	0.00	0.00	468	0.00	0.00	0.00	0.00
470	417.36	497.36	96.88	469	0.00	0.00	0.00	0.00	470	0.00	0.00	0.00	0.00	471	0.00	0.00	0.00	0.00
473	416.97	500.49	97.31	472	0.00	0.00	0.00	0.00	473	0.00	0.00	0.00	0.00	474	0.00	0.00	0.00	0.00
476	416.56	503.62	97.74	475	0.00	0.00	0.00	0.00	476	0.00	0.00	0.00	0.00	477	0.00	0.00	0.00	0.00
479	416.12	506.74	98.17	478	0.00	0.00	0.00	0.00	479	0.00	0.00	0.00	0.00	480	0.00	0.00	0.00	0.00
482	415.66	509.86	98.60	481	0.00	0.00	0.00	0.00	482	0.00	0.00	0.00	0.00	483	0.00	0.00	0.00	0.00
485	415.17	512.98	99.03	484	0.00	0.00	0.00	0.00	485	0.00	0.00	0.00	0.00	486	0.00	0.00	0.00	0.00
488	414.67	516.09	99.46	487	0.00	0.00	0.00	0.00	488	0.00	0.00	0.00	0.00	489	0.00	0.00	0.00	0.00
491	414.14	519.20	99.89	490	0.00	0.00	0.00	0.00	491	0.00	0.00	0.00	0.00	492	0.00	0.00	0.00	0.00
494	413.58	522.31	100.32	493	0.00	0.00	0.00	0.00	494	0.00	0.00	0.00	0.00	495	0.00	0.00	0.00	0.00
497	413.01	525.41	100.75	496	0.00	0.00	0.00	0.00	497	0.00	0.00	0.00	0.00	498	0.00	0.00	0.00	0.00
500	412.41	528.51	101.18	499	0.00	0.00	0.00	0.00	500	0.00	0.00	0.00	0.00	501	0.00	0.00	0.00	0.00
503	411.78	531.60	101.61	502	0.00	0.00	0.00	0.00	503	0.00	0.00	0.00	0.00	504	0.00	0.00	0.00	0.00
506	411.14	534.69	102.04	505	0.00	0.00	0.00	0.00	506	0.00	0.00	0.00	0.00	507	0.00	0.00	0.00	0.00
509	410.47	537.77	102.47	508	0.00	0.00	0.00	0.00	509	0.00	0.00	0.00	0.00	510	0.00	0.00	0.00	0.00
512	409.77	540.85	102.90	511	0.00	0.00	0.00	0.00	512	0.00	0.00	0.00	0.00	513	0.00	0.00	0.00	0.00
515	409.06	543.92	103.33	514	0.00	0.00	0.00	0.00	515	0.00	0.00	0.00	0.00	516	0.00	0.00	0.00	0.00
518	408.32	546.99	103.76	517	0.00	0.00	0.00	0.00	518	0.00	0.00	0.00	0.00	519	0.00	0.00	0.00	0.00
521	407.56	550.05	104.19	520	0.00	0.00	0.00	0.00	521	0.00	0.00	0.00	0.00	522	0.00	0.00	0.00	0.00
524	406.77	553.11	104.62	523	0.00	0.00	0.00	0.00	524	0.00	0.00	0.00	0.00	525	0.00	0.00	0.00	0.00
527	405.97	556.16	105.05	526	0.00	0.00	0.00	0.00	527	0.00	0.00	0.00	0.00	528	0.00	0.00	0.00	0.00
530	405.13	559.20	105.48	529	0.00	0.00	0.00	0.00	530	0.00	0.00	0.00	0.00	531	0.00	0.00	0.00	0.00
533	404.28	562.24	105.91	532	0.00	0.00	0.00	0.00	533	0.00	0.00	0.00	0.00	534	0.00	0.00	0.00	0.00
536	403.41	565.27	106.34	535	0.00	0.00	0.00	0.00	536	0.00	0.00	0.00	0.00	537	0.00	0.00	0.00	0.00
539	402.51	568.29	106.77	538	0.00	0.00	0.00	0.00	539	0.00	0.00	0.00	0.00	540	0.00	0.00	0.00	0.00

Oyster Creek Raw Data for Thermal Stress at 210 seconds - No Sand

				Outside Nodes					Middle Nodes					Inside Nodes				
Node	X (inch)	Y (inch)	Theta (degrees)	Node	Radial SX (psi)	Meridional SY (psi)	Hoop SZ (psi)	SXY (psi)	Node	Radial SX (psi)	Meridional SY (psi)	Hoop SZ (psi)	SXY (psi)	Node	Radial SX (psi)	Meridional SY (psi)	Hoop SZ (psi)	SXY (psi)
542	401.58	571.31	107.20	541	0.00	0.00	0.00	0.00	542	0.00	0.00	0.00	0.00	543	0.00	0.00	0.00	0.00
545	400.84	574.32	107.63	544	0.00	0.00	0.00	0.00	545	0.00	0.00	0.00	0.00	546	0.00	0.00	0.00	0.00
548	399.67	577.32	108.06	547	0.00	0.00	0.00	0.00	548	0.00	0.00	0.00	0.00	549	0.00	0.00	0.00	0.00
551	398.68	580.32	108.49	550	0.00	0.00	0.00	0.00	551	0.00	0.00	0.00	0.00	552	0.00	0.00	0.00	0.00
554	397.67	583.31	108.92	553	0.00	0.00	0.00	0.00	554	0.00	0.00	0.00	0.00	555	0.00	0.00	0.00	0.00
557	396.64	586.29	109.35	556	0.00	0.00	0.00	0.00	557	0.00	0.00	0.00	0.00	558	0.00	0.00	0.00	0.00
560	395.58	589.26	109.78	559	0.00	0.00	0.00	0.00	560	0.00	0.00	0.00	0.00	561	0.00	0.00	0.00	0.00
563	394.50	592.23	110.21	562	0.00	0.00	0.00	0.00	563	0.00	0.00	0.00	0.00	564	0.00	0.00	0.00	0.00
566	393.40	595.18	110.64	565	0.00	0.00	0.00	0.00	566	0.00	0.00	0.00	0.00	567	0.00	0.00	0.00	0.00
569	392.28	598.13	111.07	568	0.00	0.00	0.00	0.00	569	0.00	0.00	0.00	0.00	570	0.00	0.00	0.00	0.00
572	391.13	601.07	111.50	571	0.00	0.00	0.00	0.00	572	0.00	0.00	0.00	0.00	573	0.00	0.00	0.00	0.00
575	390.73	602.10	111.65	574	0.00	0.00	0.00	0.00	575	0.00	0.00	0.00	0.00	576	0.00	0.00	0.00	0.00
578	390.32	603.12	111.80	577	0.00	0.00	0.00	0.00	578	0.00	0.00	0.00	0.00	579	0.00	0.00	0.00	0.00
581	389.91	604.14	111.95	580	0.00	0.00	0.00	0.00	581	0.00	0.00	0.00	0.00	582	0.00	0.00	0.00	0.00
584	389.50	605.16	112.10	583	0.00	0.00	0.00	0.00	584	0.00	0.00	0.00	0.00	585	0.00	0.00	0.00	0.00
587	389.08	606.18	112.25	586	0.00	0.00	0.00	0.00	587	0.00	0.00	0.00	0.00	588	0.00	0.00	0.00	0.00
590	388.67	607.20	112.40	589	0.00	0.00	0.00	0.00	590	0.00	0.00	0.00	0.00	591	0.00	0.00	0.00	0.00
593	388.24	608.21	112.55	592	0.00	0.00	0.00	0.00	593	0.00	0.00	0.00	0.00	594	0.00	0.00	0.00	0.00
596	387.82	609.23	112.70	595	0.00	0.00	0.00	0.00	596	0.00	0.00	0.00	0.00	597	0.00	0.00	0.00	0.00
599	387.40	610.24	112.85	598	0.00	0.00	0.00	0.00	599	0.00	0.00	0.00	0.00	600	0.00	0.00	0.00	0.00
602	386.97	611.26	113.00	601	0.00	0.00	0.00	0.00	602	0.00	0.00	0.00	0.00	603	0.00	0.00	0.00	0.00
605	386.88	611.39	113.02	604	0.00	0.00	0.00	0.00	605	0.00	0.00	0.00	0.00	606	0.00	0.00	0.00	0.00
608	386.11	613.20	113.29	607	0.00	0.00	0.00	0.00	608	0.00	0.00	0.00	0.00	609	0.00	0.00	0.00	0.00
611	385.33	615.01	113.56	610	0.00	0.00	0.00	0.00	611	0.00	0.00	0.00	0.00	612	0.00	0.00	0.00	0.00
614	384.54	616.81	113.83	613	0.00	0.00	0.00	0.00	614	0.00	0.00	0.00	0.00	615	0.00	0.00	0.00	0.00
617	383.74	618.61	114.09	616	0.00	0.00	0.00	0.00	617	0.00	0.00	0.00	0.00	618	0.00	0.00	0.00	0.00
620	382.93	620.41	114.36	619	0.00	0.00	0.00	0.00	620	0.00	0.00	0.00	0.00	621	0.00	0.00	0.00	0.00
623	382.11	622.20	114.63	622	0.00	0.00	0.00	0.00	623	0.00	0.00	0.00	0.00	624	0.00	0.00	0.00	0.00
626	381.29	623.98	114.90	625	0.00	0.00	0.00	0.00	626	0.00	0.00	0.00	0.00	627	0.00	0.00	0.00	0.00
629	380.45	625.77	115.17	628	0.00	0.00	0.00	0.00	629	0.00	0.00	0.00	0.00	630	0.00	0.00	0.00	0.00
632	379.61	627.55	115.44	631	0.00	0.00	0.00	0.00	632	0.00	0.00	0.00	0.00	633	0.00	0.00	0.00	0.00
635	378.76	629.32	115.70	634	0.00	0.00	0.00	0.00	635	0.00	0.00	0.00	0.00	636	0.00	0.00	0.00	0.00
638	377.91	631.09	115.97	637	0.00	0.00	0.00	0.00	638	0.00	0.00	0.00	0.00	639	0.00	0.00	0.00	0.00
641	377.04	632.86	116.24	640	0.00	0.00	0.00	0.00	641	0.00	0.00	0.00	0.00	642	0.00	0.00	0.00	0.00
644	376.16	634.63	116.51	643	0.00	0.00	0.00	0.00	644	0.00	0.00	0.00	0.00	645	0.00	0.00	0.00	0.00
647	375.28	636.39	116.78	646	0.00	0.00	0.00	0.00	647	0.00	0.00	0.00	0.00	648	0.00	0.00	0.00	0.00

				Outside Nodes					Middle Nodes					Inside Nodes				
Node	X (inch)	Y (inch)	Theta (degrees)	Node	Radial SX (psi)	Meridional SY (psi)	Hoop SZ (psi)	SXY (psi)	Node	Radial SX (psi)	Meridional SY (psi)	Hoop SZ (psi)	SXY (psi)	Node	Radial SX (psi)	Meridional SY (psi)	Hoop SZ (psi)	SXY (psi)
650	374.39	638.14	117.05	649	0.00	0.00	0.00	0.00	650	0.00	0.00	0.00	0.00	651	0.00	0.00	0.00	0.00
653	373.49	639.89	117.31	652	0.00	0.00	0.00	0.00	653	0.00	0.00	0.00	0.00	654	0.00	0.00	0.00	0.00
656	372.58	641.64	117.58	655	0.00	0.00	0.00	0.00	656	0.00	0.00	0.00	0.00	657	0.00	0.00	0.00	0.00
659	371.67	643.38	117.85	658	0.00	0.00	0.00	0.00	659	0.00	0.00	0.00	0.00	660	0.00	0.00	0.00	0.00
662	370.74	645.12	118.12	661	0.00	0.00	0.00	0.00	662	0.00	0.00	0.00	0.00	663	0.00	0.00	0.00	0.00
665	369.81	646.85	118.39	664	0.00	0.00	0.00	0.00	665	0.00	0.00	0.00	0.00	666	0.00	0.00	0.00	0.00
668	368.87	648.58	118.65	667	0.00	0.00	0.00	0.00	668	0.00	0.00	0.00	0.00	669	0.00	0.00	0.00	0.00
671	368.80	648.72	118.68	670	0.00	0.00	0.00	0.00	671	0.00	0.00	0.00	0.00	672	0.00	0.00	0.00	0.00
674	367.84	650.82	119.00	673	0.00	0.00	0.00	0.00	674	0.00	0.00	0.00	0.00	675	0.00	0.00	0.00	0.00
677	366.48	652.91	119.33	676	0.00	0.00	0.00	0.00	677	0.00	0.00	0.00	0.00	678	0.00	0.00	0.00	0.00
680	365.30	654.99	119.66	679	0.00	0.00	0.00	0.00	680	0.00	0.00	0.00	0.00	681	0.00	0.00	0.00	0.00
683	364.11	657.06	119.98	682	0.00	0.00	0.00	0.00	683	0.00	0.00	0.00	0.00	684	0.00	0.00	0.00	0.00
686	362.91	659.13	120.31	685	0.00	0.00	0.00	0.00	686	0.00	0.00	0.00	0.00	687	0.00	0.00	0.00	0.00
689	361.70	661.19	120.63	688	0.00	0.00	0.00	0.00	689	0.00	0.00	0.00	0.00	690	0.00	0.00	0.00	0.00
692	360.47	663.25	120.96	691	0.00	0.00	0.00	0.00	692	0.00	0.00	0.00	0.00	693	0.00	0.00	0.00	0.00
695	359.24	665.30	121.29	694	0.00	0.00	0.00	0.00	695	0.00	0.00	0.00	0.00	696	0.00	0.00	0.00	0.00
698	357.99	667.34	121.61	697	0.00	0.00	0.00	0.00	698	0.00	0.00	0.00	0.00	699	0.00	0.00	0.00	0.00
701	356.73	669.37	121.94	700	0.00	0.00	0.00	0.00	701	0.00	0.00	0.00	0.00	702	0.00	0.00	0.00	0.00
704	355.46	671.40	122.26	703	0.00	0.00	0.00	0.00	704	0.00	0.00	0.00	0.00	705	0.00	0.00	0.00	0.00
707	354.17	673.42	122.59	706	0.00	0.00	0.00	0.00	707	0.00	0.00	0.00	0.00	708	0.00	0.00	0.00	0.00
710	352.88	675.43	122.92	709	0.00	0.00	0.00	0.00	710	0.00	0.00	0.00	0.00	711	0.00	0.00	0.00	0.00
713	351.57	677.43	123.24	712	0.00	0.00	0.00	0.00	713	0.00	0.00	0.00	0.00	714	0.00	0.00	0.00	0.00
716	350.26	679.43	123.57	715	0.00	0.00	0.00	0.00	716	0.00	0.00	0.00	0.00	717	0.00	0.00	0.00	0.00
719	348.93	681.42	123.89	718	0.00	0.00	0.00	0.00	719	0.00	0.00	0.00	0.00	720	0.00	0.00	0.00	0.00
722	347.59	683.40	124.22	721	0.00	0.00	0.00	0.00	722	0.00	0.00	0.00	0.00	723	0.00	0.00	0.00	0.00
725	346.24	685.37	124.55	724	0.00	0.00	0.00	0.00	725	0.00	0.00	0.00	0.00	726	0.00	0.00	0.00	0.00
728	344.88	687.34	124.87	727	0.00	0.00	0.00	0.00	728	0.00	0.00	0.00	0.00	729	0.00	0.00	0.00	0.00
731	343.50	689.30	125.20	730	0.00	0.00	0.00	0.00	731	0.00	0.00	0.00	0.00	732	0.00	0.00	0.00	0.00
734	342.12	691.25	125.52	733	0.00	0.00	0.00	0.00	734	0.00	0.00	0.00	0.00	735	0.00	0.00	0.00	0.00
737	340.72	693.19	125.85	736	0.00	0.00	0.00	0.00	737	0.00	0.00	0.00	0.00	738	0.00	0.00	0.00	0.00
740	339.32	695.13	126.18	739	0.00	0.00	0.00	0.00	740	0.00	0.00	0.00	0.00	741	0.00	0.00	0.00	0.00
743	337.90	697.05	126.50	742	0.00	0.00	0.00	0.00	743	0.00	0.00	0.00	0.00	744	0.00	0.00	0.00	0.00
746	336.47	698.97	126.83	745	0.00	0.00	0.00	0.00	746	0.00	0.00	0.00	0.00	747	0.00	0.00	0.00	0.00
749	335.03	700.88	127.15	748	0.00	0.00	0.00	0.00	749	0.00	0.00	0.00	0.00	750	0.00	0.00	0.00	0.00
752	333.58	702.78	127.48	751	0.00	0.00	0.00	0.00	752	0.00	0.00	0.00	0.00	753	0.00	0.00	0.00	0.00
755	332.12	704.68	127.81	754	0.00	0.00	0.00	0.00	755	0.00	0.00	0.00	0.00	756	0.00	0.00	0.00	0.00

ister Creek Raw Data for Thermal Stress at 210 seconds - No Sand

				Outside Nodes						Middle Nodes					Inside Nodes			
Node	X (inch)	Y (inch)	Theta (degrees)	Node	Radial SX (psi)	Meridional SY (psi)	Hoop SZ (psi)	SXY (psi)	Node	Radial SX (psi)	Meridional SY (psi)	Hoop SZ (psi)	SXY (psi)	Node	Radial SX (psi)	Meridional SY (psi)	Hoop SZ (psi)	SXY (psi)
758	330.85	706.57	126.13	757	0.00	0.00	0.00	0.00	758	0.00	0.00	0.00	0.00	759	0.00	0.00	0.00	0.00
761	329.17	708.44	128.46	760	0.00	0.00	0.00	0.00	761	0.00	0.00	0.00	0.00	762	0.00	0.00	0.00	0.00
764	327.87	710.31	128.78	763	0.00	0.00	0.00	0.00	764	0.00	0.00	0.00	0.00	765	0.00	0.00	0.00	0.00
767	326.17	712.17	129.11	766	0.00	0.00	0.00	0.00	767	0.00	0.00	0.00	0.00	768	0.00	0.00	0.00	0.00
770	324.66	714.02	129.44	769	0.00	0.00	0.00	0.00	770	0.00	0.00	0.00	0.00	771	0.00	0.00	0.00	0.00
773	323.13	715.87	129.76	772	0.00	0.00	0.00	0.00	773	0.00	0.00	0.00	0.00	774	0.00	0.00	0.00	0.00
776	321.60	717.70	130.09	775	0.00	0.00	0.00	0.00	776	0.00	0.00	0.00	0.00	777	0.00	0.00	0.00	0.00
779	320.05	719.53	130.41	778	0.00	0.00	0.00	0.00	779	0.00	0.00	0.00	0.00	780	0.00	0.00	0.00	0.00
782	318.50	721.34	130.74	781	0.00	0.00	0.00	0.00	782	0.00	0.00	0.00	0.00	783	0.00	0.00	0.00	0.00
785	316.93	723.15	131.07	784	0.00	0.00	0.00	0.00	785	0.00	0.00	0.00	0.00	786	0.00	0.00	0.00	0.00
788	315.35	724.95	131.39	787	0.00	0.00	0.00	0.00	788	0.00	0.00	0.00	0.00	789	0.00	0.00	0.00	0.00
791	313.77	726.74	131.72	790	0.00	0.00	0.00	0.00	791	0.00	0.00	0.00	0.00	792	0.00	0.00	0.00	0.00
794	312.17	728.52	132.04	793	0.00	0.00	0.00	0.00	794	0.00	0.00	0.00	0.00	795	0.00	0.00	0.00	0.00
797	310.56	730.29	132.37	796	0.00	0.00	0.00	0.00	797	0.00	0.00	0.00	0.00	798	0.00	0.00	0.00	0.00
800	308.94	732.06	132.70	799	0.00	0.00	0.00	0.00	800	0.00	0.00	0.00	0.00	801	0.00	0.00	0.00	0.00
803	307.32	733.81	133.02	802	0.00	0.00	0.00	0.00	803	0.00	0.00	0.00	0.00	804	0.00	0.00	0.00	0.00
806	305.68	735.55	133.35	805	0.00	0.00	0.00	0.00	806	0.00	0.00	0.00	0.00	807	0.00	0.00	0.00	0.00
809	304.03	737.29	133.68	808	0.00	0.00	0.00	0.00	809	0.00	0.00	0.00	0.00	810	0.00	0.00	0.00	0.00
812	302.38	739.01	134.00	811	0.00	0.00	0.00	0.00	812	0.00	0.00	0.00	0.00	813	0.00	0.00	0.00	0.00
815	300.71	740.73	134.33	814	0.00	0.00	0.00	0.00	815	0.00	0.00	0.00	0.00	816	0.00	0.00	0.00	0.00
818	299.03	742.44	134.65	817	0.00	0.00	0.00	0.00	818	0.00	0.00	0.00	0.00	819	0.00	0.00	0.00	0.00
821	297.35	744.13	134.98	820	0.00	0.00	0.00	0.00	821	0.00	0.00	0.00	0.00	822	0.00	0.00	0.00	0.00
824	295.65	745.82	135.31	823	0.00	0.00	0.00	0.00	824	0.00	0.00	0.00	0.00	825	0.00	0.00	0.00	0.00
827	293.95	747.50	135.63	826	0.00	0.00	0.00	0.00	827	0.00	0.00	0.00	0.00	828	0.00	0.00	0.00	0.00
830	292.23	749.16	135.96	829	0.00	0.00	0.00	0.00	830	0.00	0.00	0.00	0.00	831	0.00	0.00	0.00	0.00
833	290.51	750.82	136.28	832	0.00	0.00	0.00	0.00	833	0.00	0.00	0.00	0.00	834	0.00	0.00	0.00	0.00
836	288.77	752.47	136.61	835	0.00	0.00	0.00	0.00	836	0.00	0.00	0.00	0.00	837	0.00	0.00	0.00	0.00
839	287.03	754.11	136.94	838	0.00	0.00	0.00	0.00	839	0.00	0.00	0.00	0.00	840	0.00	0.00	0.00	0.00
842	285.28	755.74	137.26	841	0.00	0.00	0.00	0.00	842	0.00	0.00	0.00	0.00	843	0.00	0.00	0.00	0.00
845	283.52	757.36	137.59	844	0.00	0.00	0.00	0.00	845	0.00	0.00	0.00	0.00	846	0.00	0.00	0.00	0.00
848	280.57	760.02	138.13	847	0.00	0.00	0.00	0.00	848	0.00	0.00	0.00	0.00	849	0.00	0.00	0.00	0.00
851	277.60	762.66	138.67	850	0.00	0.00	0.00	0.00	851	0.00	0.00	0.00	0.00	852	0.00	0.00	0.00	0.00
854	274.61	765.27	139.21	853	0.00	0.00	0.00	0.00	854	0.00	0.00	0.00	0.00	855	0.00	0.00	0.00	0.00
857	271.59	767.85	139.75	856	0.00	0.00	0.00	0.00	857	0.00	0.00	0.00	0.00	858	0.00	0.00	0.00	0.00
860	268.55	770.40	140.29	859	0.00	0.00	0.00	0.00	860	0.00	0.00	0.00	0.00	861	0.00	0.00	0.00	0.00
863	265.48	772.92	140.84	862	0.00	0.00	0.00	0.00	863	0.00	0.00	0.00	0.00	864	0.00	0.00	0.00	0.00

rster Creek Raw Data for Thermal Stress at 210 seconds - No Sand

				Outside Nodes						Middle Nodes					Inside Nodes			
Node	X (inch)	Y (inch)	Theta (degrees)	Node	Radial SX (psi)	Meridional SY (psi)	Hoop SZ (psi)	SXY (psi)	Node	Radial SX (psi)	Meridional SY (psi)	Hoop SZ (psi)	SXY (psi)	Node	Radial SX (psi)	Meridional SY (psi)	Hoop SZ (psi)	SXY (psi)
866	262.39	775.41	141.38	865	0.00	0.00	0.00	0.00	866	0.00	0.00	0.00	0.00	867	0.00	0.00	0.00	0.00
869	259.28	777.88	141.92	868	0.00	0.00	0.00	0.00	869	0.00	0.00	0.00	0.00	870	0.00	0.00	0.00	0.00
872	256.14	780.31	142.46	871	0.00	0.00	0.00	0.00	872	0.00	0.00	0.00	0.00	873	0.00	0.00	0.00	0.00
875	252.98	782.72	143.00	874	0.00	0.00	0.00	0.00	875	0.00	0.00	0.00	0.00	876	0.00	0.00	0.00	0.00
878	251.40	783.85	143.26	877	0.00	0.00	0.00	0.00	878	0.00	0.00	0.00	0.00	879	0.00	0.00	0.00	0.00
881	249.98	784.97	143.51	880	0.00	0.00	0.00	0.00	881	0.00	0.00	0.00	0.00	882	0.00	0.00	0.00	0.00
884	247.27	786.96	143.97	883	0.00	0.00	0.00	0.00	884	0.00	0.00	0.00	0.00	885	0.00	0.00	0.00	0.00
887	244.55	788.92	144.43	886	0.00	0.00	0.00	0.00	887	0.00	0.00	0.00	0.00	888	0.00	0.00	0.00	0.00
890	241.81	790.87	144.89	889	0.00	0.00	0.00	0.00	890	0.00	0.00	0.00	0.00	891	0.00	0.00	0.00	0.00
893	239.05	792.79	145.34	892	0.00	0.00	0.00	0.00	893	0.00	0.00	0.00	0.00	894	0.00	0.00	0.00	0.00
896	236.28	794.69	145.80	895	0.00	0.00	0.00	0.00	896	0.00	0.00	0.00	0.00	897	0.00	0.00	0.00	0.00
899	233.49	796.57	146.26	898	0.00	0.00	0.00	0.00	899	0.00	0.00	0.00	0.00	900	0.00	0.00	0.00	0.00
902	230.69	798.42	146.72	901	0.00	0.00	0.00	0.00	902	0.00	0.00	0.00	0.00	903	0.00	0.00	0.00	0.00
905	225.89	801.86	147.52	904	0.00	0.00	0.00	0.00	905	0.00	0.00	0.00	0.00	906	0.00	0.00	0.00	0.00
908	221.39	805.58	148.32	907	0.00	0.00	0.00	0.00	908	0.00	0.00	0.00	0.00	909	0.00	0.00	0.00	0.00
911	217.22	809.07	149.09	910	0.00	0.00	0.00	0.00	911	0.00	0.00	0.00	0.00	912	0.00	0.00	0.00	0.00
914	213.41	814.38	149.85	913	0.00	0.00	0.00	0.00	914	0.00	0.00	0.00	0.00	915	0.00	0.00	0.00	0.00
917	209.99	819.19	150.57	916	0.00	0.00	0.00	0.00	917	0.00	0.00	0.00	0.00	918	0.00	0.00	0.00	0.00
920	206.97	824.28	151.25	919	0.00	0.00	0.00	0.00	920	0.00	0.00	0.00	0.00	921	0.00	0.00	0.00	0.00
923	204.38	829.57	151.89	922	0.00	0.00	0.00	0.00	923	0.00	0.00	0.00	0.00	924	0.00	0.00	0.00	0.00
926	202.23	835.08	152.47	925	0.00	0.00	0.00	0.00	926	0.00	0.00	0.00	0.00	927	0.00	0.00	0.00	0.00
929	200.55	840.74	153.01	928	0.00	0.00	0.00	0.00	929	0.00	0.00	0.00	0.00	930	0.00	0.00	0.00	0.00
932	199.34	846.52	153.48	931	0.00	0.00	0.00	0.00	932	0.00	0.00	0.00	0.00	933	0.00	0.00	0.00	0.00
935	198.61	852.38	153.90	934	0.00	0.00	0.00	0.00	935	0.00	0.00	0.00	0.00	936	0.00	0.00	0.00	0.00
938	198.37	858.28	154.25	937	0.00	0.00	0.00	0.00	938	0.00	0.00	0.00	0.00	939	0.00	0.00	0.00	0.00
941	198.31	858.78	154.28	940	0.00	0.00	0.00	0.00	941	0.00	0.00	0.00	0.00	942	0.00	0.00	0.00	0.00
944	198.32	860.78	154.39	943	0.00	0.00	0.00	0.00	944	0.00	0.00	0.00	0.00	945	0.00	0.00	0.00	0.00
947	198.32	862.78	154.50	946	0.00	0.00	0.00	0.00	947	0.00	0.00	0.00	0.00	948	0.00	0.00	0.00	0.00
950	198.32	863.78	154.55	949	0.00	0.00	0.00	0.00	950	0.00	0.00	0.00	0.00	951	0.00	0.00	0.00	0.00
953	198.32	864.78	154.61	952	0.00	0.00	0.00	0.00	953	0.00	0.00	0.00	0.00	954	0.00	0.00	0.00	0.00
956	198.32	865.78	154.66	955	0.00	0.00	0.00	0.00	956	0.00	0.00	0.00	0.00	957	0.00	0.00	0.00	0.00
959	198.32	866.78	154.71	958	0.00	0.00	0.00	0.00	959	0.00	0.00	0.00	0.00	960	0.00	0.00	0.00	0.00
962	198.32	867.78	154.76	961	0.00	0.00	0.00	0.00	962	0.00	0.00	0.00	0.00	963	0.00	0.00	0.00	0.00
965	198.32	868.83	154.82	964	0.00	0.00	0.00	0.00	965	0.00	0.00	0.00	0.00	966	0.00	0.00	0.00	0.00
968	198.32	869.88	154.87	967	0.00	0.00	0.00	0.00	968	0.00	0.00	0.00	0.00	969	0.00	0.00	0.00	0.00
971	198.32	870.93	154.93	970	0.00	0.00	0.00	0.00	971	0.00	0.00	0.00	0.00	972	0.00	0.00	0.00	0.00

Dyster Creek Raw Data for Thermal Stress at 210 seconds - No Sand

				Outside Nodes					Middle Nodes					Inside Nodes				
Node	X (inch)	Y (inch)	Theta (degrees)	Node	Radial SX (psi)	Meridional SY (psi)	Hoop SZ (psi)	SXY (psi)	Node	Radial SX (psi)	Meridional SY (psi)	Hoop SZ (psi)	SXY (psi)	Node	Radial SX (psi)	Meridional SY (psi)	Hoop SZ (psi)	SXY (psi)
974	198.32	871.98	154.98	973	0.00	0.00	0.00	0.00	974	0.00	0.00	0.00	0.00	975	0.00	0.00	0.00	0.00
977	198.32	873.03	155.04	976	0.00	0.00	0.00	0.00	977	0.00	0.00	0.00	0.00	978	0.00	0.00	0.00	0.00
980	198.32	874.08	155.09	979	0.00	0.00	0.00	0.00	980	0.00	0.00	0.00	0.00	981	0.00	0.00	0.00	0.00
983	198.32	875.13	155.15	982	0.00	0.00	0.00	0.00	983	0.00	0.00	0.00	0.00	984	0.00	0.00	0.00	0.00
986	198.32	876.18	155.20	985	0.00	0.00	0.00	0.00	986	0.00	0.00	0.00	0.00	987	0.00	0.00	0.00	0.00
989	198.32	877.23	155.25	988	0.00	0.00	0.00	0.00	989	0.00	0.00	0.00	0.00	990	0.00	0.00	0.00	0.00
992	198.32	878.28	155.31	991	0.00	0.00	0.00	0.00	992	0.00	0.00	0.00	0.00	993	0.00	0.00	0.00	0.00
995	198.32	880.55	155.42	994	0.00	0.00	0.00	0.00	995	0.00	0.00	0.00	0.00	996	0.00	0.00	0.00	0.00
998	198.32	882.81	155.53	997	0.00	0.00	0.00	0.00	998	0.00	0.00	0.00	0.00	999	0.00	0.00	0.00	0.00
1001	198.32	885.08	155.64	1000	0.00	0.00	0.00	0.00	1001	0.00	0.00	0.00	0.00	1002	0.00	0.00	0.00	0.00
1004	198.32	887.34	155.75	1003	0.00	0.00	0.00	0.00	1004	0.00	0.00	0.00	0.00	1005	0.00	0.00	0.00	0.00
1007	198.32	889.61	155.86	1006	0.00	0.00	0.00	0.00	1007	0.00	0.00	0.00	0.00	1008	0.00	0.00	0.00	0.00
1010	198.32	891.88	155.97	1009	0.00	0.00	0.00	0.00	1010	0.00	0.00	0.00	0.00	1011	0.00	0.00	0.00	0.00
1013	198.32	894.14	156.08	1012	0.00	0.00	0.00	0.00	1013	0.00	0.00	0.00	0.00	1014	0.00	0.00	0.00	0.00
1016	198.32	896.41	156.19	1015	0.00	0.00	0.00	0.00	1016	0.00	0.00	0.00	0.00	1017	0.00	0.00	0.00	0.00
1019	198.32	898.67	156.29	1018	0.00	0.00	0.00	0.00	1019	0.00	0.00	0.00	0.00	1020	0.00	0.00	0.00	0.00
1022	198.32	900.94	156.40	1021	0.00	0.00	0.00	0.00	1022	0.00	0.00	0.00	0.00	1023	0.00	0.00	0.00	0.00
1025	198.32	903.20	156.50	1024	0.00	0.00	0.00	0.00	1025	0.00	0.00	0.00	0.00	1026	0.00	0.00	0.00	0.00
1028	198.32	905.47	156.61	1027	0.00	0.00	0.00	0.00	1028	0.00	0.00	0.00	0.00	1029	0.00	0.00	0.00	0.00
1031	198.32	907.73	156.71	1030	0.00	0.00	0.00	0.00	1031	0.00	0.00	0.00	0.00	1032	0.00	0.00	0.00	0.00
1034	198.32	910.00	156.81	1033	0.00	0.00	0.00	0.00	1034	0.00	0.00	0.00	0.00	1035	0.00	0.00	0.00	0.00
1037	198.32	912.27	156.91	1036	0.00	0.00	0.00	0.00	1037	0.00	0.00	0.00	0.00	1038	0.00	0.00	0.00	0.00
1040	198.32	914.53	157.01	1039	0.00	0.00	0.00	0.00	1040	0.00	0.00	0.00	0.00	1041	0.00	0.00	0.00	0.00
1043	198.32	916.80	157.11	1042	0.00	0.00	0.00	0.00	1043	0.00	0.00	0.00	0.00	1044	0.00	0.00	0.00	0.00
1046	198.32	919.06	157.21	1045	0.00	0.00	0.00	0.00	1046	0.00	0.00	0.00	0.00	1047	0.00	0.00	0.00	0.00
1049	198.32	921.33	157.31	1048	0.00	0.00	0.00	0.00	1049	0.00	0.00	0.00	0.00	1050	0.00	0.00	0.00	0.00
1052	198.32	923.59	157.41	1051	0.00	0.00	0.00	0.00	1052	0.00	0.00	0.00	0.00	1053	0.00	0.00	0.00	0.00
1055	198.32	925.86	157.50	1054	0.00	0.00	0.00	0.00	1055	0.00	0.00	0.00	0.00	1056	0.00	0.00	0.00	0.00
1058	198.32	928.13	157.60	1057	0.00	0.00	0.00	0.00	1058	0.00	0.00	0.00	0.00	1059	0.00	0.00	0.00	0.00
1061	198.32	930.39	157.69	1060	0.00	0.00	0.00	0.00	1061	0.00	0.00	0.00	0.00	1062	0.00	0.00	0.00	0.00
1064	198.32	932.66	157.79	1063	0.00	0.00	0.00	0.00	1064	0.00	0.00	0.00	0.00	1065	0.00	0.00	0.00	0.00
1067	198.32	934.92	157.88	1066	0.00	0.00	0.00	0.00	1067	0.00	0.00	0.00	0.00	1068	0.00	0.00	0.00	0.00
1070	198.32	937.19	157.97	1069	0.00	0.00	0.00	0.00	1070	0.00	0.00	0.00	0.00	1071	0.00	0.00	0.00	0.00
1073	198.32	939.45	158.06	1072	0.00	0.00	0.00	0.00	1073	0.00	0.00	0.00	0.00	1074	0.00	0.00	0.00	0.00
1076	198.32	941.72	158.16	1075	0.00	0.00	0.00	0.00	1076	0.00	0.00	0.00	0.00	1077	0.00	0.00	0.00	0.00
1079	198.32	943.98	158.25	1078	0.00	0.00	0.00	0.00	1079	0.00	0.00	0.00	0.00	1080	0.00	0.00	0.00	0.00

Dyster Creek Raw Data for Thermal Stress at 210 seconds - No Sand

				Outside Nodes							Middle Nodes						Inside Nodes		
Node	X (inch)	Y (inch)	Theta (degrees)	Node	Radial SX (psi)	Meridional SY (psi)	Hoop SZ (psi)	SXY (psi)	Node	Radial SX (psi)	Meridional SY (psi)	Hoop SZ (psi)	SXY (psi)	Node	Radial SX (psi)	Meridional SY (psi)	Hoop SZ (psi)	SXY (psi)
1082	198.32	946.25	158.34	1081	0.00	0.00	0.00	0.00	1082	0.00	0.00	0.00	0.00	1083	0.00	0.00	0.00	0.00
1085	198.32	948.25	158.41	1084	0.00	0.00	0.00	0.00	1085	0.00	0.00	0.00	0.00	1086	0.00	0.00	0.00	0.00
1088	198.32	950.25	158.49	1087	0.00	0.00	0.00	0.00	1088	0.00	0.00	0.00	0.00	1089	0.00	0.00	0.00	0.00
1091	198.32	952.25	158.57	1090	0.00	0.00	0.00	0.00	1091	0.00	0.00	0.00	0.00	1092	0.00	0.00	0.00	0.00
1094	198.32	954.25	158.65	1093	0.00	0.00	0.00	0.00	1094	0.00	0.00	0.00	0.00	1095	0.00	0.00	0.00	0.00
1097	198.32	956.25	158.72	1096	0.00	0.00	0.00	0.00	1097	0.00	0.00	0.00	0.00	1098	0.00	0.00	0.00	0.00
1100	198.32	957.28	158.76	1099	0.00	0.00	0.00	0.00	1100	0.00	0.00	0.00	0.00	1101	0.00	0.00	0.00	0.00
1103	198.32	958.16	158.79	1102	0.00	0.00	0.00	0.00	1103	0.00	0.00	0.00	0.00	1104	0.00	0.00	0.00	0.00
1106	198.32	959.11	158.83	1105	0.00	0.00	0.00	0.00	1106	0.00	0.00	0.00	0.00	1107	0.00	0.00	0.00	0.00
1109	198.32	960.06	158.87	1108	0.00	0.00	0.00	0.00	1109	0.00	0.00	0.00	0.00	1110	0.00	0.00	0.00	0.00
1112	198.32	961.01	158.90	1111	0.00	0.00	0.00	0.00	1112	0.00	0.00	0.00	0.00	1113	0.00	0.00	0.00	0.00
1115	198.32	961.97	158.94	1114	0.00	0.00	0.00	0.00	1115	0.00	0.00	0.00	0.00	1116	0.00	0.00	0.00	0.00
1118	198.32	962.92	158.97	1117	0.00	0.00	0.00	0.00	1118	0.00	0.00	0.00	0.00	1119	0.00	0.00	0.00	0.00
1121	198.32	963.87	159.01	1120	0.00	0.00	0.00	0.00	1121	0.00	0.00	0.00	0.00	1122	0.00	0.00	0.00	0.00
1124	198.32	964.82	159.04	1123	0.00	0.00	0.00	0.00	1124	0.00	0.00	0.00	0.00	1125	0.00	0.00	0.00	0.00
1127	198.32	965.78	159.08	1126	0.00	0.00	0.00	0.00	1127	0.00	0.00	0.00	0.00	1128	0.00	0.00	0.00	0.00
1130	198.32	965.88	159.08	1129	0.00	0.00	0.00	0.00	1130	0.00	0.00	0.00	0.00	1131	0.00	0.00	0.00	0.00
1133	198.32	966.25	159.10	1132	0.00	0.00	0.00	0.00	1133	0.00	0.00	0.00	0.00	1134	0.00	0.00	0.00	0.00
1136	198.32	966.63	159.11	1135	0.00	0.00	0.00	0.00	1136	0.00	0.00	0.00	0.00	1137	0.00	0.00	0.00	0.00
1139	198.32	966.73	159.11	1138	0.00	0.00	0.00	0.00	1139	0.00	0.00	0.00	0.00	1140	0.00	0.00	0.00	0.00
1142	198.32	967.73	159.15	1141	0.00	0.00	0.00	0.00	1142	0.00	0.00	0.00	0.00	1143	0.00	0.00	0.00	0.00
1145	198.32	968.73	159.19	1144	0.00	0.00	0.00	0.00	1145	0.00	0.00	0.00	0.00	1146	0.00	0.00	0.00	0.00
1148	198.32	969.73	159.22	1147	0.00	0.00	0.00	0.00	1148	0.00	0.00	0.00	0.00	1149	0.00	0.00	0.00	0.00
1151	198.32	970.73	159.26	1150	0.00	0.00	0.00	0.00	1151	0.00	0.00	0.00	0.00	1152	0.00	0.00	0.00	0.00
1154	198.32	971.73	159.30	1153	0.00	0.00	0.00	0.00	1154	0.00	0.00	0.00	0.00	1155	0.00	0.00	0.00	0.00
1157	198.32	972.73	159.33	1158	0.00	0.00	0.00	0.00	1157	0.00	0.00	0.00	0.00	1158	0.00	0.00	0.00	0.00
1160	198.32	973.73	159.37	1159	0.00	0.00	0.00	0.00	1160	0.00	0.00	0.00	0.00	1161	0.00	0.00	0.00	0.00
1163	198.32	974.73	159.40	1162	0.00	0.00	0.00	0.00	1163	0.00	0.00	0.00	0.00	1164	0.00	0.00	0.00	0.00
1166	198.32	975.73	159.44	1165	0.00	0.00	0.00	0.00	1166	0.00	0.00	0.00	0.00	1167	0.00	0.00	0.00	0.00
1169	198.32	976.73	159.47	1168	0.00	0.00	0.00	0.00	1169	0.00	0.00	0.00	0.00	1170	0.00	0.00	0.00	0.00
1172	198.32	978.93	159.55	1171	0.00	0.00	0.00	0.00	1172	0.00	0.00	0.00	0.00	1173	0.00	0.00	0.00	0.00
1175	198.32	981.13	159.63	1174	0.00	0.00	0.00	0.00	1175	0.00	0.00	0.00	0.00	1176	0.00	0.00	0.00	0.00
1178	198.32	983.33	159.71	1177	0.00	0.00	0.00	0.00	1178	0.00	0.00	0.00	0.00	1179	0.00	0.00	0.00	0.00
1181	198.32	985.53	159.78	1180	0.00	0.00	0.00	0.00	1181	0.00	0.00	0.00	0.00	1182	0.00	0.00	0.00	0.00
1184	198.32	987.73	159.86	1183	0.00	0.00	0.00	0.00	1184	0.00	0.00	0.00	0.00	1185	0.00	0.00	0.00	0.00
1187	198.32	989.94	159.93	1186	0.00	0.00	0.00	0.00	1187	0.00	0.00	0.00	0.00	1188	0.00	0.00	0.00	0.00

lyster Creek Raw Data for Thermal Stress at 210 seconds - No Sand

				Outside Nodes					Middle Nodes					Inside Nodes			
Node	X (inch)	Y (inch)	Theta (degrees)	Node	Radial SX (psi)	Meridional SY (psi)	Hoop SZ (psi)	SXY (psi)	Node	Radial SX (psi)	Meridional SY (psi)	Hoop SZ (psi)	SXY (psi)	Node	Radial SX (psi)	Meridional SY (psi)	Hoop SZ (psi)	SXY (psi)
1190	198.32	992.14	160.01	1189	0.00	0.00	0.00	0.00	1190	0.00	0.00	0.00	0.00	1191	0.00	0.00	0.00	0.00
1193	198.32	994.34	160.08	1192	0.00	0.00	0.00	0.00	1193	0.00	0.00	0.00	0.00	1194	0.00	0.00	0.00	0.00
1196	198.32	996.54	160.16	1195	0.00	0.00	0.00	0.00	1196	0.00	0.00	0.00	0.00	1197	0.00	0.00	0.00	0.00
1199	198.32	998.74	160.23	1198	0.00	0.00	0.00	0.00	1199	0.00	0.00	0.00	0.00	1200	0.00	0.00	0.00	0.00
1202	198.32	1000.94	160.30	1201	0.00	0.00	0.00	0.00	1202	0.00	0.00	0.00	0.00	1203	0.00	0.00	0.00	0.00
1205	198.32	1003.15	160.37	1204	0.00	0.00	0.00	0.00	1205	0.00	0.00	0.00	0.00	1206	0.00	0.00	0.00	0.00
1208	198.32	1005.35	160.45	1207	0.00	0.00	0.00	0.00	1208	0.00	0.00	0.00	0.00	1209	0.00	0.00	0.00	0.00
1211	198.32	1007.55	160.52	1210	0.00	0.00	0.00	0.00	1211	0.00	0.00	0.00	0.00	1212	0.00	0.00	0.00	0.00
1214	198.32	1009.75	160.59	1213	0.00	0.00	0.00	0.00	1214	0.00	0.00	0.00	0.00	1215	0.00	0.00	0.00	0.00
1217	198.32	1010.70	160.62	1216	0.00	0.00	0.00	0.00	1217	0.00	0.00	0.00	0.00	1218	0.00	0.00	0.00	0.00
1220	198.32	1011.66	160.65	1219	0.00	0.00	0.00	0.00	1220	0.00	0.00	0.00	0.00	1221	0.00	0.00	0.00	0.00
1223	198.32	1012.61	160.68	1222	0.00	0.00	0.00	0.00	1223	0.00	0.00	0.00	0.00	1224	0.00	0.00	0.00	0.00
1226	198.32	1013.56	160.71	1225	0.00	0.00	0.00	0.00	1226	0.00	0.00	0.00	0.00	1227	0.00	0.00	0.00	0.00
1229	198.32	1014.51	160.74	1228	0.00	0.00	0.00	0.00	1229	0.00	0.00	0.00	0.00	1230	0.00	0.00	0.00	0.00
1232	198.32	1015.47	160.77	1231	0.00	0.00	0.00	0.00	1232	0.00	0.00	0.00	0.00	1233	0.00	0.00	0.00	0.00
1235	198.32	1016.42	160.80	1234	0.00	0.00	0.00	0.00	1235	0.00	0.00	0.00	0.00	1236	0.00	0.00	0.00	0.00
1238	198.32	1017.37	160.83	1237	0.00	0.00	0.00	0.00	1238	0.00	0.00	0.00	0.00	1239	0.00	0.00	0.00	0.00
1241	198.32	1018.32	160.86	1240	0.00	0.00	0.00	0.00	1241	0.00	0.00	0.00	0.00	1242	0.00	0.00	0.00	0.00
1244	198.32	1019.28	160.89	1243	0.00	0.00	0.00	0.00	1244	0.00	0.00	0.00	0.00	1245	0.00	0.00	0.00	0.00
1247	198.32	1019.38	160.89	1246	0.00	0.00	0.00	0.00	1247	0.00	0.00	0.00	0.00	1248	0.00	0.00	0.00	0.00
1250	198.32	1019.75	160.90	1249	0.00	0.00	0.00	0.00	1250	0.00	0.00	0.00	0.00	1251	0.00	0.00	0.00	0.00
1253	198.32	1020.13	160.91	1252	0.00	0.00	0.00	0.00	1253	0.00	0.00	0.00	0.00	1254	0.00	0.00	0.00	0.00
1256	198.32	1020.23	160.92	1255	0.00	0.00	0.00	0.00	1256	0.00	0.00	0.00	0.00	1257	0.00	0.00	0.00	0.00
1259	198.32	1021.23	160.95	1258	0.00	0.00	0.00	0.00	1259	0.00	0.00	0.00	0.00	1260	0.00	0.00	0.00	0.00
1262	198.32	1022.23	160.98	1261	0.00	0.00	0.00	0.00	1262	0.00	0.00	0.00	0.00	1263	0.00	0.00	0.00	0.00
1265	198.32	1023.23	161.01	1264	0.00	0.00	0.00	0.00	1265	0.00	0.00	0.00	0.00	1266	0.00	0.00	0.00	0.00
1268	198.32	1024.23	161.04	1267	0.00	0.00	0.00	0.00	1268	0.00	0.00	0.00	0.00	1269	0.00	0.00	0.00	0.00
1271	198.32	1025.23	161.07	1270	0.00	0.00	0.00	0.00	1271	0.00	0.00	0.00	0.00	1272	0.00	0.00	0.00	0.00
1274	198.32	1026.23	161.10	1273	0.00	0.00	0.00	0.00	1274	0.00	0.00	0.00	0.00	1275	0.00	0.00	0.00	0.00
1277	198.32	1027.23	161.13	1276	0.00	0.00	0.00	0.00	1277	0.00	0.00	0.00	0.00	1278	0.00	0.00	0.00	0.00
1280	198.32	1028.23	161.16	1279	0.00	0.00	0.00	0.00	1280	0.00	0.00	0.00	0.00	1281	0.00	0.00	0.00	0.00
1283	198.32	1029.23	161.19	1282	0.00	0.00	0.00	0.00	1283	0.00	0.00	0.00	0.00	1284	0.00	0.00	0.00	0.00
1286	198.32	1030.23	161.22	1285	0.00	0.00	0.00	0.00	1286	0.00	0.00	0.00	0.00	1287	0.00	0.00	0.00	0.00
1289	198.32	1032.65	161.29	1288	0.00	0.00	0.00	0.00	1289	0.00	0.00	0.00	0.00	1290	0.00	0.00	0.00	0.00
1292	198.32	1035.08	161.36	1291	0.00	0.00	0.00	0.00	1292	0.00	0.00	0.00	0.00	1293	0.00	0.00	0.00	0.00
1295	198.32	1037.51	161.44	1294	0.00	0.00	0.00	0.00	1295	0.00	0.00	0.00	0.00	1296	0.00	0.00	0.00	0.00

Oyster Creek Raw Data for Thermal Stress at 210 seconds - No Sand

				Outside Nodes					Middle Nodes					Inside Nodes				
Node	X (inch)	Y (inch)	Theta (degrees)	Node	Radial SX (psi)	Meridional SY (psi)	Hoop SZ (psi)	SXY (psi)	Node	Radial SX (psi)	Meridional SY (psi)	Hoop SZ (psi)	SXY (psi)	Node	Radial SX (psi)	Meridional SY (psi)	Hoop SZ (psi)	SXY (psi)
1296	198.32	1039.94	161.51	1297	0.00	0.00	0.00	0.00	1298	0.00	0.00	0.00	0.00	1299	0.00	0.00	0.00	0.00
1301	198.32	1042.36	161.58	1300	0.00	0.00	0.00	0.00	1301	0.00	0.00	0.00	0.00	1302	0.00	0.00	0.00	0.00
1304	198.32	1044.79	161.65	1303	0.00	0.00	0.00	0.00	1304	0.00	0.00	0.00	0.00	1305	0.00	0.00	0.00	0.00
1307	198.32	1047.22	161.72	1306	0.00	0.00	0.00	0.00	1307	0.00	0.00	0.00	0.00	1308	0.00	0.00	0.00	0.00
1310	198.32	1049.65	161.78	1309	0.00	0.00	0.00	0.00	1310	0.00	0.00	0.00	0.00	1311	0.00	0.00	0.00	0.00
1313	198.32	1052.07	161.85	1312	0.00	0.00	0.00	0.00	1313	0.00	0.00	0.00	0.00	1314	0.00	0.00	0.00	0.00
1316	198.32	1054.50	161.92	1315	0.00	0.00	0.00	0.00	1316	0.00	0.00	0.00	0.00	1317	0.00	0.00	0.00	0.00
1319	198.32	1055.47	161.95	1318	0.00	0.00	0.00	0.00	1319	0.00	0.00	0.00	0.00	1320	0.00	0.00	0.00	0.00
1322	198.32	1058.43	161.97	1321	0.00	0.00	0.00	0.00	1322	0.00	0.00	0.00	0.00	1323	0.00	0.00	0.00	0.00
1325	198.32	1057.40	162.00	1324	0.00	0.00	0.00	0.00	1325	0.00	0.00	0.00	0.00	1326	0.00	0.00	0.00	0.00
1328	198.32	1058.36	162.03	1327	0.00	0.00	0.00	0.00	1328	0.00	0.00	0.00	0.00	1329	0.00	0.00	0.00	0.00
1331	198.32	1059.33	162.05	1330	0.00	0.00	0.00	0.00	1331	0.00	0.00	0.00	0.00	1332	0.00	0.00	0.00	0.00
1334	198.32	1060.29	162.08	1333	0.00	0.00	0.00	0.00	1334	0.00	0.00	0.00	0.00	1335	0.00	0.00	0.00	0.00
1337	198.32	1061.26	162.11	1336	0.00	0.00	0.00	0.00	1337	0.00	0.00	0.00	0.00	1338	0.00	0.00	0.00	0.00
1340	198.32	1062.22	162.13	1339	0.00	0.00	0.00	0.00	1340	0.00	0.00	0.00	0.00	1341	0.00	0.00	0.00	0.00
1343	198.32	1063.19	162.16	1342	0.00	0.00	0.00	0.00	1343	0.00	0.00	0.00	0.00	1344	0.00	0.00	0.00	0.00
1346	198.32	1064.15	162.18	1345	0.00	0.00	0.00	0.00	1346	0.00	0.00	0.00	0.00	1347	0.00	0.00	0.00	0.00
1349	198.32	1064.25	162.19	1348	0.00	0.00	0.00	0.00	1349	0.00	0.00	0.00	0.00	1350	0.00	0.00	0.00	0.00
1352	198.32	1064.50	162.19	1351	0.00	0.00	0.00	0.00	1352	0.00	0.00	0.00	0.00	1353	0.00	0.00	0.00	0.00
1355	198.32	1064.75	162.20	1354	0.00	0.00	0.00	0.00	1355	0.00	0.00	0.00	0.00	1356	0.00	0.00	0.00	0.00
1358	198.32	1064.85	162.20	1357	0.00	0.00	0.00	0.00	1358	0.00	0.00	0.00	0.00	1359	0.00	0.00	0.00	0.00
1361	198.32	1065.85	162.23	1360	0.00	0.00	0.00	0.00	1361	0.00	0.00	0.00	0.00	1362	0.00	0.00	0.00	0.00
1364	198.32	1066.85	162.26	1363	0.00	0.00	0.00	0.00	1364	0.00	0.00	0.00	0.00	1365	0.00	0.00	0.00	0.00
1367	198.32	1067.85	162.28	1366	0.00	0.00	0.00	0.00	1367	0.00	0.00	0.00	0.00	1368	0.00	0.00	0.00	0.00
1370	198.32	1068.85	162.31	1369	0.00	0.00	0.00	0.00	1370	0.00	0.00	0.00	0.00	1371	0.00	0.00	0.00	0.00
1373	198.32	1069.85	162.34	1372	0.00	0.00	0.00	0.00	1373	0.00	0.00	0.00	0.00	1374	0.00	0.00	0.00	0.00
1376	198.32	1070.85	162.36	1375	0.00	0.00	0.00	0.00	1376	0.00	0.00	0.00	0.00	1377	0.00	0.00	0.00	0.00
1379	198.32	1071.85	162.39	1378	0.00	0.00	0.00	0.00	1379	0.00	0.00	0.00	0.00	1380	0.00	0.00	0.00	0.00
1382	198.32	1072.85	162.42	1381	0.00	0.00	0.00	0.00	1382	0.00	0.00	0.00	0.00	1383	0.00	0.00	0.00	0.00
1385	198.32	1073.85	162.44	1384	0.00	0.00	0.00	0.00	1385	0.00	0.00	0.00	0.00	1386	0.00	0.00	0.00	0.00
1388	198.32	1074.85	162.47	1387	0.00	0.00	0.00	0.00	1388	0.00	0.00	0.00	0.00	1389	0.00	0.00	0.00	0.00
1391	198.32	1077.07	162.53	1390	0.00	0.00	0.00	0.00	1391	0.00	0.00	0.00	0.00	1392	0.00	0.00	0.00	0.00
1394	198.32	1079.28	162.58	1393	0.00	0.00	0.00	0.00	1394	0.00	0.00	0.00	0.00	1395	0.00	0.00	0.00	0.00
1397	198.32	1081.50	162.64	1396	0.00	0.00	0.00	0.00	1397	0.00	0.00	0.00	0.00	1398	0.00	0.00	0.00	0.00
1400	198.32	1083.71	162.70	1399	0.00	0.00	0.00	0.00	1400	0.00	0.00	0.00	0.00	1401	0.00	0.00	0.00	0.00
1403	198.32	1085.93	162.76	1402	0.00	0.00	0.00	0.00	1403	0.00	0.00	0.00	0.00	1404	0.00	0.00	0.00	0.00

Oyster Creek Raw Data for Thermal Stress at 210 seconds - No Sand

				Outside Nodes					Middle Nodes					Inside Nodes			
Node	X (inch)	Y (inch)	Theta (degrees)	Node	Radial SX (psi)	Meridional SY (psi)	Hoop SZ (psi)	SXY (psi)	Node	Radial SX (psi)	Meridional SY (psi)	Hoop SZ (psi)	SXY (psi)	Node	Radial SX (psi)	Meridional SY (psi)	Hoop SZ (psi)	SXY (psi)
1406	198.32	1088.14	182.81	1405	0.00	0.00	0.00	0.00	1406	0.00	0.00	0.00	0.00	1407	0.00	0.00	0.00	0.00
1408	198.32	1090.36	182.87	1408	0.00	0.00	0.00	0.00	1409	0.00	0.00	0.00	0.00	1410	0.00	0.00	0.00	0.00
1412	198.32	1092.57	182.92	1411	0.00	0.00	0.00	0.00	1412	0.00	0.00	0.00	0.00	1413	0.00	0.00	0.00	0.00
1415	198.32	1094.79	182.98	1414	0.00	0.00	0.00	0.00	1415	0.00	0.00	0.00	0.00	1416	0.00	0.00	0.00	0.00
1418	198.32	1097.00	183.03	1417	0.00	0.00	0.00	0.00	1418	0.00	0.00	0.00	0.00	1419	0.00	0.00	0.00	0.00
1421	198.32	1098.00	183.06	1420	0.00	0.00	0.00	0.00	1421	0.00	0.00	0.00	0.00	1422	0.00	0.00	0.00	0.00
1424	198.32	1099.00	183.08	1423	0.00	0.00	0.00	0.00	1424	0.00	0.00	0.00	0.00	1425	0.00	0.00	0.00	0.00
1427	198.32	1100.00	183.11	1426	0.00	0.00	0.00	0.00	1427	0.00	0.00	0.00	0.00	1428	0.00	0.00	0.00	0.00
1430	198.32	1101.00	183.13	1429	0.00	0.00	0.00	0.00	1430	0.00	0.00	0.00	0.00	1431	0.00	0.00	0.00	0.00
1433	198.32	1102.00	183.15	1432	0.00	0.00	0.00	0.00	1433	0.00	0.00	0.00	0.00	1434	0.00	0.00	0.00	0.00
1436	198.32	1103.00	183.18	1435	0.00	0.00	0.00	0.00	1436	0.00	0.00	0.00	0.00	1437	0.00	0.00	0.00	0.00
1438	198.32	1104.00	183.20	1438	0.00	0.00	0.00	0.00	1439	0.00	0.00	0.00	0.00	1440	0.00	0.00	0.00	0.00
1442	198.32	1105.00	183.23	1441	0.00	0.00	0.00	0.00	1442	0.00	0.00	0.00	0.00	1443	0.00	0.00	0.00	0.00
1445	198.32	1106.00	183.25	1444	0.00	0.00	0.00	0.00	1445	0.00	0.00	0.00	0.00	1446	0.00	0.00	0.00	0.00
1448	198.32	1107.00	183.28	1447	0.00	0.00	0.00	0.00	1448	0.00	0.00	0.00	0.00	1449	0.00	0.00	0.00	0.00
1451	198.47	1108.25	183.29	1450	0.00	0.00	0.00	0.00	1451	0.00	0.00	0.00	0.00	1452	0.00	0.00	0.00	0.00
1454	198.63	1109.50	183.31	1453	0.00	0.00	0.00	0.00	1454	0.00	0.00	0.00	0.00	1455	0.00	0.00	0.00	0.00
					97	94	88	97		101	101	86	98		96	96	86	99
					1072.89	11000.93	12454.55	2643.90		-391.95	974.74	12806.75	-727.93		289.00	-9856.70	-13918.42	-564.47

AN ASME SECTION VIII EVALUATION OF THE OYSTER CREEK DRYWELL FOR WITHOUT SAND CASE PART 2 STABILITY ANALYSIS

February 1991

prepared for

GPU Nuclear Corporation
Parsippany, New Jersey

prepared by

GE Nuclear Energy
San Jose, California

AN ASME SECTION VIII EVALUATION OF THE OYSTER CREEK DRYWELL FOR WITHOUT SAND CASE PART 2 STABILITY ANALYSIS

Prepared by: _____
C.D. Frederickson, Senior Engineer
Materials Monitoring &
Structural Analysis Services

Reviewed by: _____
H. S. Mehta, Principal Engineer
Materials Monitoring &
Structural Analysis Services

Approved by: _____
S. Ranganath, Manager
Materials Monitoring &
Structural Analysis Services

TABLE OF CONTENTS

		Page
1.	INTRODUCTION	1-1
	1.1 General	1-1
	1.2 Report Outline	1-1
	1.3 References	1-2
2.	BUCKLING ANALYSIS METHODOLOGY	2-1
	2.1 Basic Approach	2-1
	2.2 Determination of Capacity Reduction Factor	2-2
	2.3 Modification of Capacity Reduction Factor for Hoop Stress	2-3
	2.4 Determination of Plasticity Reduction Factor	2-4
	2.5 References	2-5
3.	FINITE ELEMENT MODELING AND ANALYSIS	3-1
	3.1 Finite Element Buckling Analysis Methodology	3-1
	3.2 Finite Element Model	3-2
	3.3 Drywell Materials	3-3
	3.4 Boundary Conditions	3-3
	3.5 Loads	3-4
	3.6 Stress Results	3-7
	3.7 Theoretical Elastic Buckling Stress Results	3-9
	3.8 References	3-10
4.	ALLOWABLE BUCKLING STRESS EVALUATION	4-1
5.	SUMMARY AND CONCLUSIONS	5-1

LIST OF TABLES

Table No.	Title	Page No.
3-1	Oyster Creek Drywell Shell Thicknesses	3-11
3-2	Cylinder Stiffener Locations and Section Properties	3-12
3-3	Material Properties for SA-212 Grade B Steel	3-12
3-4	Oyster Creek Drywell Load Combinations	3-13
3-5	Adjusted Weight Densities of Shell to Account for Compressible Material Weight	3-14
3-6	Oyster Creek Drywell Additional Weights - Refueling	3-15
3-7	Oyster Creek Drywell Additional Weights - Post-Accident	3-16
3-8	Hydrostatic Pressures for Post-Accident, Flooded Cond.	3-17
3-9	Meridional Seismic Stresses at Four Sections	3-18
3-10	Application of Loads to Match Seismic Stresses - Refueling Case	3-19
3-11	Application of Loads to Match Seismic Stresses - Post-Accident Case	3-20
4-1	Calculation of Allowable Buckling Stresses - Refueling	4-2
4-2	Calculation of Allowable Buckling Stresses - Post-Accident	4-3
5-1	Buckling Analysis Summary	5-2

LIST OF FIGURES

Figure No.	Title	Page No.
1-1	Drywell Configuration	1-3
2-1	Capacity Reduction Factors for Local Buckling of Stiffened and Unstiffened Spherical Shells	2-7
2-2	Experimental Data Showing Increase in Compressive Buckling Stress Due to Internal Pressure	2-8
2-3	Design Curve to Account for Increase in Compressive Buckling Stress due to Internal Pressure	2-9
2-4	Plasticity Reduction Factors for Inelastic Buckling	2-10
3-1	Oyster Creek Drywell Geometry	3-21
3-2	Oyster Creek Drywell 3-D Finite Element Model	3-22
3-3	Closeup of Lower Drywell Section of FEM (Outside View)	3-23
3-4	Closeup of Lower Drywell Section of FEM (Inside View)	3-24
3-5	Boundary Conditions of Finite Element Model	3-25
3-6	Application of Loading to Simulate Seismic Bending	3-26
3-7	Meridional Stresses - Refueling Case	3-27
3-8	Lower Drywell Meridional Stresses - Refueling Case	3-28

LIST OF FIGURES

Figure No.	Title	Page No.
3-9	Circumferential Stresses - Refueling Case	3-29
3-10	Lower Drywell Circumferential Stresses - Refueling Case	3-30
3-11	Meridional Stresses - Post-Accident Case	3-31
3-12	Lower Drywell Meridional Stresses - Post-Accident Case	3-32
3-13	Circumferential Stresses - Post-Accident Case	3-33
3-14	Lower Drywell Circumferential Stresses - Post-Accident Case	3-34
3-15	Symmetric and Asymmetric Buckling Modes	3-35
3-16	Symmetric Buckling Mode Shape - Refueling Case	3-36
3-17	Asymmetric Buckling Mode Shape - Refueling Case	3-37
3-18	Buckling Mode Shape - Post-Accident Case	3-38

1. INTRODUCTION

1.1 General

To address local wall thinning of the Oyster Creek drywell, GPUN has prepared a supplementary report to the Code stress report of record [1-1] which is divided into two parts. Part 1 includes all of the Code stress analysis results other than the buckling capability for the drywell shell [1-2]. Part 2 addresses the buckling capability of the drywell shell shown in Figure 1-1 [1-3]. The supplementary report for the degraded drywell is for the present configuration (with sand support in the lower sphere). One option which is being considered by GPUN to mitigate further corrosion in the sandbed region is to remove the sand. Reference 1-4 and this report evaluate the influence of removing the sand on the code stress analysis and buckling evaluation, respectively. Buckling of the entire drywell shell is considered in this analysis with the sandbed region being the area of primary concern.

1.2 *Report Outline*

Section 2 of this report outlines the methodology used in the buckling capability evaluation. Finite element modeling, analysis and results are described in section 3. Evaluation of the allowable compressive buckling stresses and comparisons with the calculated compressive stresses for the limiting load combinations are covered in section 4. Section 5 presents the summary of results and conclusions.

1.3 References

1-1 "Structural Design of the Pressure Suppression Containment Vessels," by Chicago Bridge & Iron Co.,Contract # 9-0971, 1965.

1-2 "An ASME Section VIII Evaluation of the Oyster Creek Drywell - Part 1 Stress Analysis." GE Report No. 9-1, DRF# 00664, November 1990, prepared for GPUN.

1-3 "An ASME Section VIII Evaluation of the Oyster Creek Drywell - Part 2 Stability Analysis," GE Report No. 9-2, DRF# 00664, November 1990, prepared for GPUN.

1-4 "An ASME Section VIII Evaluation of the Oyster Creek Drywell - Part 1 Stress Analysis." GE Report No. 9-3, DRF# 00664, February 1991, prepared for GPUN.

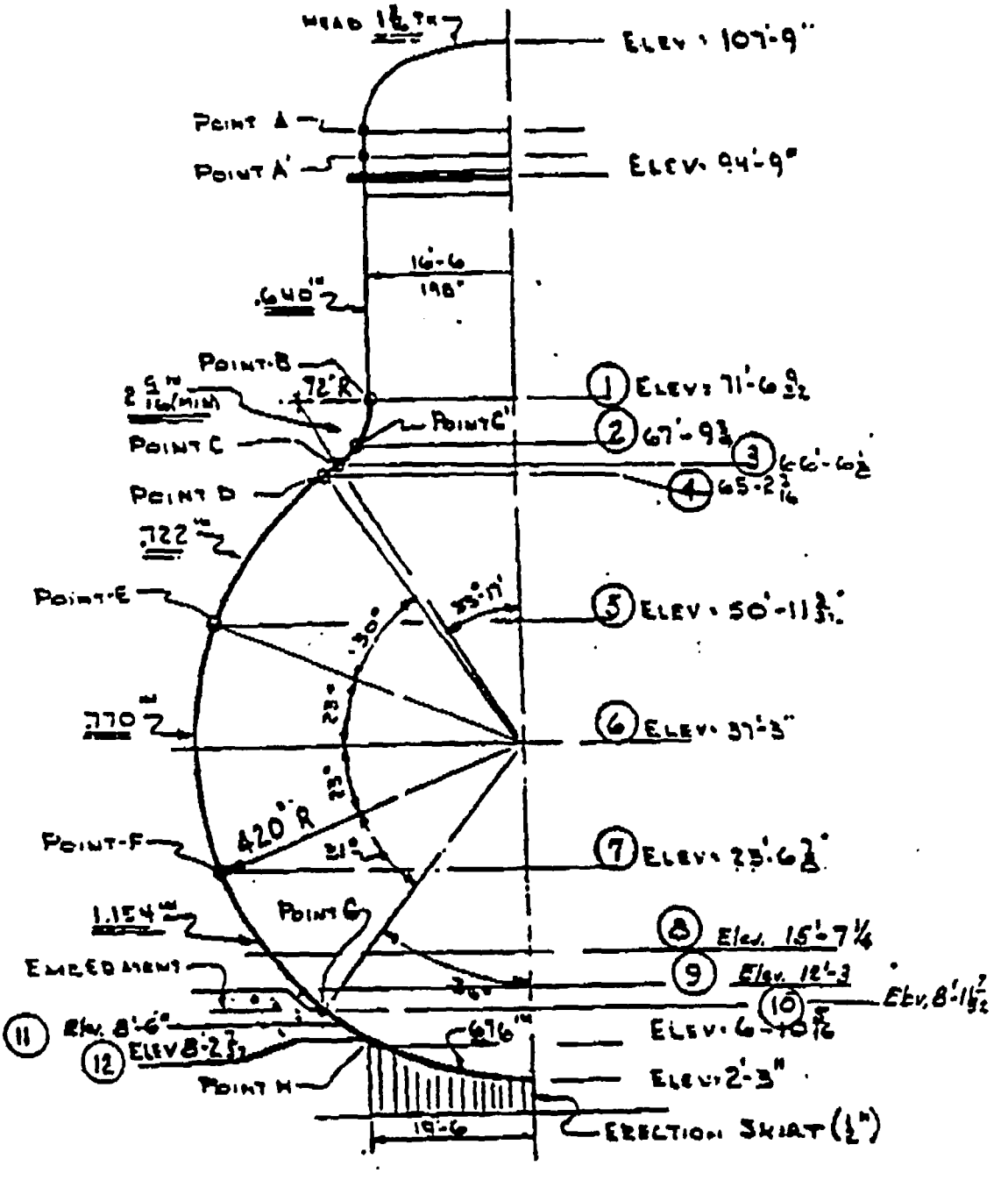

Figure 1-1 Drywell Configuration

2. BUCKLING ANALYSIS METHODOLOGY

2.1 Basic Approach

The basic approach used in the buckling evaluation follows the methodology outlined in the ASME Code Case N-284 [2-1 and 2-2]. Following the procedure of this Code Case, the allowable compressive stress is evaluated in three steps.

In the first step, a theoretical elastic buckling stress, σ_{ie}, is determined. This value may be calculated either by classical buckling equations or by finite element analysis. Since the drywell shell geometry is complex, a three dimensional finite element analysis approach is followed using the eigenvalue extraction technique. More details on the eigenvalue determination are given in Section 3.

In the second step, the theoretical elastic buckling stress is modified by the appropriate capacity and plasticity reduction factors. The capacity reduction factor, α_i, accounts for the difference between classical buckling theory and actual tested buckling stresses for fabricated shells. This difference is due to imperfections inherent in fabricated shells, not accounted for in classical buckling theory, which can cause significant reductions in the critical buckling stress. Thus, the elastic buckling stress for fabricated shells is given by the product of the theoretical elastic buckling stress and the capacity reduction factor, i.e., $\sigma_{ie}\alpha_i$. When the elastic buckling stress exceeds the proportional limit of the material, a plasticity reduction factor, η_i, is used to account for non-linear material behavior. The inelastic buckling stress for fabricated shells is given by $\eta_i\alpha_i\sigma_{ie}$.

In the final step, the allowable compressive stress is obtained by dividing the buckling stress calculated in the second step by the safety factor, FS:

$$\text{Allowable Compressive Stress} = \eta_i\alpha_i\sigma_{ie}/FS$$

In Reference 2-1, the safety factor for the Design and Level A & B service conditions is specified as 2.0. A safety factor of 1.67 is specified for Level C service conditions (such as the post-accident condition).

The determination of appropriate values for capacity and plasticity reduction factors is discussed next.

2.2 Determination of Capacity Reduction Factor

The capacity reduction factor, α_i, is used to account for reductions in actual buckling strength due to the existence of geometric imperfections. The capacity reduction factors given in Reference 2-1 are based on extensive data compiled by Miller [2-3]. The factors appropriate for a spherical shell geometry such as that of the drywell in the sandbed region, are shown in Figure 2-1 (Figure 1512-1 of Reference 2-1). The tail (flat) end of the curves are used for unstiffened shells. The curve marked 'Uniaxial compression' is applicable since the stress state in the sandbed region is compressive in the meridional direction but tensile in the circumferential direction. From this curve, α_i is determined to be 0.207.

The preceding value of the capacity reduction factor is very conservative for two reasons. First, it is based on the assumption that the spherical shell has a uniform thickness equal to the reduced thickness. However, the drywell shell has a greater thickness above the sandbed region which would reinforce the sandbed region. Second, it is assumed that the circumferential stress is zero. The tensile circumferential stress has the effect of rounding the shell and reducing the effect of imperfections introduced during the fabrication and construction phase. A modification of the α_i value to account for the presence of tensile circumferential stress is discussed in Subsection 2.3.

The capacity reduction factor values given in Reference 2-1 are applicable to shells which meet the tolerance requirements of NE-4220

of Section III [2-4]. Reference 2-5 compares the tolerance requirements of NE-4220 to the requirements to which the Oyster Creek drywell shell was fabricated. The comparison shows that the Oyster Creek drywell shell was erected to the tolerance requirements of NE-4220. Therefore, although the Oyster Creek drywell is not a Section III, NE vessel, it is justified to use the approach outlined in Code Case N-284.

2.3 Modification of Capacity Reduction Factor for Hoop Stress

The orthogonal tensile stress has the effect of rounding fabricated shells and reducing the effect of imperfections on the buckling strength. The Code Case N-284 [2-1 and 2-2] notes in the last paragraph of Article 1500 that, "The influence of internal pressure on a shell structure may reduce the initial imperfections and therefore higher values of capacity reduction factors may be acceptable. Justification for higher values of α_i must be given in the Design report."

Haris, et al [2-6] present the most comprehensive set of test data which clearly show that internal pressure in the form of hoop tension, increases the axial buckling stress. Reference 2-6 also contains data from References 2-7 and 2-8. Baker [2-9] and, in a recent book, Bushnell [2-10] also endorse References 2-6 and 2-7 in discussing the effect of internal pressure on the buckling capability of cylindrical shells. Based on References 2-6, Johnson [2-11] recommends a procedure to account for this increase in buckling capability. The data reported in Reference 2-6 are first discussed to show the reasonableness of the procedure recommended by Johnson.

Figure 2-2 (Figure 13 from Reference 2-6) shows the experimental data from several sources showing the increase in compressive buckling stress due to internal pressure. The curve recommended by Johnson corresponds to the '90% Probability Curve' in Figure 2-2. As shown later in Tables 4-1 and 4-2, the values of nondimensional pressure parameter (the abscissa in Figure 2-2) in the buckling analysis

presented in this report, are between 0.1 and 1.0. In this range, the '90% Probability Curve' in Figure 2-2 is also a lower bound to the experimental data. This clearly shows that the use of Johnson's procedure in this report assures conservative results (i.e., the procedure predicts a smaller increase in the compressive buckling stress than that indicated by the experimental data). The implementation of Johnson's procedure in this evaluation is described next.

The buckling stress in uniaxial compression for a sphere of uniform thickness is given by the following:

$$S_c = (0.605)(0.207)\ Et/R$$

Where, 0.605 is a constant, 0.207 is the capacity reduction factor and E,t and R are Young's Modulus, wall thickness and radius, respectively. In the presence of a tensile stress such as that produced by an internal pressure, p, the modified buckling stress is as follows:

$$S_{c,mod} = [(0.605)(0.207) + \Delta C]\ Et/R$$

Where ΔC is given in graphical form in Figure 2-3. As can be seen in Figure 2-3, ΔC is a function of the parameter $X=(p/4E)(2R/t)^2$. When the tensile stress magnitude, S, is known, the equivalent internal pressure can be calculated using the expression:

$$p = 2tS/R$$

The ΔC term is then incorporated in the capacity reduction factor itself by defining a modified capacity reduction factor, $\alpha_{i,mod}$:

$$\alpha_{i,mod} = 0.207 + \Delta C/0.605$$

2.4 Determination of Plasticity Reduction Factor

When the elastic buckling stress exceeds the proportional limit of the

material, a plasticity reduction factor, η_i, is used to account for the non-linear material behavior. The inelastic buckling stress for fabricated shells is given by $\eta_i \alpha_i \sigma_{ie}$. Reference 2-2 gives the mathematical expressions shown below [Article -1611 (a)] to calculate the plasticity reduction factor for the meridional direction elastic buckling stress. Δ is equal to $\alpha_i \sigma_{ie}/\sigma_y$ and σ_y is the material yield strength. Figure 2-4 shows the relationship in graphical form.

$$
\begin{aligned}
\eta_i &= 1.0 && \text{if } \Delta \leq 0.55 \\
&= (0.45/\Delta) + 0.18 && \text{if } 0.55 < \Delta \leq 1.6 \\
&= 1.31/(1+1.15\Delta) && \text{if } 1.6 < \Delta \leq 6.25 \\
&= 1/\Delta && \text{if } \Delta > 6.25
\end{aligned}
$$

2.5 References

2-1 ASME Boiler and Pressure Vessel Code Case N-284, "Metal Containment Shell Buckling Design Methods, Section III, Division 1, Class MC", Approved August 25, 1980.

2-2 Letter (1985) from C.D. Miller to P. Raju; Subject: Recommended Revisions to ASME Code Case N-284.

2-3 Miller, C.D., "Commentary on the Metal Containment Shell Buckling Design Methods of the ASME Boiler and Pressure Vessel Code," December 1979.

2-4 ASME Boiler & Pressure Vessel Code, Section III, Nuclear Power Plant Components.

2-5 "Justification for Use of Section III, Subsection NE, Guidance in Evaluating the Oyster Creek Drywell," Appendix A to letter dated December 21, 1990 from H.S. Mehta of GE to S.C. Tumminelli of GPUN.

2-6 Harris, L.A., et al, "The Stability of Thin-Walled Unstiffened Circular Cylinders Under Axial Compression Including the Effects of Internal Pressure," Journal of the Aeronautical Sciences, Vol. 24, No. 8 (August 1957), pp. 587-596.

2-7 Lo, H., Crate, H., and Schwartz, E.B., "Buckling of Thin-Walled Cylinder Under Axial Compression and Internal Pressure," NACA TN 2021, January 1950.

2-8 Fung, Y.C., and Sechler, E.E., "Buckling of Thin-Walled Circular Cylinders Under Axial Compression and Internal Pressure," Journal of the Aeronautical Sciences, Vol. 24, No. 5, pp. 351-356, May 1957.

2-9 Baker, E.H., et al., "Shell Analysis Manual," NASA, CR-912 (April 1968).

2-10 Bushnell, D., "Computerized Buckling Analysis of Shells," Kluwer Academic Publishers, 1989 (Chapter 5).

2-11 Johnson, B.G., "Guide to Stability Design Criteria for Metal Structures," Third Edition (1976), John Wiley & Sons.

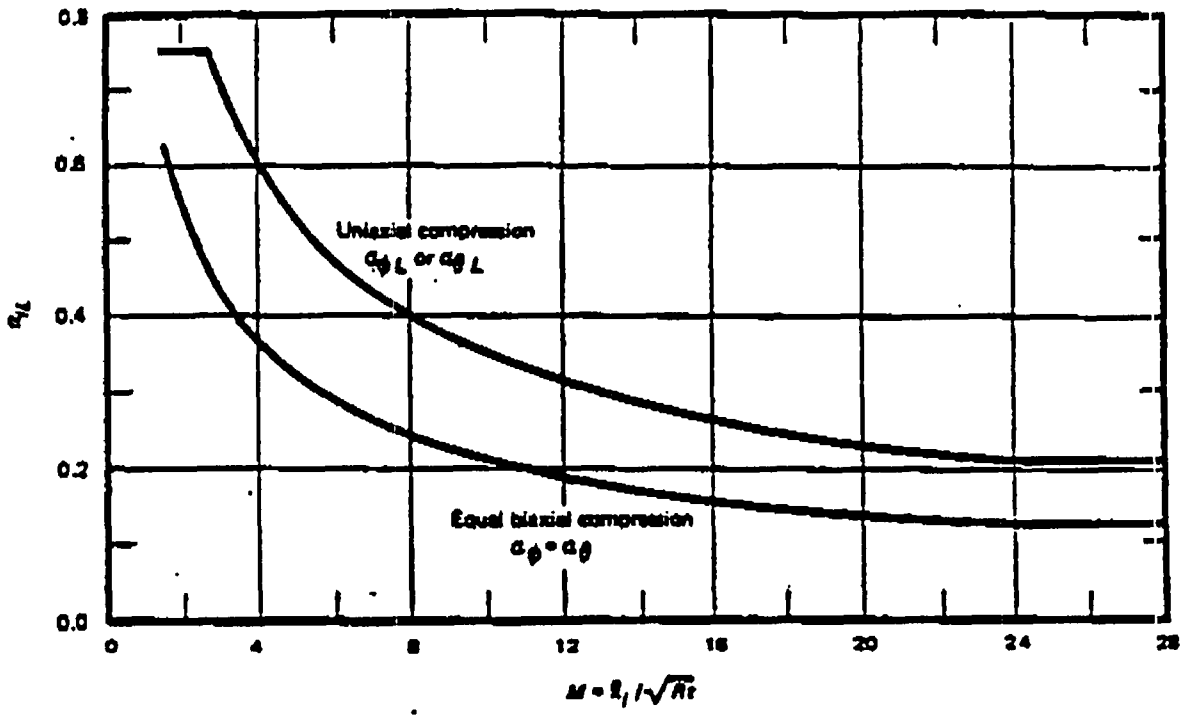

Figure 2-1 Capacity Reduction Factors for Local Buckling of Stiffened and Unstiffened Spherical Shells

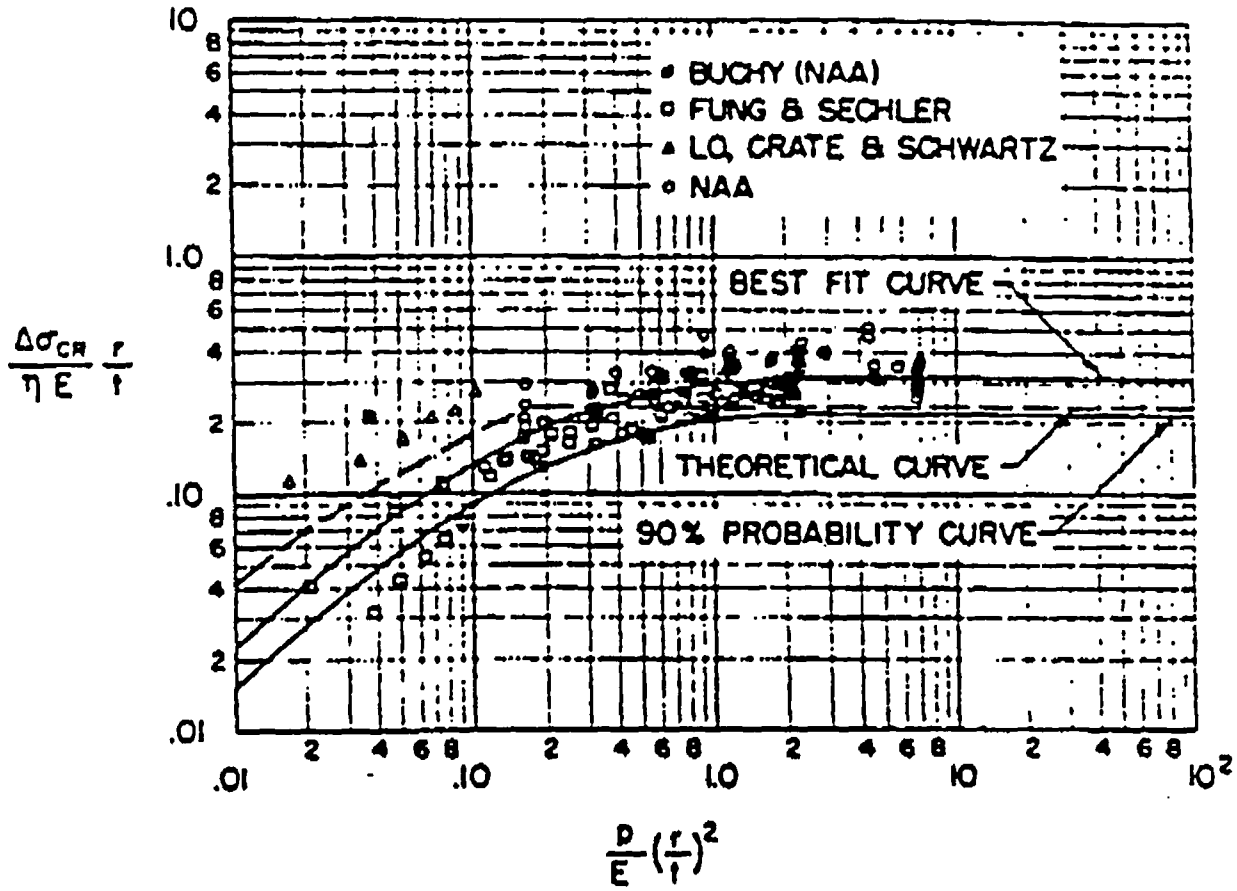

Figure 2-2 Experimental Data Showing Increase in Compressive Buckling Stress Due to Internal Pressure (Reference 2-6)

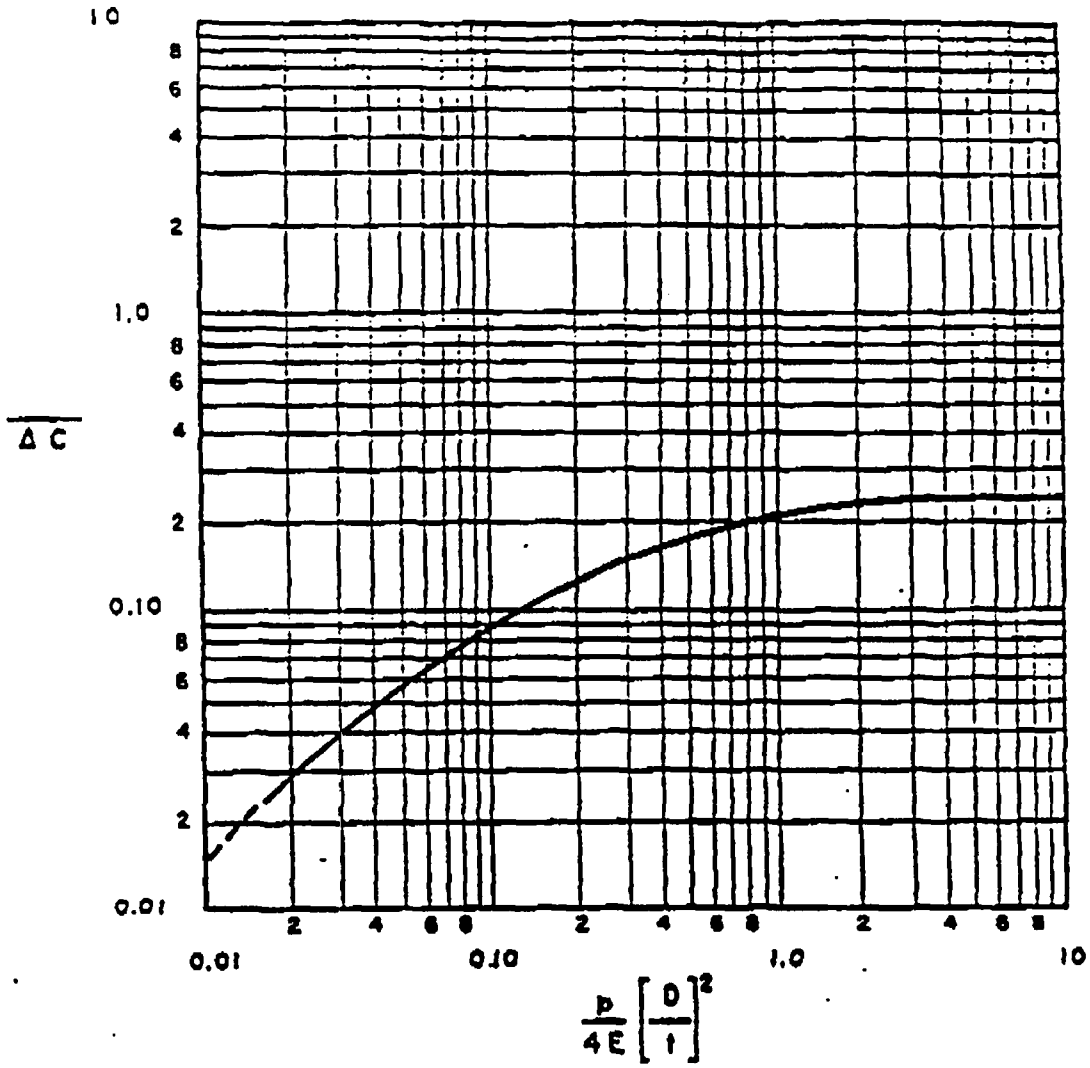

Figure 2-3 Design Curve to Account for Increase in Compressive Buckling Stress Due to Internal Pressure (Reference 2-11)

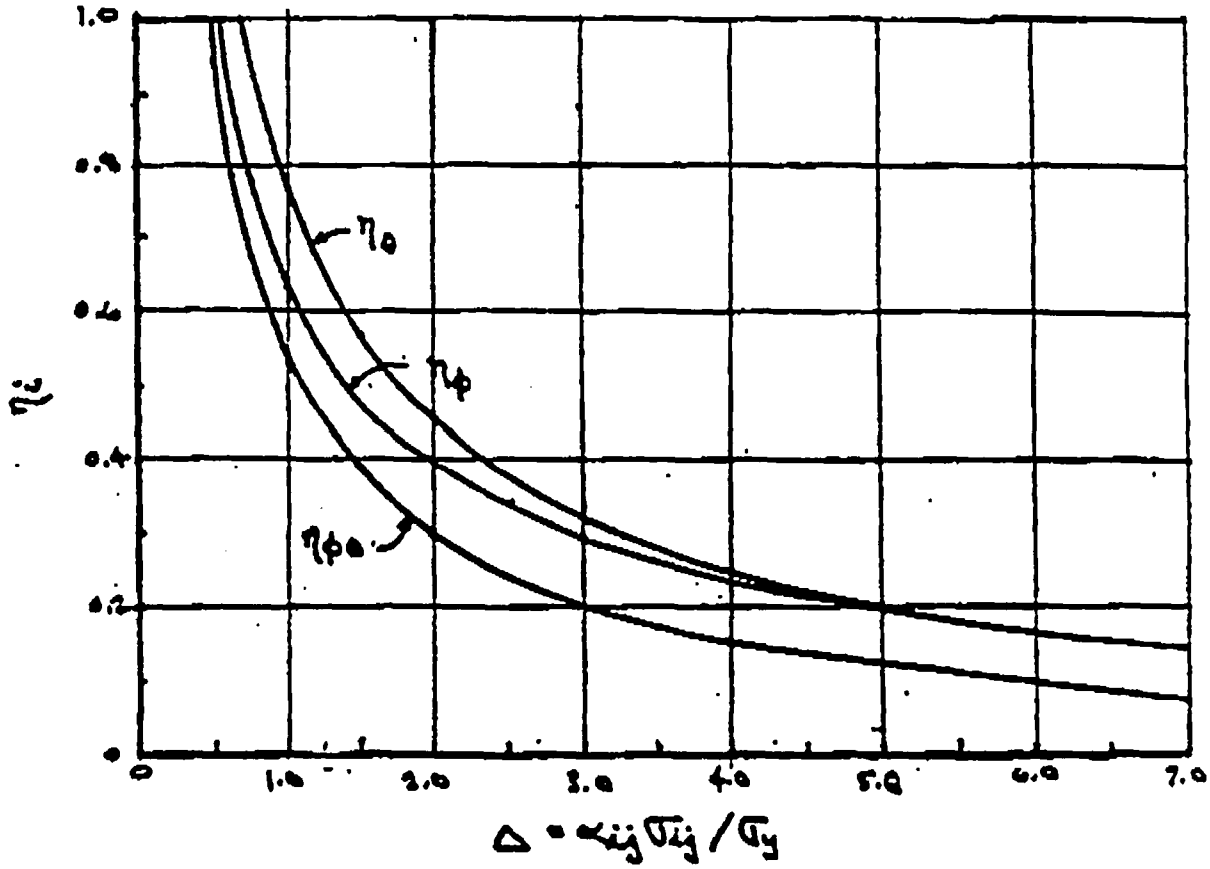

Figure 2-4 Plasticity Reduction Factors for Inelastic Buckling

3. FINITE ELEMENT MODELING AND ANALYSIS

3.1 Finite Element Buckling Analysis Methodology

This evaluation of the Oyster Creek Drywell buckling capability uses the Finite Element Analysis (FEA) program ANSYS [Reference 3-1]. The ANSYS program uses a two step eigenvalue formulation procedure to perform linear elastic buckling analysis. The first step is a static analysis of the structure with all anticipated loads applied. The structural stiffness matrix, [K], the stress stiffness matrix, [S], and the applied stresses, σ_{ap}, are developed and saved from this static analysis. A buckling pass is then run to solve for the eigenvalue or load factor, λ, for which elastic buckling is predicted using the equation:

$$([K] + \lambda [S]) \{u\} = 0$$

where: λ is the eigenvalue or load factor.
$\{u\}$ is the eigenvector representing the buckled shape of the structure.

This load factor is a multiplier for the applied stress state at which the onset of elastic buckling will theoretically occur. All applied loads (pressures, forces, gravity, etc...) are scaled equally. For example, a load factor of 4 would indicate that the structure would buckle for a load condition four times that defined in the stress pass. The critical stress, σ_{cr}, at a certain location of the structure is thus calculated as:

$$\sigma_{cr} = \lambda \sigma_{ap}$$

This theoretical elastic buckling stress is then modified by the capacity and plasticity reduction factors to determine the predicted buckling stress of the fabricated structure as discussed in Section 2. This stress is further reduced by a factor of safety to determine the allowable compressive stress.

3.2 Finite Element Model

The Oyster Creek drywell has been previously analyzed using a simplified axisymmetric model to evaluate the buckling capability in the sandbed region [Reference 3-2]. This type of analysis conservatively neglects the vents and reinforcements around the vents which significantly increase the stiffness of the shell near the sandbed region. In order to more accurately determine the buckling capability of the drywell, a three dimensional finite element model is developed.

The geometry of the Oyster Creek drywell is shown in Figure 3-1. Taking advantage of symmetry of the drywell with 10 vents, a 36° section is modeled. Figure 3-2 illustrates the finite element model of the drywell. This model includes the drywell shell from the base of the sandbed region to the top of the elliptical head and the vent and vent header. The torus is not included in this model because the bellows provide a very flexible connection which does not allow significant structural interaction between the drywell and torus.

Figure 3-3 shows a more detailed view of the lower section of the drywell model. The various colors on Figures 3-2 and 3-3 represent the different shell thicknesses of the drywell and vent. Nominal or as-designed thicknesses, summarized in Table 3-1, are used for the drywell shell for all regions other than the sandbed region. The sandbed region shown in blue in Figure 3-3 is considered to have a thickness of 0.736 inch. This is the 95% confidence projected thickness to outage 14R. Figure 3-4 shows the view from the inside of the drywell with the gussets and the vent jet deflector.

The drywell and vent shell are modeled using the 3-dimensional plastic quadrilateral shell (STIF43) element. Although this element has plastic capabilities, this analysis is conducted using only elastic behavior. This element type was chosen over the elastic quadrilateral shell (STIF63) element because it is better suited for modeling curved surfaces.

At a distance of 76 inches from the drywell shell, the vent is simplified using beam elements. The transition from shell to beam elements is made by extending rigid beam elements from a node along the centerline of the vent radially outward to each of the shell nodes of the vent. ANSYS STIF4 beam elements are then connected to this centerline node to model the axial and bending stiffness of the vent and header. Spring (STIF14) elements are used to model the vertical header supports inside the torus. ANSYS STIF4 beam elements are also used to model the stiffeners in the cylindrical region of the upper drywell. The section properties of these stiffeners are summarized in Table 3-2.

3.3 Drywell Materials

The drywell shell is fabricated from SA-212, Grade B high tensile strength carbon-silicon steel plates for boilers and other pressure vessels ordered to SA-300 specifications. The mechanical properties for this material at room temperature are shown in Table 3-3. These are the properties used in the finite element analysis. For the perforated vent jet deflector, the material properties were modified to account for the reduction in stiffness due to the perforations.

3.4 Boundary Conditions

Symmetric boundary conditions are defined for both edges of the 36° drywell model for the static stress analysis as shown on Figure 3-5. This allows the nodes at this boundary to expand radially outward from the drywell centerline and vertically, but not in the circumferential direction. Rotations are also fixed in two directions to prevent the boundary from rotating out of the plane of symmetry. Nodes at the bottom edge of the drywell are fixed in all directions to simulate the fixity of the shell within the concrete foundation. Nodes at the end of the header support spring elements are also fixed.

3.5 Loads

The loads are applied to the drywell finite element model in the manner which most accurately represents the actual loads anticipated on the drywell. Details on the application of loads are discussed in the following paragraphs.

3.5.1 Load Combinations

All load combinations to be considered on the drywell are summarized on Table 3-4. The most limiting load combinations in terms of possible buckling are those which cause the most compressive stresses in the sandbed region. Many of the design basis load combinations include high internal pressures which would create tensile stresses in the shell and help prevent buckling. The most severe design load combination identified for the buckling analysis of the drywell is the refueling condition (Case IV). This load combination consists of the following loads:

Dead weight of vessel, penetrations, compressible material, equipment supports and welding pads.
Live loads of welding pads and equipment door
Weight of refueling water
External Pressure of 2 psig
Seismic inertia and deflection loads for unflooded condition

The normal operation condition with seismic is very similar to this condition, however, it will be less severe due to the absence of the refueling water and equipment door weight.
The most severe load combination for the emergency condition is for the post-accident (Case VI) load combination including:

Dead weight of vessel, penetrations, compressible material and equipment supports
Live load of personnel lock
Hydrostatic Pressure of Water for Drywell Flooded to 74'-5"
External Pressure of 2 psig
Seismic inertia and deflection loads for flooded condition

The application of these loads is described in more detail in the following sections.

3.5.2 Gravity Loads

The gravity loads include dead weight loads of the drywell shell, weight of the compressible material and penetrations and live loads. The drywell shell loads are imposed on the model by defining the weight density of the shell material and applying a vertical acceleration of 1.0 g to simulate gravity. The ANSYS program automatically distributes the loads consistent with the mass and acceleration. The compressible material weight of 10 lb/ft^2 is added by adjusting the weight density of the shell to also include the compressible material. The adjusted weight densities for the various shell thicknesses are summarized in Table 3-5. The compressible material is assumed to cover the entire drywell shell (not including the vent) up to the elevation of the flange.

The additional dead weights, penetration weights and live loads are applied as additional nodal masses to the model. As shown on Table 3-6 for the refueling case, the total additional mass is summed for each 5 foot elevation of the drywell. The total is then divided by 10 for the 36° section assuming that the mass is evenly distributed around the perimeter of the drywell. The resulting mass is then applied uniformly to a set of nodes at the desired elevation as shown on Table 3-6. These applied masses automatically impose gravity loads on the drywell model with the defined acceleration of 1g. The same method is used to apply the additional masses to the model for the post-accident case as summarized in Table 3-7.

3.5.3 Pressure Loads

The 2 psi external pressure load for the refueling case is applied to the external faces of all of the drywell and vent shell elements. The compressive axial stress at the transition from vent shell to beam elements is simulated by applying equivalent axial forces to the nodes of the shell elements.

Considering the post-accident case, the drywell is assumed to be flooded to elevation 74'-6" (894 inches). Using a water density of 62.3 lb/ft^3 (0.0361 lb/in^3), the pressure gradient versus elevation is calculated as shown in Table 3-8. The hydrostatic pressure at the bottom of the sandbed region is calculated to be 28.3 psi. According to the elevation of the element centerline, the appropriate pressures are applied to the inside surface of the shell elements.

3.5.4 Seismic Loads

Seismic stresses have been calculated for the Oyster Creek Drywell in Part 1 of this report, Reference 3-3. Meridional stresses are imposed on the drywell during a seismic event due to a 0.058" deflection of the reactor building and due to horizontal and vertical inertial loads on the drywell.

The meridional stresses due to a seismic event are imposed on the 3-D drywell model by applying downward forces at four elevations of the model (A: 23'-7",B: 37'-3",C: 50'-11" and D: 88'-9") as shown on Figure 3-6. Using this method, the meridional stresses calculated in Reference 3-3 are duplicated at four sections of the drywell including 1) the mid-elevation of the sandbed region, 2) 17.25° below the equator, 3) 5.75° above the equator and 4) just above the knuckle region. These four sections were chosen to most accurately represent the load distribution in the lower drywell while also providing a reasonably accurate stress distribution in the upper drywell.

To find the correct loads to match the seismic stresses, the total seismic stress (due to reactor building deflection and horizontal and vertical inertia) are obtained from Reference 3-3 at the four sections of interest. The four sections and the corresponding meridional stresses for the refueling and post-accident seismic cases are summarized in Table 3-9.

Unit loads are then applied to the 3-D model in separate load steps at each elevation shown in Figure 3-6. The resulting stresses at the four sections of interest are then averaged for each of the applied unit loads. By solving four equations with four unknowns, the correct loads are determined to match the stresses shown in Table 3-9 at the four sections. The calculation for the correct loads are shown on Tables 3-10 and 3-11 for the refueling and post-accident cases, respectively.

3.6 Stress Results

The resulting stresses for the two load combinations described in section 3.5 are summarized in this section.

3.6.1 Refueling Condition Stress Results

The resulting stress distributions for the refueling condition are shown in Figures 3-7 through 3-10. The red colors represent the most tensile stresses and the blue colors, the most compressive. Figures 3-7 and 3-8 show the meridional stresses for the entire drywell and lower drywell. The circumferential stresses for the same areas are shown on Figures 3-9 and 3-10. The resulting average meridional stress at the mid-elevation of the sandbed region was found to be:

$$\sigma_{Rm} = -7580 \text{ psi}$$

The circumferential stress averaged from the bottom to the top of the sandbed region is;

σ_{Rc} = 4490 psi

3.6.2 Post-Accident Condition Stress Results

The application of all of the loads described for the post-accident condition results in the stress distributions shown in Figures 3-11 through 3-14. The red colors represent the most tensile stresses and the blue colors, the most compressive. Figures 3-11 and 3-12 show the meridional stresses for the entire drywell and lower drywell. The circumferential stresses for the same areas are shown on Figures 3-13 and 3-14. The resulting average meridional stress at mid-elevation of the sandbed region was found to be;

σ_{PAm} = -11960 psi

The circumferential stress averaged from the bottom to the top of the sandbed region is;

σ_{PAc} = +20080 psi

3.7 Theoretical Elastic Buckling Stress Results

After completion of the stress runs for the Refueling and Post-Accident load combinations, the eigenvalue buckling runs are made as described in Section 3.1. This analysis determines the theoretical elastic buckling loads and buckling mode shapes.

3.7.1 Refueling Condition Buckling Results

As shown on Figure 3-15, it is possible for the drywell to buckle in two different modes. In the case of symmetric buckling shown on Figure 3-15, each edge of the 36° drywell model experiences radial displacement with no rotation. This mode is simulated by applying symmetric boundary conditions to the 3-D model the same as used for the stress run. Using these boundary conditions for the refueling case, the critical load factor was found to be 7.67 with the critical buckling occurring in the sandbed region. The critical buckling mode shape is shown in Figure 3-16 for symmetric boundary conditions. The red color indicates sections of the shell which displace radially outward and the blue, those areas which displace inward.

The first four buckling modes were computed in this eigenvalue buckling analysis with no buckling modes found outside the sandbed region for a load factor as high as 9.94. Therefore, buckling is not a concern outside of the sandbed region.

It is also possible for the drywell to buckle in the asymmetric manner shown in Figure 3-15. For this mode, the edges of the 3-D model are allowed to rotate but are restrained from expanding radially. This case is considered by applying asymmetric boundary conditions at the edges of the 3-D model. With the two pass approach used by ANSYS, it is possible to study asymmetric buckling of the drywell when the stresses are found based on symmetric boundary conditions. The resulting load factor found using asymmetric boundary conditions is 10.13. The mode shape for this case is shown on Figure 3-17.

Because the load factor is lower for symmetric boundary conditions with the same applied stress, the symmetric buckling condition is more limiting. Multiplying the load factor of 7.67 by the average meridional stress from section 3.6.1, the theoretical elastic buckling stress is found to be;

$$\sigma_{Rie} = 7.67 \times (7580 \text{ psi}) = 58{,}100 \text{ psi}$$

3.7.2 Post-Accident Condition Buckling Results

Considering the post-accident case with symmetric boundary conditions, the load factor was calculated as 5.18. Multiplying this load factor by the applied stress from section 3.6.2 results in a theoretical elastic buckling stress of

$$\sigma_{PAie} = 5.18 \times (11960 \text{ psi}) = 61{,}950 \text{ psi}$$

The critical mode shape for this condition is shown in Figure 3-18. Again, the critical buckling mode is in the sandbed region.

3.8 References

3-1 DeSalvo, G.J., Ph.D, and Gorman, R.W., "ANSYS Engineering Analysis System User's Manual, Revision 4.4," Swanson Analysis Systems, Inc., May 1, 1989.

3-2 GPUN Specification SP-1302-53-044, Technical Specification for Primary Containment Analysis - Oyster Creek Nuclear Generating Station; Rev. 2, October 1990.

3-3 "An ASME Section VIII Evaluation of the Oyster Creek Drywell - Part 1 Stress Analysis," GE Report No. 9-1, DRF # 00664, November 1990, prepared for GPUN.

Table 3-1

Oyster Creek Drywell Shell Thicknesses

Section	Thickness (in.)
Sandbed Region	0.736 *
Lower Sphere	1.154
Mid Sphere	0.770
Upper Sphere	0.722
Knuckle	2.5625
Cylinder	0.640
Reinforcement Below Flange	1.250
Reinforcement Above Flange	1.500
Elliptical Head	1.1875
Ventline Reinforcement	2.875
Gussets	0.875
Vent Jet Deflector	2.500
Ventline Connection	2.500
Upper Ventline	0.4375
Lower Ventline	0.250

* 95% confidence projected thickness to 14R.

Table 3-2

Cylinder Stiffener Locations and Section Properties

Elevation (in)	Height (in)	Width (in)	Area (in^2)	Bending Inertia (in^4) Horizontal	Vertical
966.3	0.75	6.0	4.5	13.5	0.211
1019.8	0.75	6.0	4.5	13.5	0.211
1064.5	0.50	6.0	3.0	9.0	0.063
1113.0(1)	2.75 1.00	7.0 7.38	26.6	387.5	12.75
1131.0	1.0	12.0	12.0	144.0	1.000

(1) - This stiffener is made up of 2 beam sections, one 2.75x7" and one 1.0x7.375"

Table 3-3

Material Properties for SA-212 Grade B Steel

Material Property	Value
Young's Modulus	29.6×10^6 psi
Yield Strength	38000 psi
Poisson's Ratio	0.3
Density	0.283 lb/in^3

Table 3-4

Oyster Creek Drywell Load Combinations

CASE I - INITIAL TEST CONDITION
Deadweight + Design Pressure (62 psi) + Seismic (2 x DBE)

CASE II - FINAL TEST CONDITION
Deadweight + Design Pressure (35 psi) + Seismic (2 x DBE)

CASE III - NORMAL OPERATING CONDITION
Deadweight + Pressure (2 psi external) + Seismic (2 x DBE)

CASE IV - REFUELING CONDITION
Deadweight + Pressure (2 psi external) + Water Load + Seismic (2 x DBE)

CASE V - ACCIDENT CONDITION
Deadweight + Pressure(62 psi @ 175°F or 35 psi @ 281°F) + Seismic (2 x DBE)

CASE VI - POST ACCIDENT CONDITION
Deadweight + Water Load @ 74'6" + Seismic (2 x DBE)

Table 3-5

Adjusted Weight Densities of Shell to Account for Compressible Material Weight

Shell Thickness (in.)	Adjusted Weight Density (lb/in^3)
1.154	0.343
0.770	0.373
0.722	0.379
2.563	0.310
0.640	0.392
1.250	0.339

Table 3-6

Oyster Creek Drywell Additional Weights - Refueling Condition

ELEVATION (feet)	DEAD WEIGHT (lbf)	PENETR. WEIGHT (lbf)	& MISC. LOADS (lbf)	TOTAL LOAD (lbf)	5 FOOT RANGE LOAD	LOAD PER 36 DEG. (lbf)	# OF ELEMENTS	NODES OF APPLICATION	LOAD PER FULL NODE (lbf)	LOAD PER HALF NODE (lbf)
15.56	50000			50000						
16		188100		188100						
20		11200		11200						
** 15-20					229300	22930	6	116-119	3822	1911
22#	556000			556000						
** 21-25#					556000	55600	8	161-169	6950	3475
28		11100		11100						
30	64100	51500		115600						
30.25	105000		100000	205000						
** 26-30					331700	33170	8	179-187	4146	2073
31		16500		16500						
32		750		750						
33		15450		15450						
34		28050		28050						
35		1500		1500						
** 31-35					62250	6225	8	188-196	778	389
36		1550		1550						
40	41000	43350		84350						
** 36-40					85900	8590	8	197-205	1074	537
50#	1102000			1102000						
** 45-50#					1102000	110200	8	418-426	13775	6888
54		7850		7850						
** 51-55					7850	785	8	436-444	98	49
56	56400		24000	80400						
60	95200	700	20000	115900						
** 56-60					196300	19630	8	454-482	2454	1227
65	52000		20000	72000						
** 61-65					72000	7200	8	472-480	900	450
70		5750		5750						
** 66-70					5750	575	8	508-516	72	36
73		8850		8850						
** 71-75					8850	885	8	526-534	111	55
82.17	21650			21650						
** 81-85					21650	2165	8	553-561	271	135
87		1000		1000						
90		15000		15000						
** 86-90					16000	1600	8	571-579	200	100
93.75	20700			20700						
94.75#			698000	698000						
95.75	20100			20100						
** 91-96					738800	73880	8	589-597	9235	4618
TOTALS:	2184150	388200	862000	3434350	3434350	343435				

- LOAD TO BE APPLIED IN VERTICAL DIRECTION ONLY.
& - MISCELLANEOUS LOADS INCLUDE 698000 LB WATER WEIGHT AT 94.75 FT. ELEVATION 100000 LB EQUIPMENT DOOR WEIGHT AT 30.25 FT. ELEVATION AND WELD PAD LIVE LOADS OF 24000, 20000 AND 20000 AT 58, 60 AND 65 FT. ELEVATIONS

REFWGT.WK1

Table 3-7

Oyster Creek Drywell Additional Weights - Post-Accident Condition

ELEVATION (feet)	DEAD WEIGHT (lbf)	PENETR. WEIGHT (lbf)	& MISC. LOADS (lbf)	TOTAL LOAD (lbf)	5 FOOT RANGE LOAD	LOAD PER 36 DEG. (lbf)	# OF ELEMENTS	NODES OF APPLICATION	LOAD PER FULL NODE (lbf)	LOAD PER HALF NODE (lbf)
15.56	50000			50000						
16		168100		168100						
20		11200		11200						
** 15-20					229300	22930	6	116-119	3822	1911
22#	556000			556000						
** 21-25#					556000	55600	8	161-169	6950	3475
26		11100		11100						
30	64100	51500		115600						
30.25	105000			105000						
** 26-30					231700	23170	8	179-187	2896	1448
31		16500		16500						
32		750		750						
33		15450		15450						
34		28050		28050						
35		1500		1500						
** 31-35					62250	6225	8	188-196	778	389
38		1550		1550						
40	41000	43350		84350						
** 36-40					85900	8590	8	197-205	1074	537
50#	1102000			1102000						
** 45-50#					1102000	110200	8	418-426	13775	6888
54		7850		7850						
** 51-55					7850	785	8	436-444	98	49
58	56400			56400						
60	95200	700		95900						
** 56-60					152300	15230	8	454-462	1904	952
65	52000			52000						
** 61-65					52000	5200	8	472-480	650	325
70		5750		5750						
** 66-70					5750	575	8	508-516	72	36
73		8850		8850						
** 71-75					8850	885	8	526-534	111	55
82.17	21650			21650						
** 81-85					21650	2165	8	553-561	271	135
87		1000		1000						
90		15000		15000						
** 86-90					16000	1600	8	571-579	200	100
93.75	20700			20700						
95.75	20100			20100						
** 91-96					40800	4080	8	589-597	510	255
TOTALS:	2184150	388200	0	2572350	2572350	257235				

- LOAD TO BE APPLIED IN VERTICAL DIRECTION ONLY.
& - NO MISCELLANEOUS LOADS FOR THIS CONDITION.

FLOODWGT.WK1

Table 3-8

Hydrostatic Pressures for Post-Accident, Flooded Condition

WATER DENSITY: 62.32 lb/ft3
0.03606 lb/in3

FLOODED ELEV: 74.5 ft
894 inches

ELEMENTS ABOVE NODES	ANGLE ABOVE EQUATOR (degrees)	ELEVATION (inch)	DEPTH (inch)	PRESSURE (psi)	ELEMENTS
27	-53.32	110.2	783.8	28.3	1-12
40	-51.97	116.2	777.8	28.1	13-24
53	-50.62	122.4	771.6	27.8	25-36
66	-49.27	128.8	765.2	27.6	37-48
79	-47.50	137.3	756.7	27.3	49-51, 61-66 ,55-57
92	-46.20	143.9	750.1	27.1	52-54, 138-141 ,58-60
102	-44.35	153.4	740.6	26.7	142-147, 240-242, 257-259
108	-41.89	166.6	727.4	26.2	148-151, 243, 256
112	-39.43	180.2	713.8	25.7	152-155, 244, 255
116	-36.93	194.6	699.4	25.2	156-159, 245, 254
120	-34.40	209.7	684.3	24.7	160-165, 246, 253
124	-31.87	225.2	668.8	24.1	166-173, 247, 252
130	-29.33	241.3	652.7	23.5	174-183, 248-251
138	-26.80	257.6	636.4	23.0	184-195
148	-24.27	274.4	619.6	22.3	196-207
161	-20.13	302.5	591.5	21.3	208-215
170	-14.38	342.7	551.3	19.9	216-223
179	-8.63	384.0	510.0	18.4	224-231
188	-2.88	425.9	468.1	16.9	232-239
197	2.88	468.1	425.9	15.4	430-437
400	8.63	510.0	384.0	13.8	438-445
409	14.38	551.3	342.7	12.4	446-453
418	20.13	591.5	302.5	10.9	454-461
427	25.50	627.8	266.2	9.6	462-469
436	30.50	660.2	233.8	8.4	470-477
445	35.50	690.9	203.1	7.3	478-485
454	40.50	719.8	174.2	6.3	486-493
463	45.50	746.6	147.4	5.3	494-501
472	50.50	771.1	122.9	4.4	502-509
481	54.86	790.5	103.5	3.7	510-517
490	-	805.6	88.4	3.2	518-525
499	-	820.7	73.3	2.6	526-533
508	-	835.7	58.3	2.1	534-541
517	-	850.8	43.2	1.6	542-549
526	-	885.3	8.7	0.3	550-557
-	-	187.3	706.7	25.5	340-399 (Ventline)

FLOODP.WK1

Table 3-9

Meridional Seismic Stresses at Four Sections

Section	Elevation (inches)	2-D Shell Model Node	Meridional Stresses Refueling (psi)	Meridional Stresses Post-Accident (psi)
A) Middle of Sandbed	119	32	1258	1288
B) 17.25° Below Equator	323	302	295	585
C) 5.75° Above Equator	489	461	214	616
D) Above Knuckle	1037	1037	216	808

Table 3-10

Application of Loads to Match Seismic Stresses - Refueling Case

COMPRESSIVE STRESSES FROM 2-D ANALYSIS	SECTION: / 2-D NODE: / ELEV:	2-D SEISMIC STRESSES AT SECTION (psi) 1 / 32 / 119.3"	2 / 302 / 322.5"	3 / 461 / 489.1"	4 / 1037 / 912.3"
0.058" SEISMIC DEFLECTION:		788.67	155.54	103.48	85.31
HORIZ. PLUS VERTICAL SEISMIC INERTIA:		469.55	139.44	110.13	130.21
TOTAL SEISMIC COMPRESSIVE STRESSES:		1258.22	294.98	213.59	215.52

3-D INPUT LOAD SECTION	INPUT 3-D UNIT LOAD DESCRIPTION	SECTION: / 3-D NODES: / ELEV:	3-D STRESSES AT SECTION (psi) 1 / 53-65 / 119.3"	2 / 170-178 / 322.5"	3 / 400-408 / 489.1"	4 / 526-534 / 912.3"
A	1000 lbs at nodes 563 through 569		85.43	37.94	34.94	55.23
B	500 lbs at 427&435, 1000 lbs at 428-434		89.88	39.92	36.76	0.00
C	500 lbs at 197&205, 1000 lbs at 198-204		97.64	43.37	0.00	0.00
D	500 lbs at 161&169, 1000 lbs at 162-168		89.85	0.00	0.00	0.00
	DESIRED COMPRESSIVE STRESSES (psi):		1258.22	294.98	213.59	215.52

3-D INPUT LOAD SECTION	LOAD TO BE APPLIED TO MATCH 2-D STRESSES		RESULTING STRESSES AT SECTION (psi)			
A	3902.2		333.37	148.05	136.34	215.52
B	2101.4		188.87	83.89	77.25	0.00
C	1453.6		141.93	63.04	0.00	0.00
D	6611.6		594.05	0.00	0.00	0.00
		SUM:	1258.22	294.98	213.59	215.52

SEISUNFL.WK1

Table 3-11

Application of Loads to Match Seismic Stresses - Post-Accident Case

COMPRESSIVE STRESSES FROM 2-D ANALYSIS	SECTION:	1	2	3	4
	2-D NODE:	32	302	461	1037
	ELEV:	119.3"	322.5"	489.1"	912.3"
		2-D SEISMIC STRESSES AT SECTION (psi)			
0.058" SEISMIC DEFLECTION:		788.67	155.54	103.46	85.31
HORIZ. PLUS VERTICAL SEISMIC INERTIA:		499.79	429.39	512.76	723.14
TOTAL SEISMIC COMPRESSIVE STRESSES:		1288.46	584.93	616.22	808.45

3-D INPUT LOAD SECTION	INPUT 3-D UNIT LOAD DESCRIPTION	SECTION:	1	2	3	4
		3-D NODES:	53-65	170-178	400-408	528-534
		ELEV:	119.3"	322.5"	489.1"	912.3"
			3-D STRESSES AT SECTION (psi)			
A	1000 lbs at nodes 563 through 569		85.43	37.94	34.94	55.23
B	500 lbs at 427&435, 1000 lbs at 428-434		89.88	39.92	36.76	0.00
C	500 lbs at 197&205, 1000 lbs at 198-204		97.64	43.37	0.00	0.00
D	500 lbs at 161&169, 1000 lbs at 162-168		89.85	0.00	0.00	0.00
	DESIRED COMPRESSIVE STRESSES (psi):		1288.46	584.93	616.22	808.45

3-D INPUT LOAD SECTION	LOAD TO BE APPLIED TO MATCH 2-D STRESSES		RESULTING STRESSES AT SECTION (psi)			
A	14637.9		1250.51	555.36	511.45	808.45
B	2850.2		256.17	113.78	104.77	0.00
C	-1941.7		-189.58	-84.21	0.00	0.00
D	-318.8		-28.64	0.00	0.00	0.00
		SUM:	1288.46	584.93	616.22	808.45

SEISFL.WK1

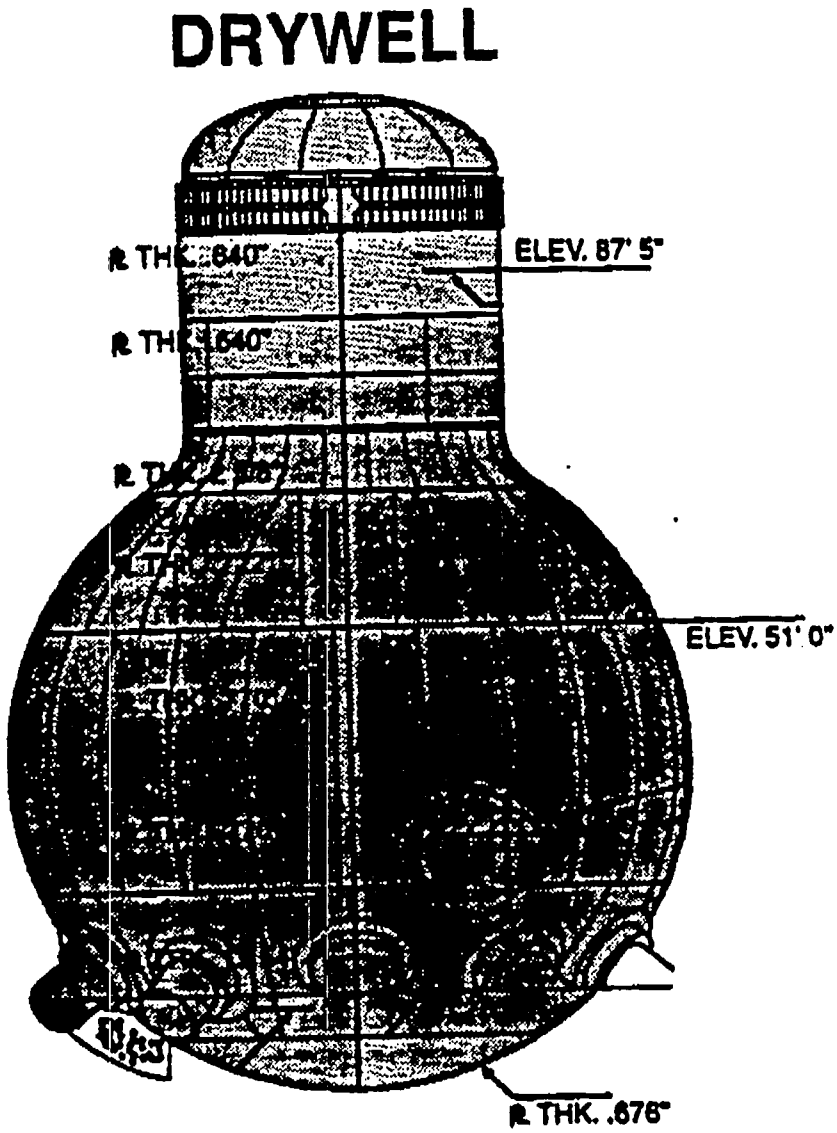

Figure 3-1. Oyster Creek Drywell Geometry

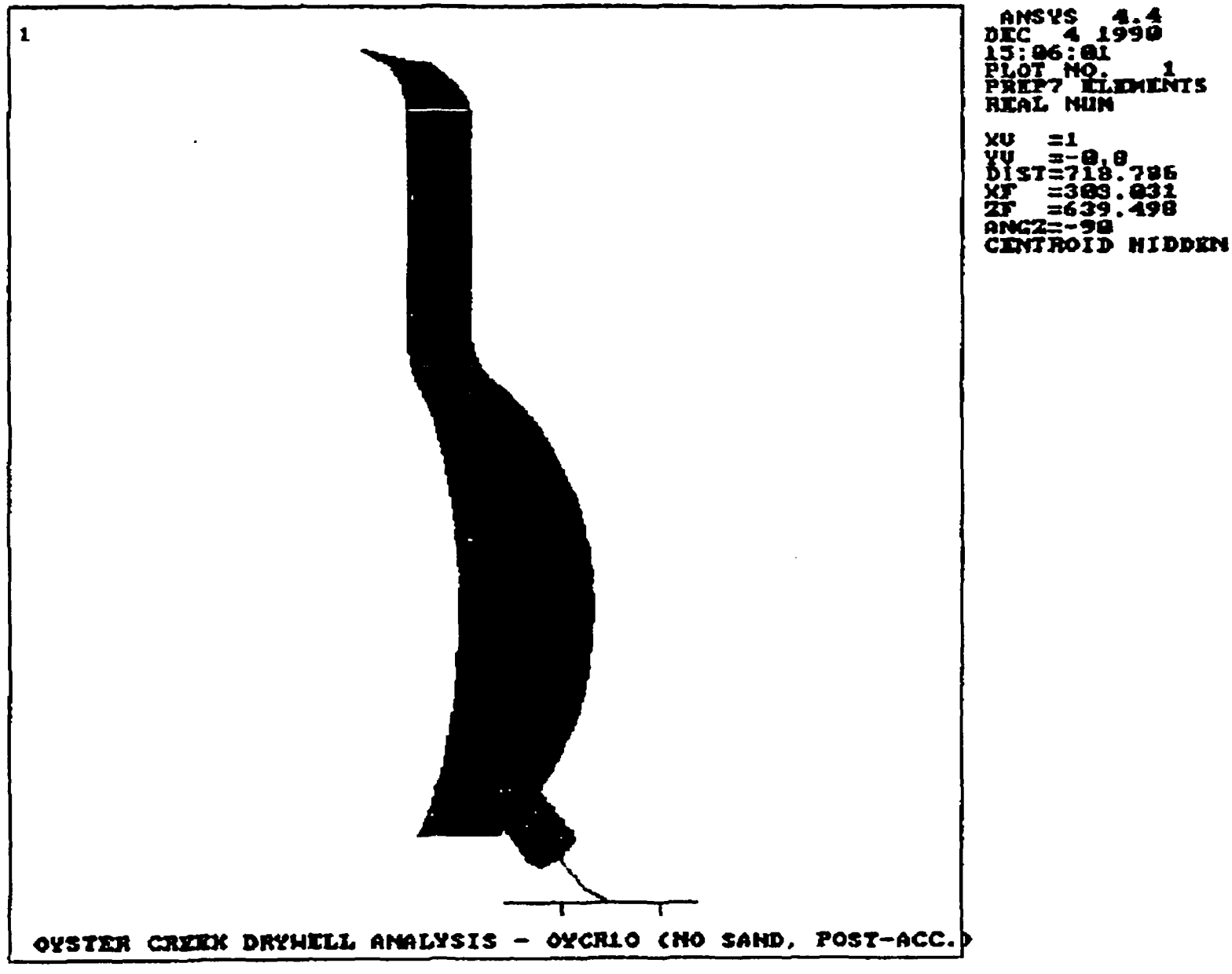

Figure 3-2. Oyster Creek Drywell 3-D Finite Element Model

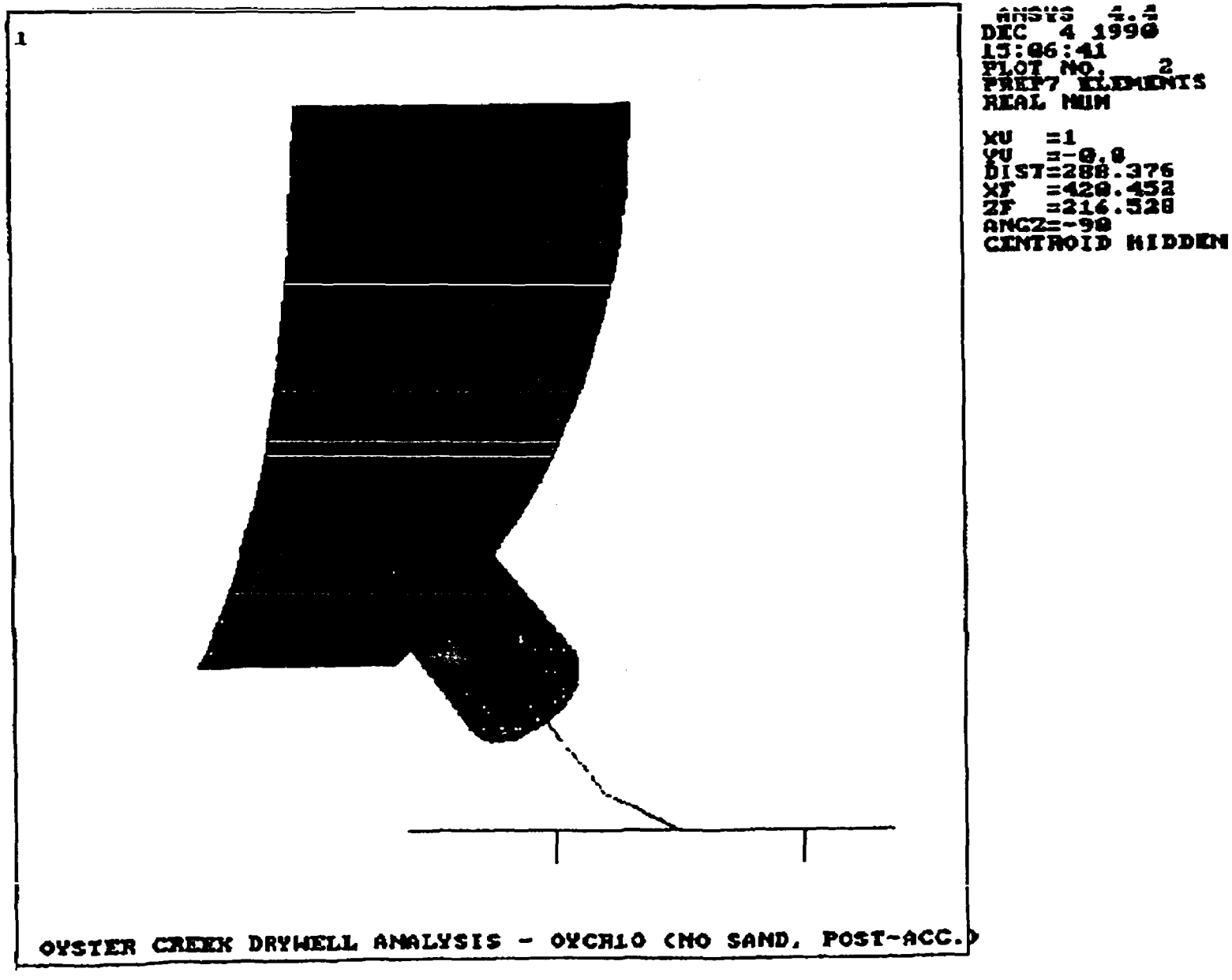

Figure 3-3. Closeup of Lower Drywell Section of FEM (Outside View)

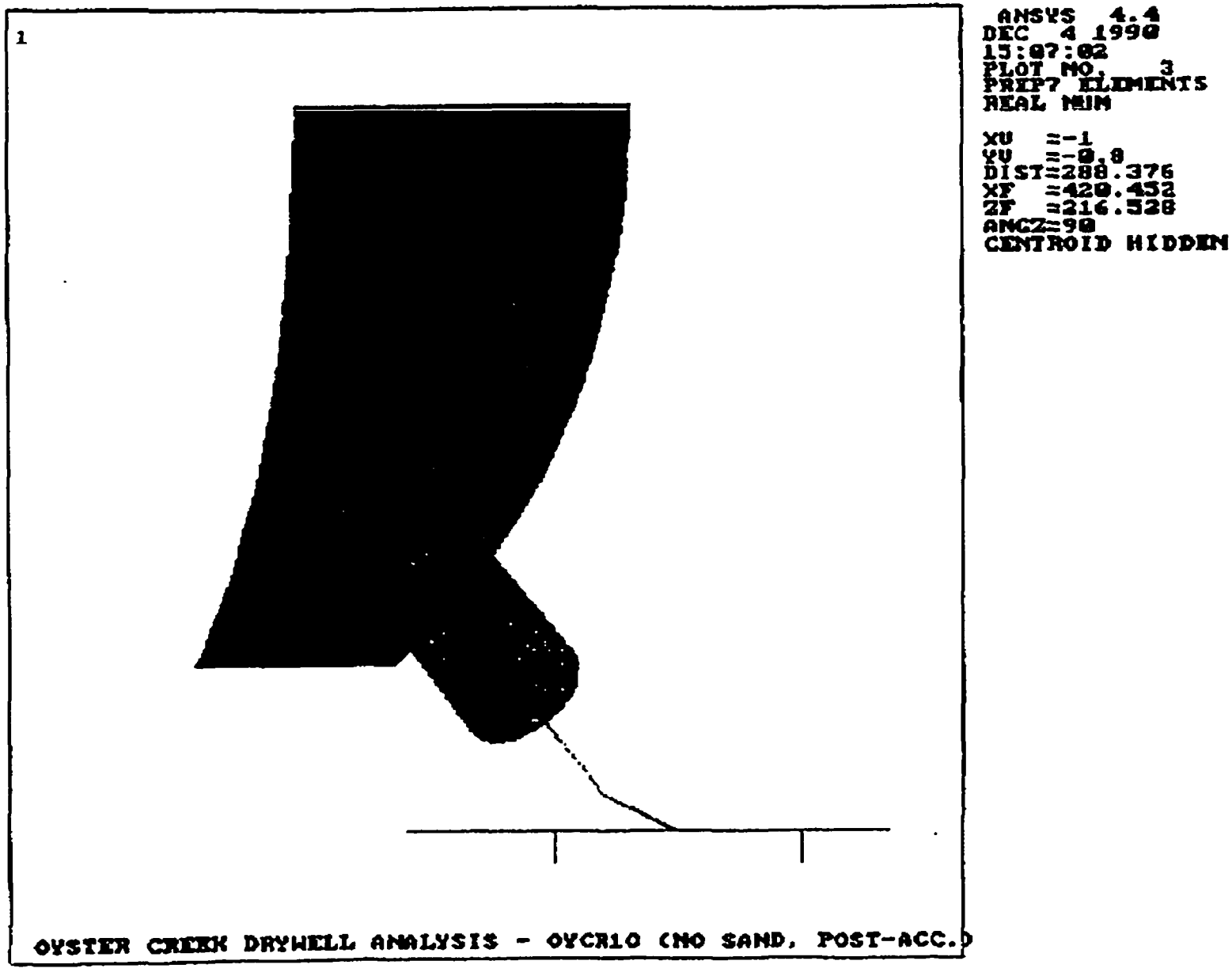

Figure 3.4 Closeup of Lower Drywell Section of FEM (Inside View)

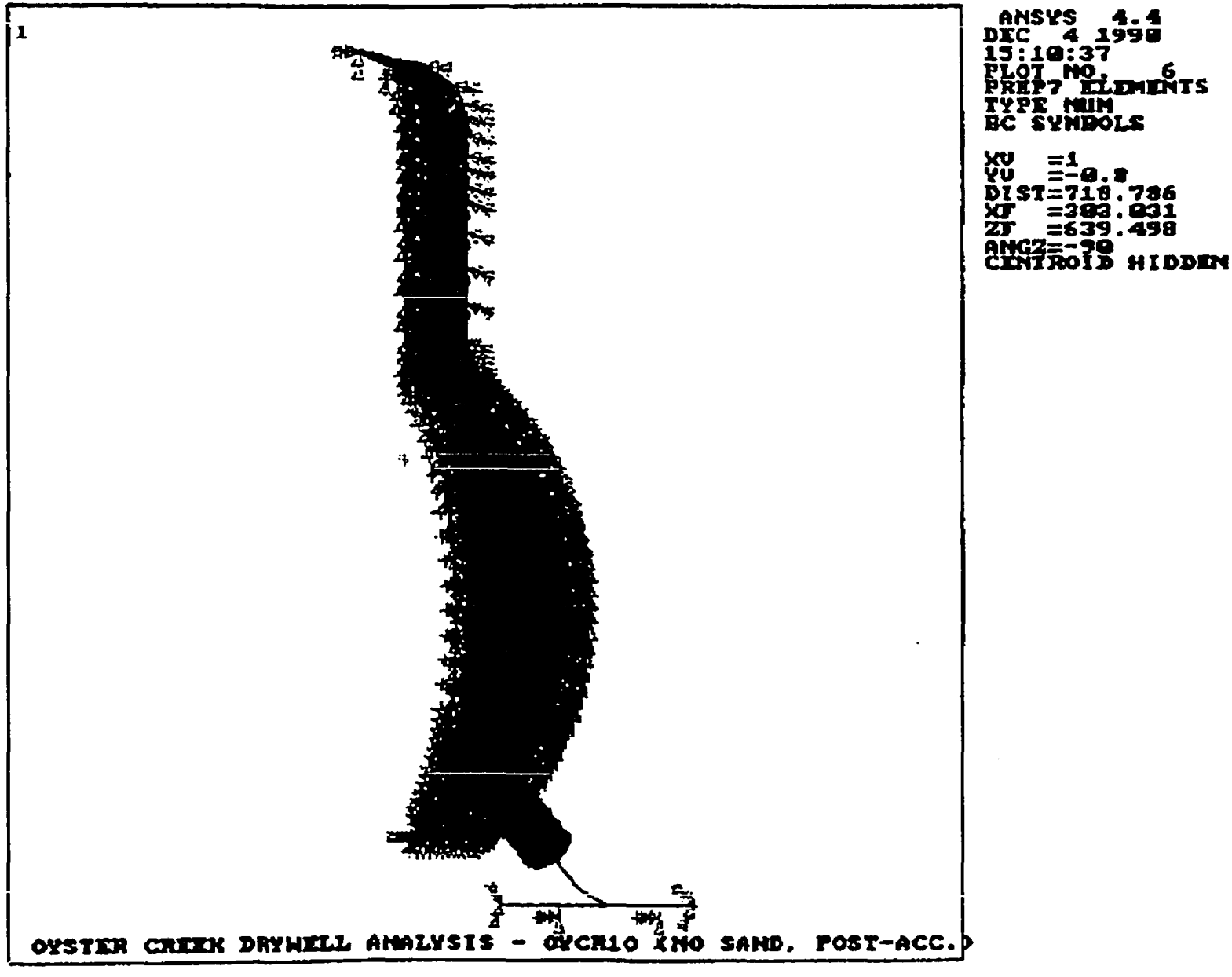

Figure 3-5 Boundary Conditions of Finite Element Model

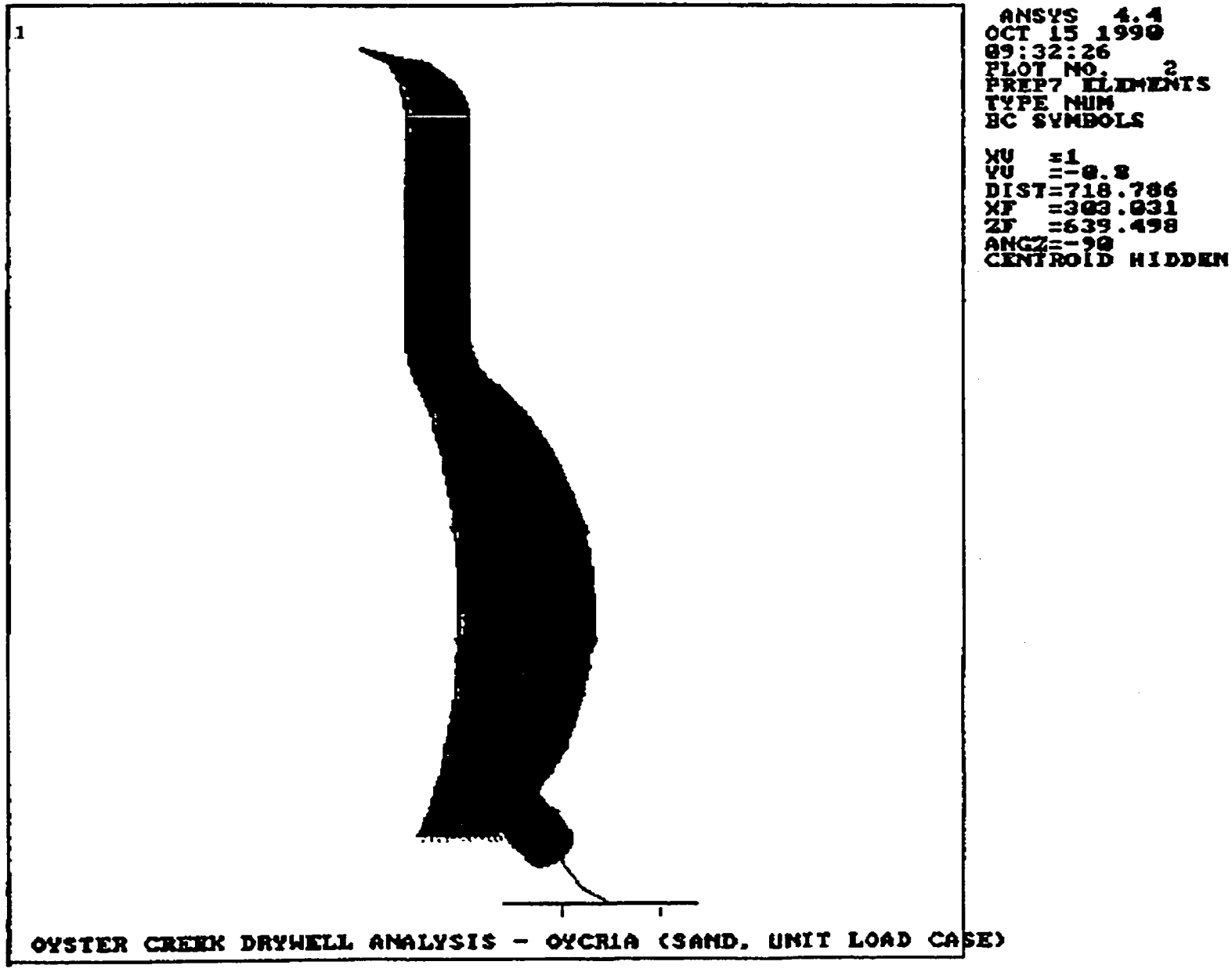

Figure 3.6 Application of Loading to Simulate Seismic Loading

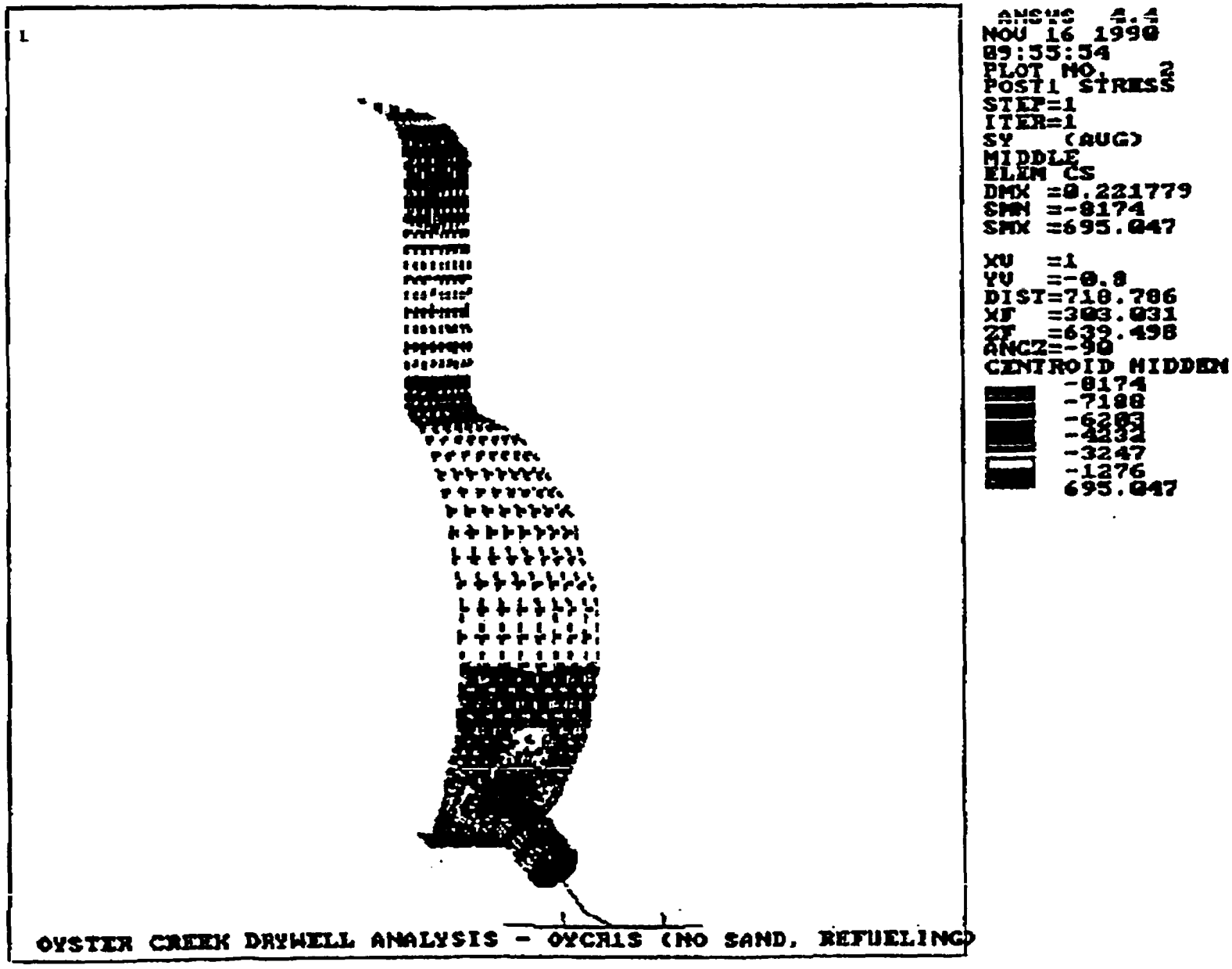

Figure 3-7. Meridional Stresses - Refueling Case

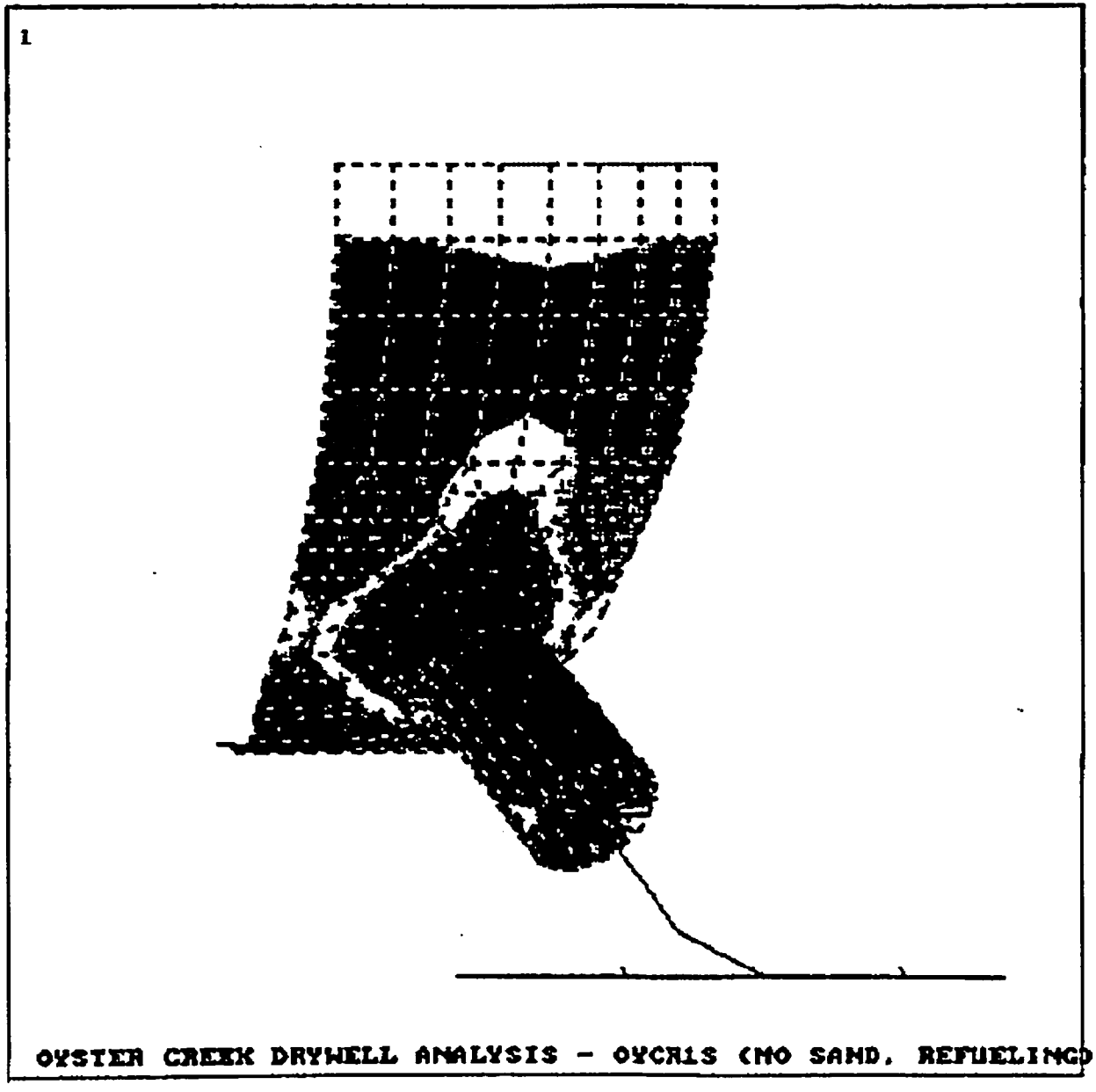
1
ANSYS 4.4
NOV 16 1990
09:57:29
PLOT NO. 4
POST1 STRESS
STEP=1
ITER=1
SY (AVG)
MIDDLE
ELEM CS
DMX =0.139473
SMN =-8174
SMX =695.047
XV =1
YV =-0.8
DIST=288.376
XF =420.452
ZF =216.528
ANGZ=-90
CENTROID HIDDEN
-8174
-7188
-6203
-4232
-3247
-1276
695.047
OYSTER CREEK DRYWELL ANALYSIS - OYCR1S (NO SAND, REFUELING)

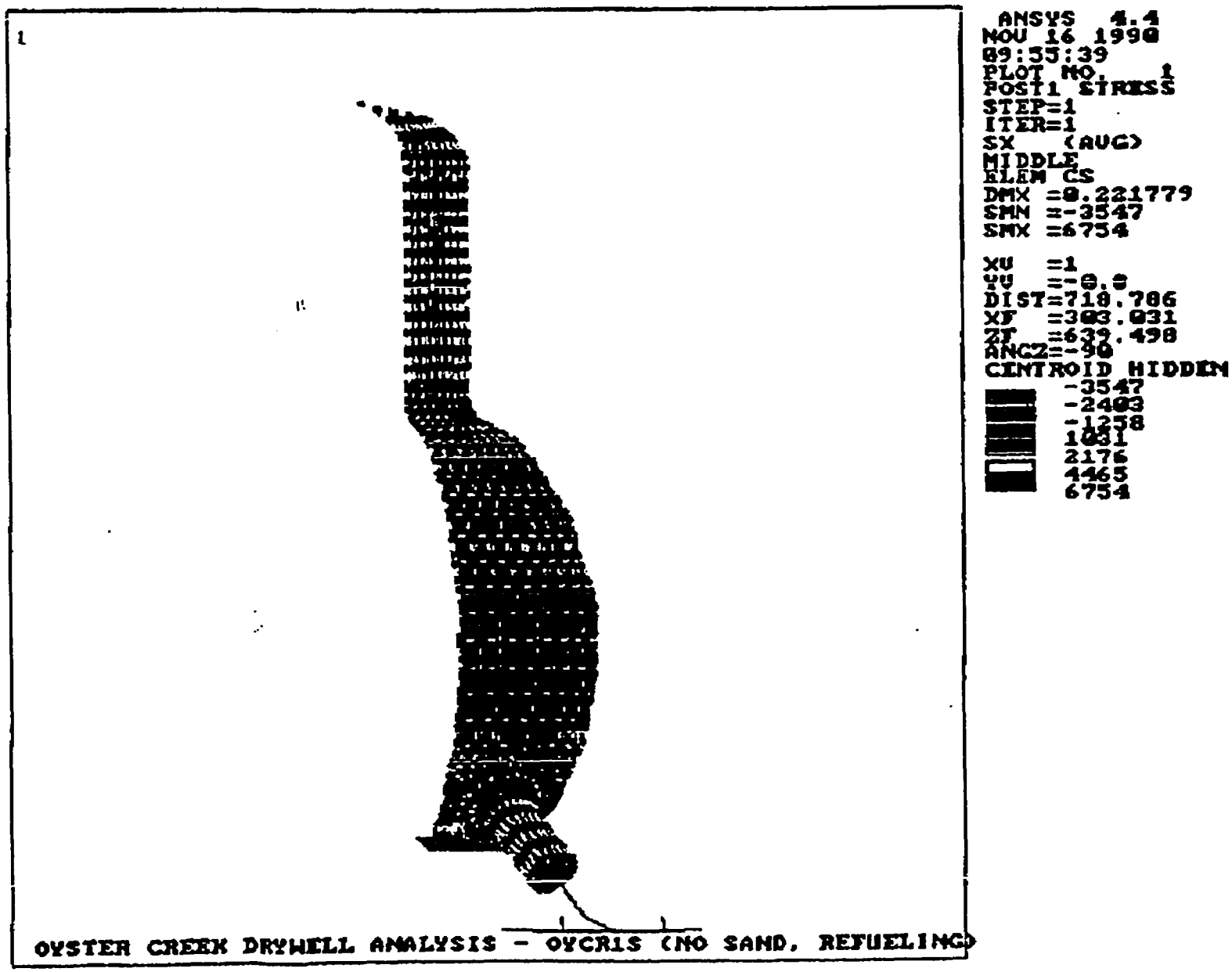

Figure 3.9 Circumferential Stresses - Refueling Case

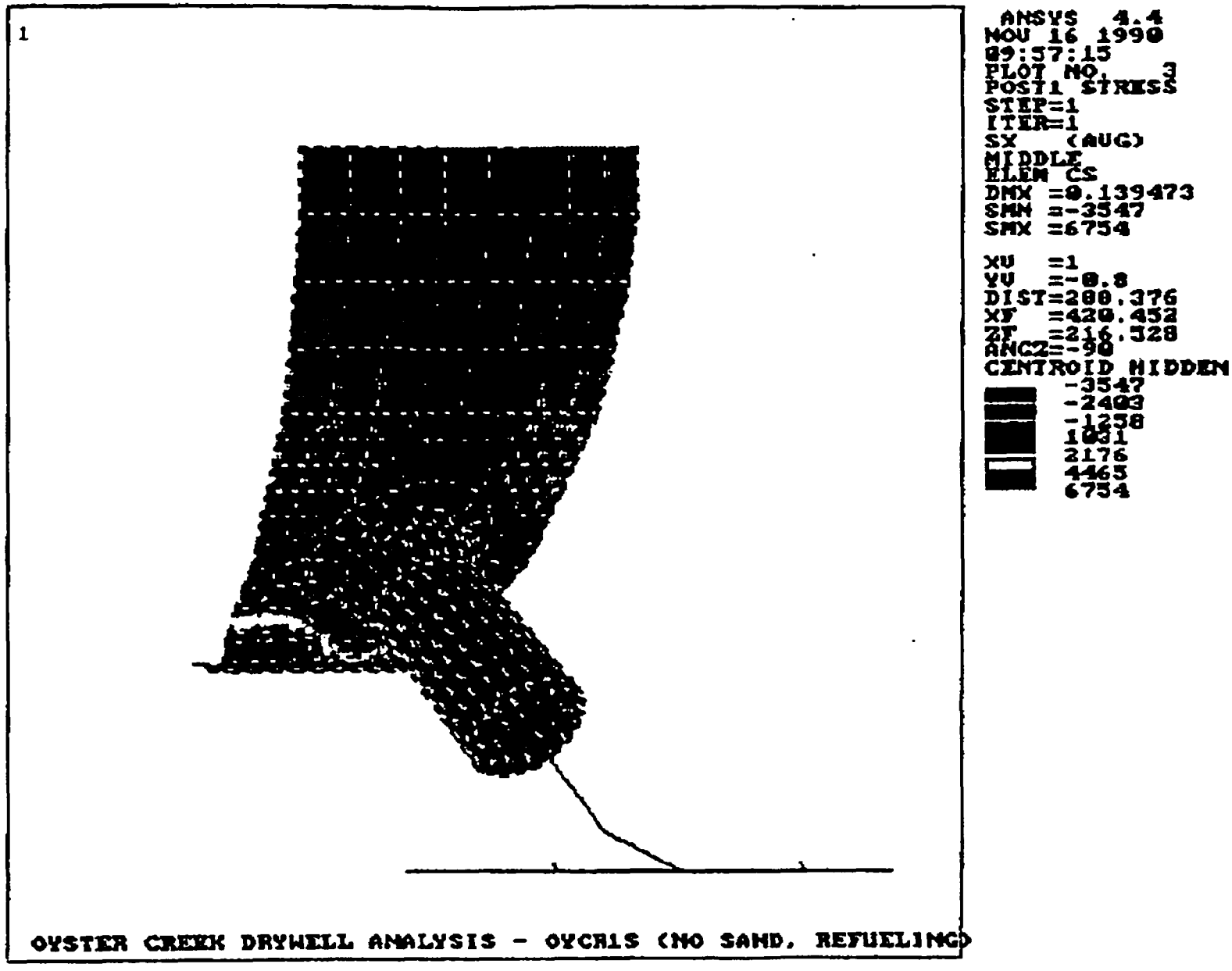

Figure 3-10. Lower Drywell Circumferential Stresses - Refueling Case

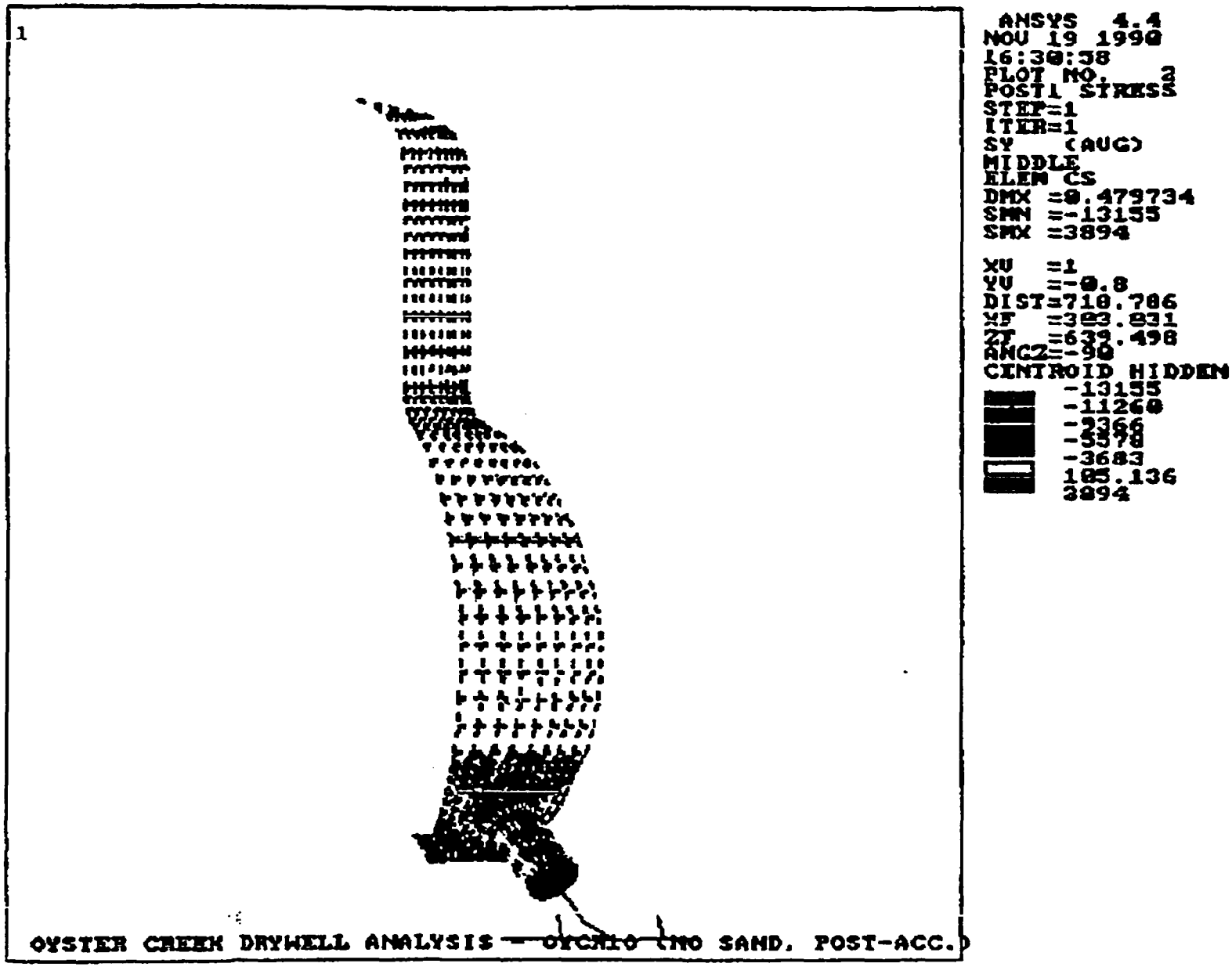

Figure 3-11. Meridional Stresses - Post-Accident Case

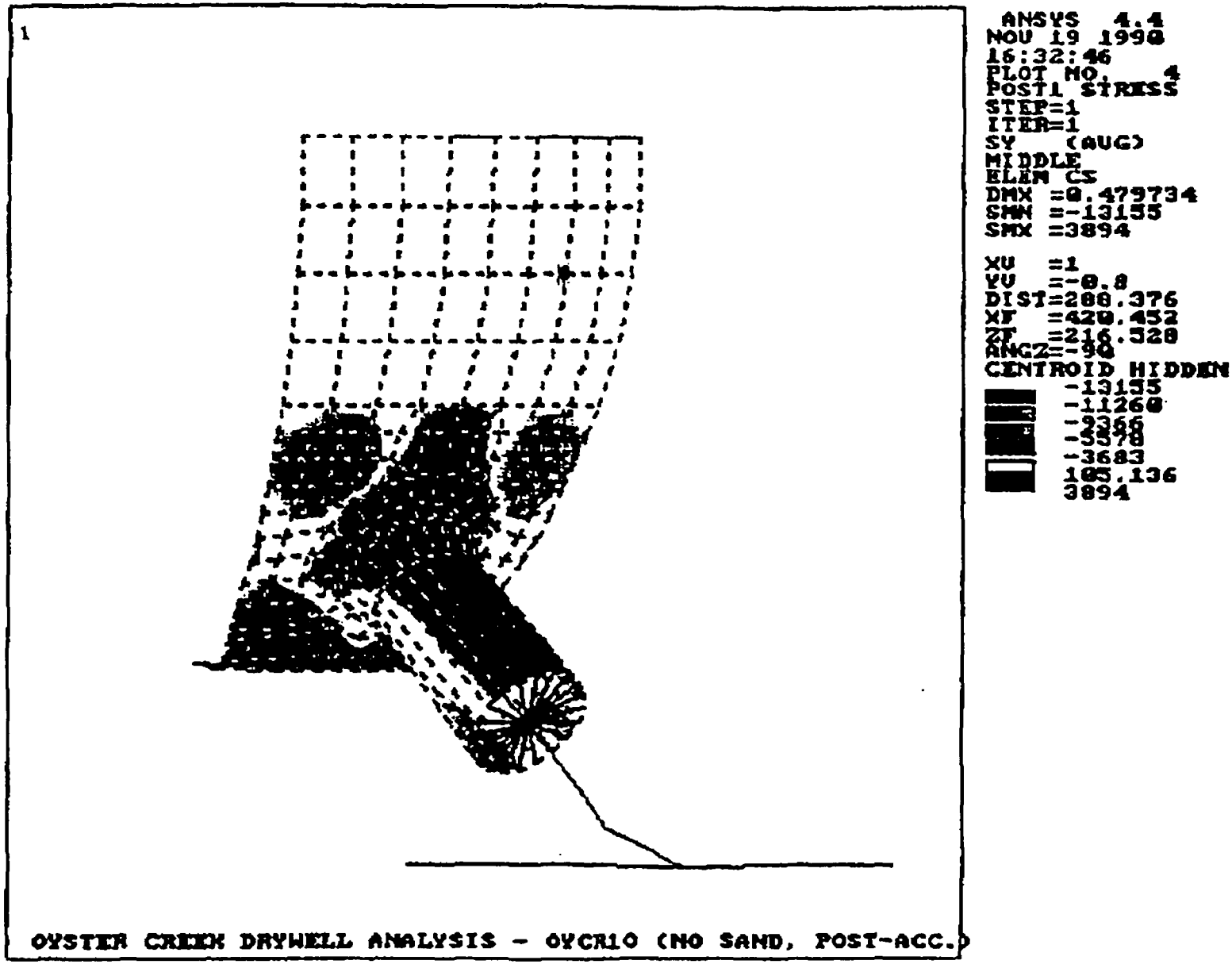

Figure 3-12. Lower Drywell Meridional Stresses - Post-Accident Case

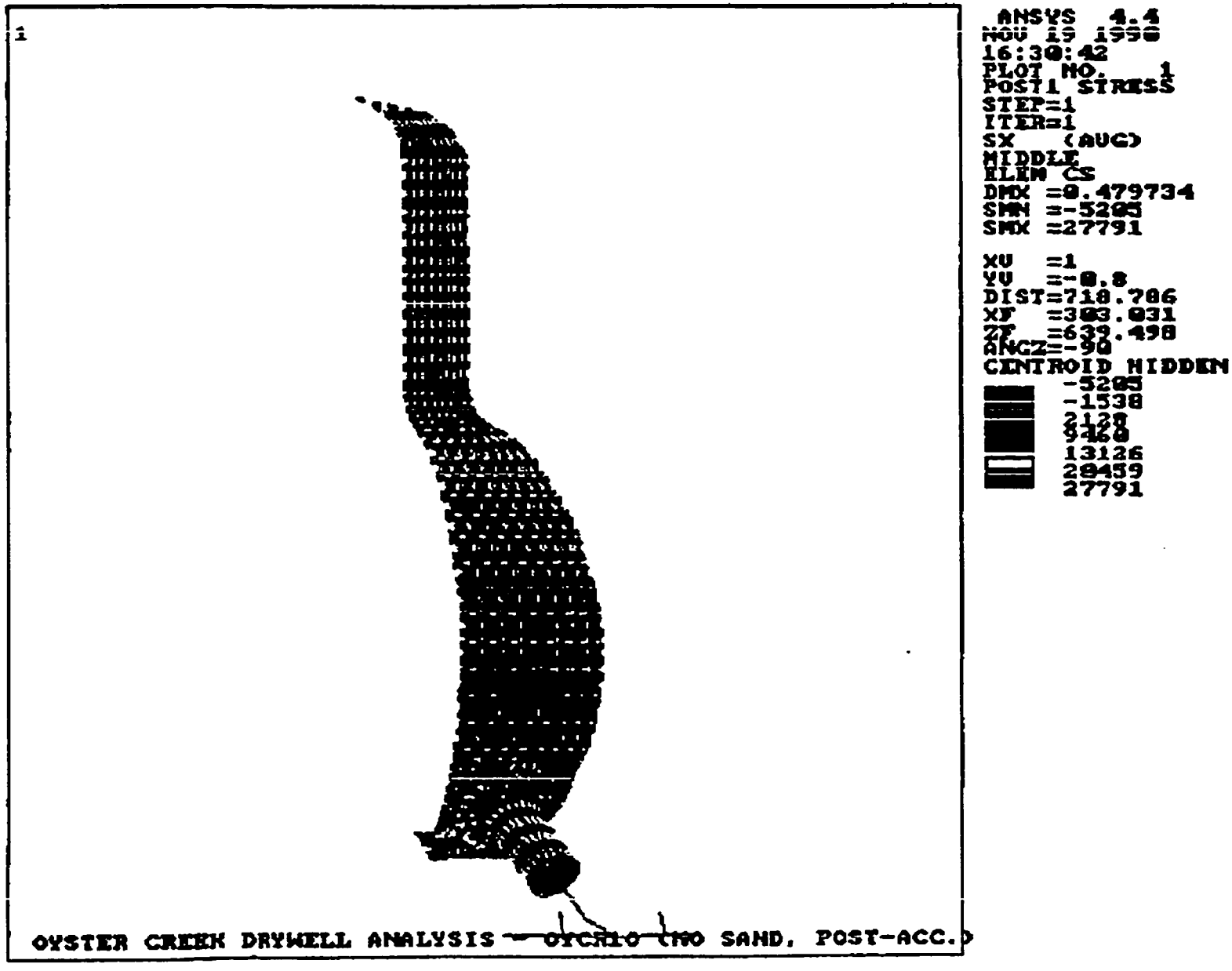

Figure 3-13. Circumferential Stresses - Post-Accident Case

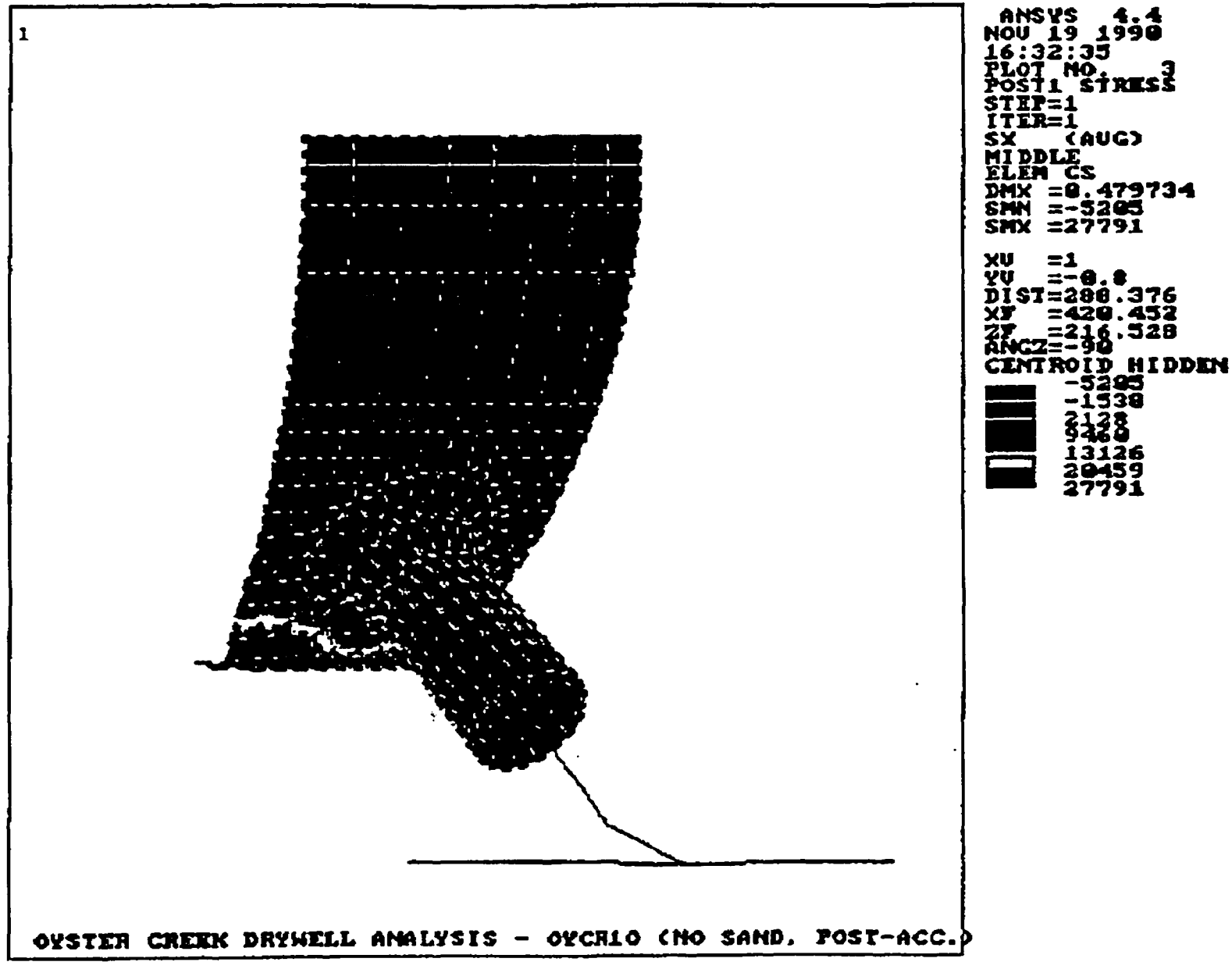

Figure 3-14. Lower Drywell Circumferential Stresses - Post-Accident Case

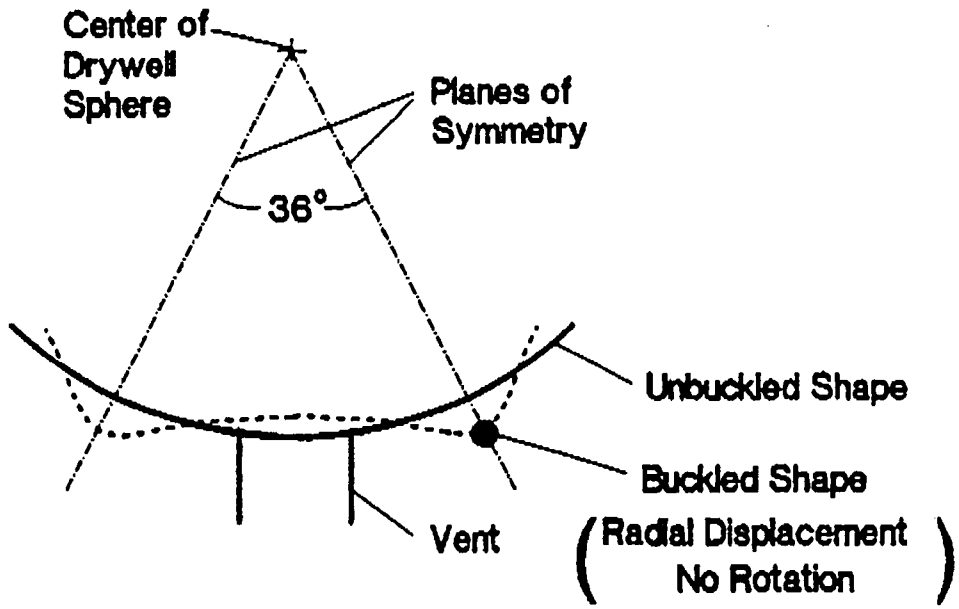

Symmetric Buckling of Drywell

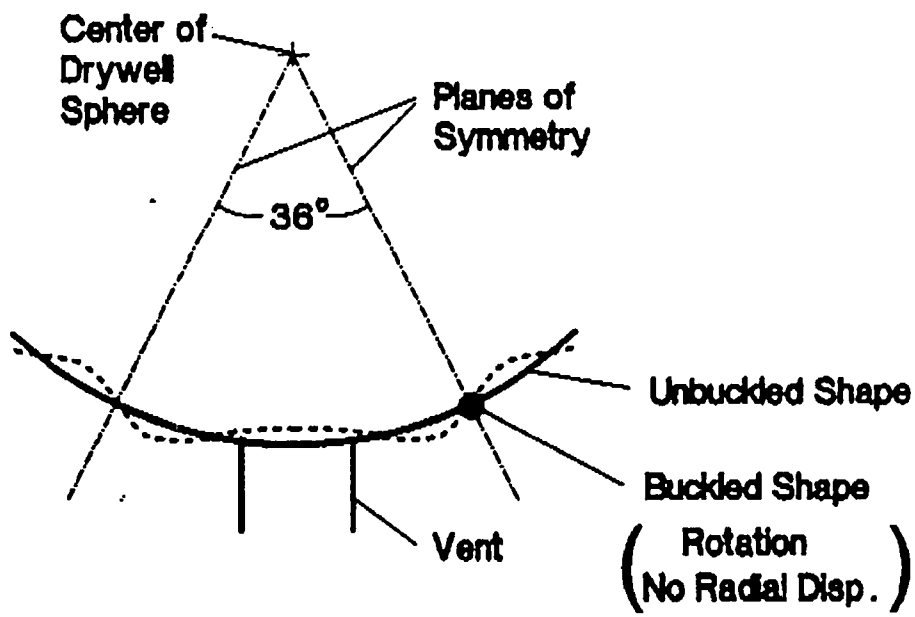

Asymmetric Buckling of Drywell

SYM.DRW

Figure 3-15. Symmetric and Asymmetric Buckling Modes

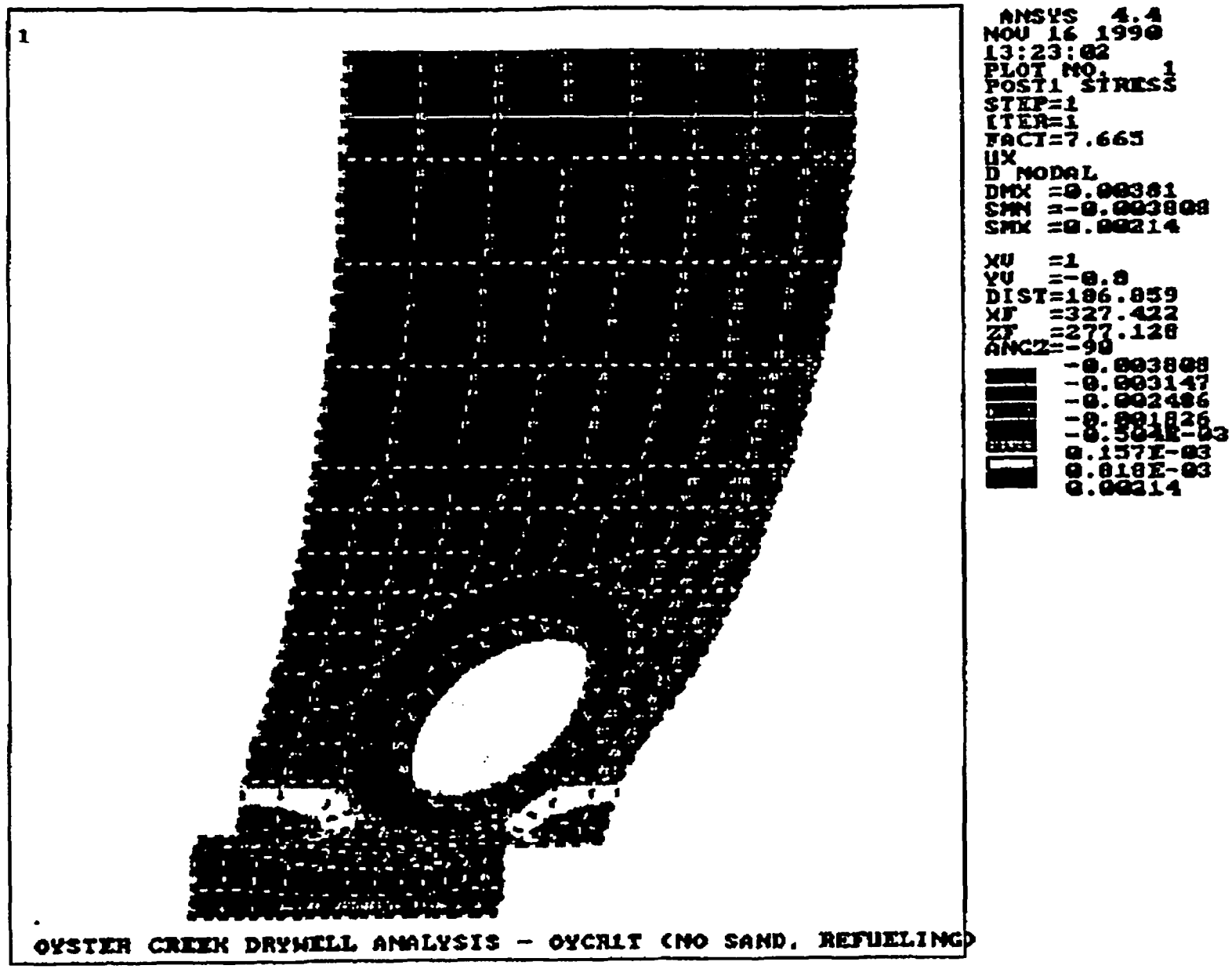

Figure 3-16. Symmetric Buckling Mode Shape - Refueling Case

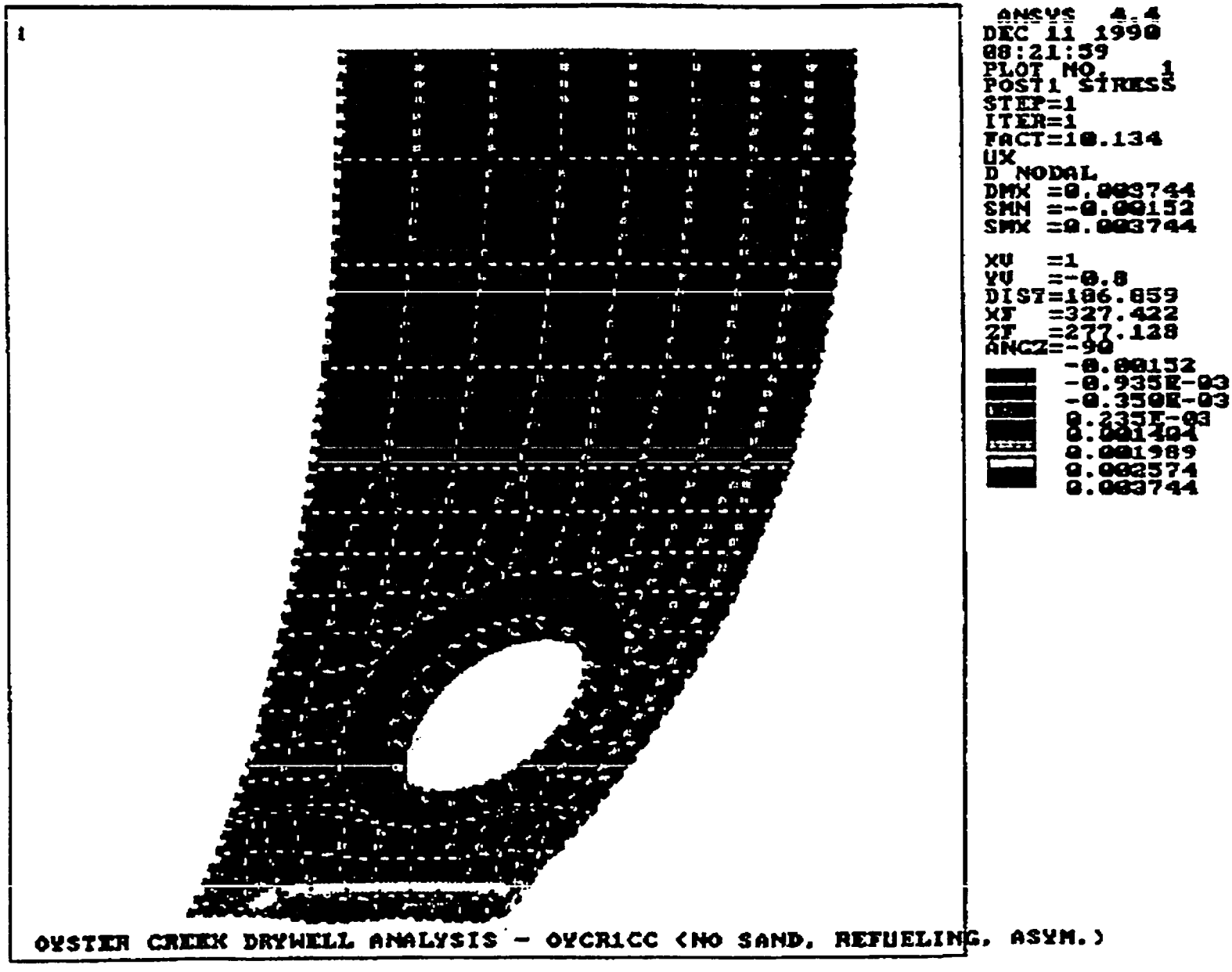

Figure 3.17 Asymmetric Buckling Mode Shape - Refueling Case

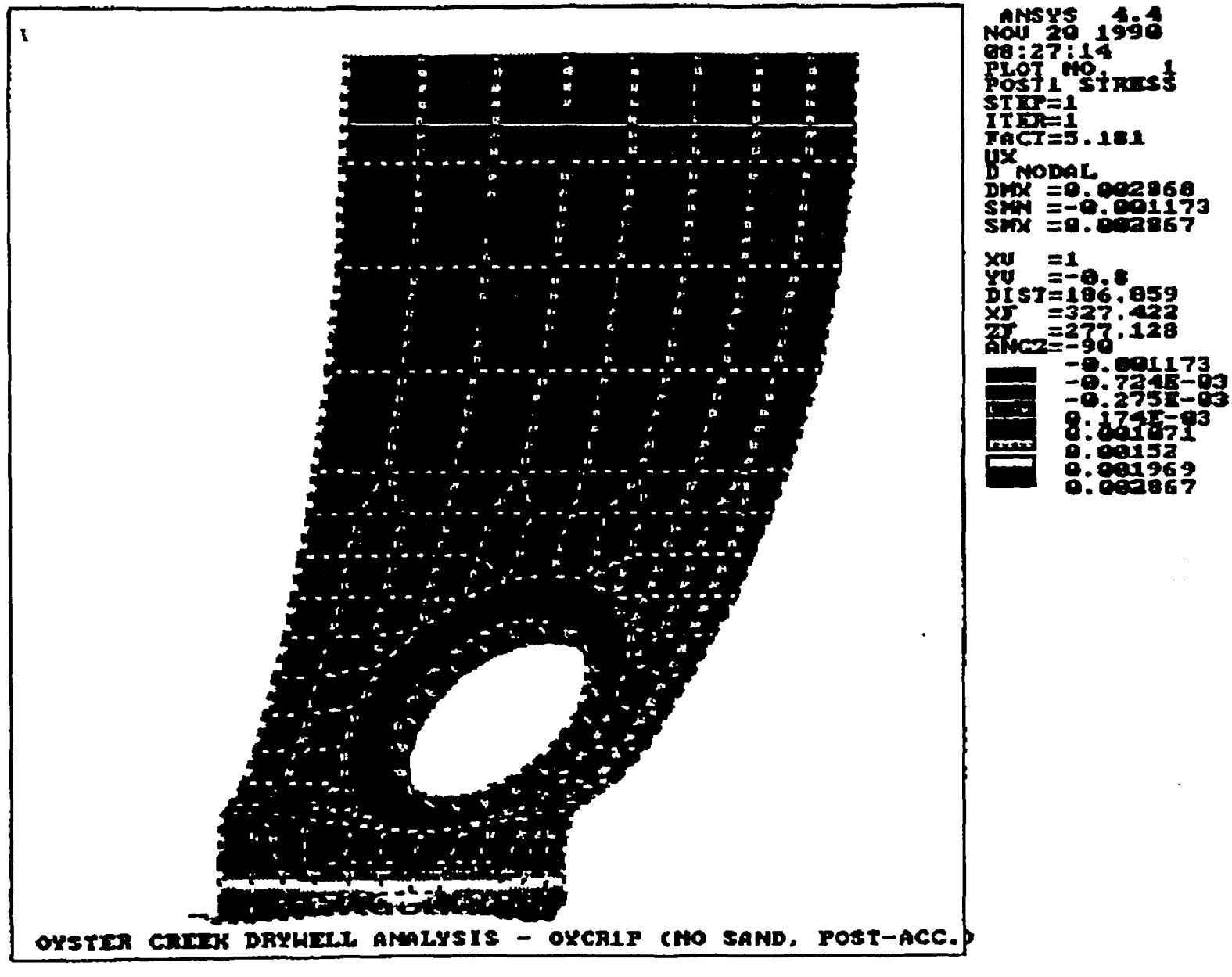

Figure 3-18 Buckling Mode Shape - Post Accident Case

4. ALLOWABLE BUCKLING STRESS EVALUATION

Applying the methodology described in Section 2 for the modification of the theoretical elastic buckling stress, the allowable compressive stresses are now calculated. Tables 4-1 and 4-2 summarize the calculation of the allowable buckling stresses for the Refueling and Post-Accident conditions, respectively. The modified capacity reduction factors are first calculated as described in sections 2.2 and 2.3. After reducing the theoretical instability stress by this reduction factor, the plasticity reduction factor is calculated and applied. The resulting inelastic buckling stresses are then divided by the factor of safety of 2.0 for the Refueling case and 1.67 for the Post-Accident case to obtain the final allowable compressive stresses.

The allowable compressive stress for the Refueling case is 10.65 ksi. Since the applied compressive stress is 7.58 ksi, there is a 41% margin. The allowable compressive stress for the Post-Accident, flooded case is 13.77 ksi. This results in a margin of 15% for the applied compressive stress of 11.96 ksi.

Table 4-1

Calculation of Allowable Buckling Stresses - Refueling Case

Parameter	Value
Theoretical Elastic Instability Stress, σ_{ie} (ksi)	58.10
Capacity Reduction Factor, α_i	0.207
Circumferential Stress, σ_c (ksi)	4.49
Equivalent Pressure, p (psi)	15.74
"X" Parameter	0.173
ΔC	0.118
Modified Capacity Reduction Factor, $\alpha_{i,mod}$	0.402
Elastic Buckling Stress, $\sigma_e = \alpha_{i,mod}\,\sigma_{ie}$ (ksi)	23.34
Proportional Limit Ratio, $\Delta = \sigma_e/\sigma_y$	0.614
Plasticity Reduction Factor, η_i	0.913
Inelastic Buckling Stress, $\sigma_i = \eta_i\sigma_e$ (ksi)	21.30
Factor of Safety, FS	2.0
Allowable Compressive Stress, $\sigma_{all} = \sigma_i/FS$ (ksi)	10.65
Applied Compressive Meridional Stress, σ_m (ksi)	7.58
Margin = $[(\sigma_i/\sigma_m) - 1] \times 100\%$	41%

Table 4-2

Calculation of Allowable Buckling Stresses - Post-Accident Case

Parameter	Value
Theoretical Elastic Instability Stress, σ_{ie} (ksi)	61.95
Capacity Reduction Factor, α_i	0.207
Circumferential Stress, σ_c (ksi)	20.08
Equivalent Pressure, p (psi)	70.38
"X" Parameter	0.774
ΔC	0.195
Modified Capacity Reduction Factor, $\alpha_{i,mod}$	0.529
Elastic Buckling Stress, $\sigma_e = \alpha_{i,mod}\ \sigma_{ie}$ (ksi)	32.74
Proportional Limit Ratio, $\Delta = \sigma_e/\sigma_y$	0.862
Plasticity Reduction Factor, η_i	0.702
Inelastic Buckling Stress, $\sigma_i = \eta_i\sigma_e$ (ksi)	22.99
Factor of Safety, FS	1.67
Allowable Compressive Stress, $\sigma_{all} = \sigma_i/FS$ (ksi)	13.77
Applied Compressive Meridional Stress, σ_m (ksi)	11.96
Margin = $[(\sigma_i/\sigma_m) - 1] \times 100\%$	15%

5. SUMMARY AND CONCLUSIONS

The results of this buckling analysis for the refueling and post-accident load combinations are summarized in Table 5-1. The applied and allowable compressive meridional stresses shown in Table 5-1 are for the sandbed region which is the most limiting region in terms of buckling. This analysis demonstrates that the Oyster Creek drywell has adequate margin against buckling with no sand support for an assumed sandbed shell thickness of 0.736 inch. This thickness is the 95% confidence projected thickness for the 14R outage.

Table 5-1

Buckling Analysis Summary

	Load Combination	
	Refueling	Post-Accident
Service Condition	Design	Level C
Factor of Safety Applied	2.00	1.67
Applied Compressive Meridional Stress (ksi)	7.58	11.96
Allowable Compressive Meridional Stress (ksi)	10.65	13.77
Buckling Margin	41%	15%